전파간섭계와 ALMA 소개

2019.07.29 — 08.02
소백산 천문대
2019 ALMA 여름학교

권우진
Woojin Kwon

Radio observations

$\boxed{\theta \sim \lambda/D}$

- To achieve 1 arc-second resolution
  at λ = 500 nm: D ~ 10 cm
  at λ = 1 mm : D ~ 200 m

- Difficulties in building a big radio telescope:
  1. The required tracking accuracy ~ $\theta/10$ but the best mechanical tracking and pointing accuracy ~ 1" due to
     - Gravitational sagging
     - Antenna deformations caused by differential solar heating
     - Wind gusts
  2. Surface accuracy ~ $\lambda/20$

What radio interferometers look like?

- Arrays: e.g., JVLA, SMA, NOEMA, ALMA
- Very Long Baseline Interferometers: e.g., KVN

ALMA 인류 역사상 가장 규모가 큰 천문대

ALMA 인류 역사상 가장 규모가 큰 천문대

References

- **Essential Radio Astronomy (3.7)**
  J. J. Condon and S. M. Ransom, NRAO
  https://science.nrao.edu/opportunities/courses/era/

- Fundamentals of Radio Astronomy (ch. 5, 6)
  J. M. Marr, R. L. Snell, and S. E. Kurtz

- Tools of Radio Astronomy
  K. Rohlfs and T. L. Wilson

- Interferometry and Synthesis in Radio Astronomy
  A. Richard Thompson, James M. Moran, and George W. Swenson, Jr.

- Synthesis Imaging in Radio Astronomy
  Astronomical Society of the Pacific Conference Series (Volume 180)

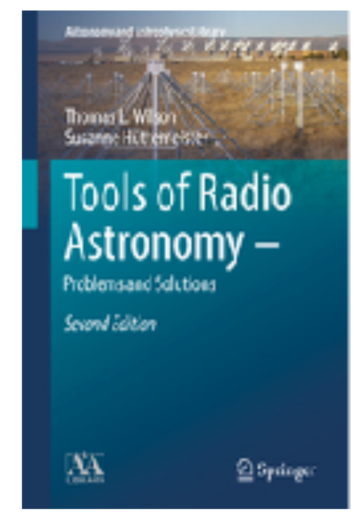

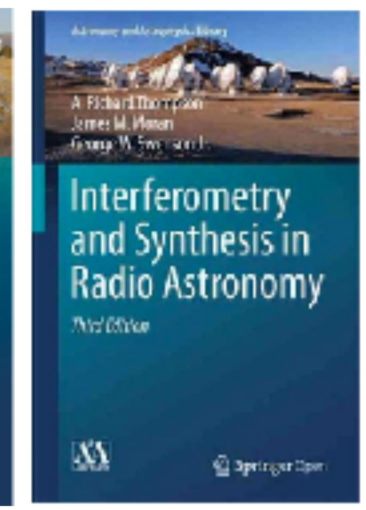

Fourier transform

$$\boxed{F(s) \equiv \int_{-\infty}^{\infty} f(x) \;\; e^{-2\pi i s x} \, dx,}$$

$$\boxed{f(x) \equiv \int_{-\infty}^{\infty} F(s) \;\; e^{2\pi i s x} \, ds,}$$

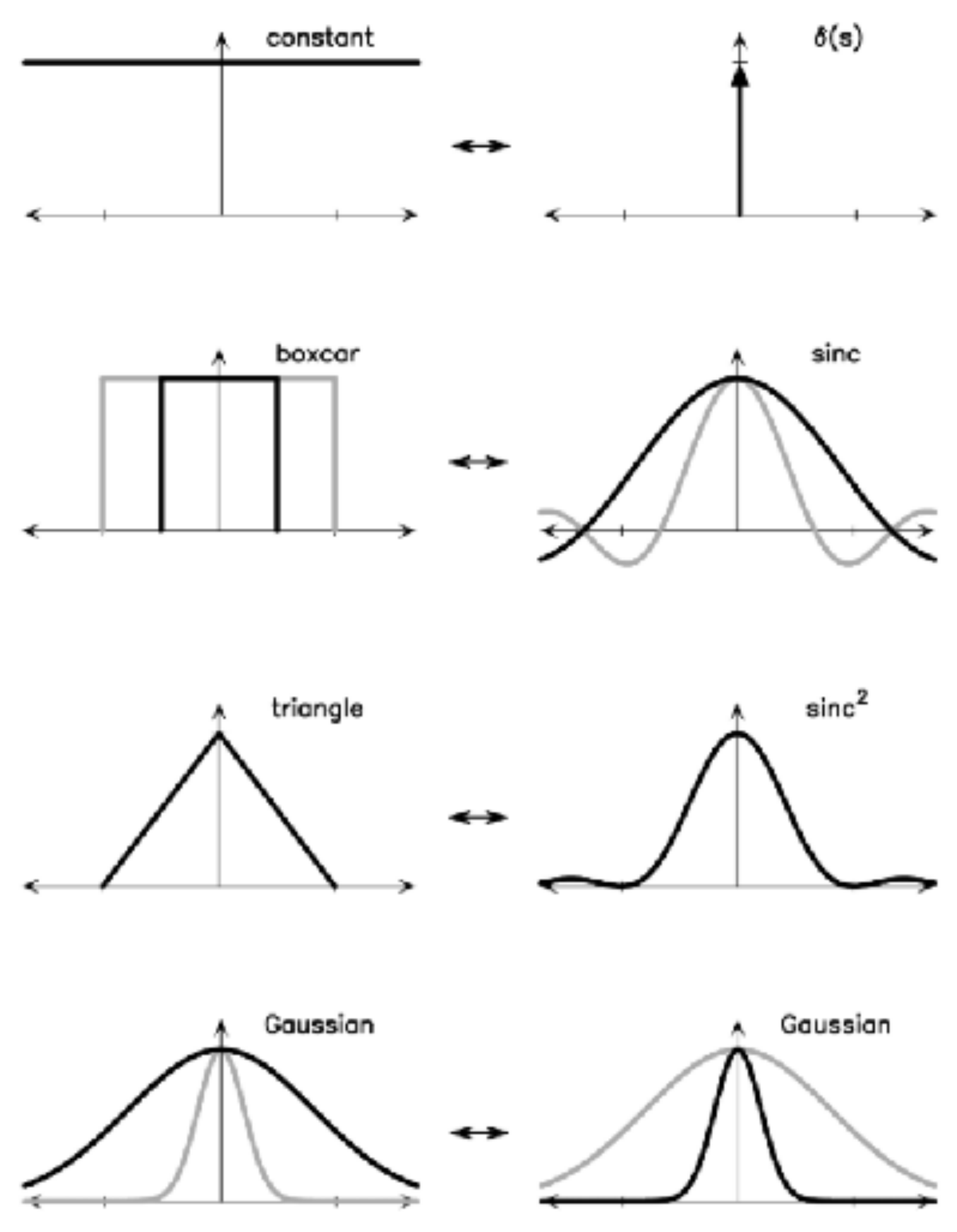

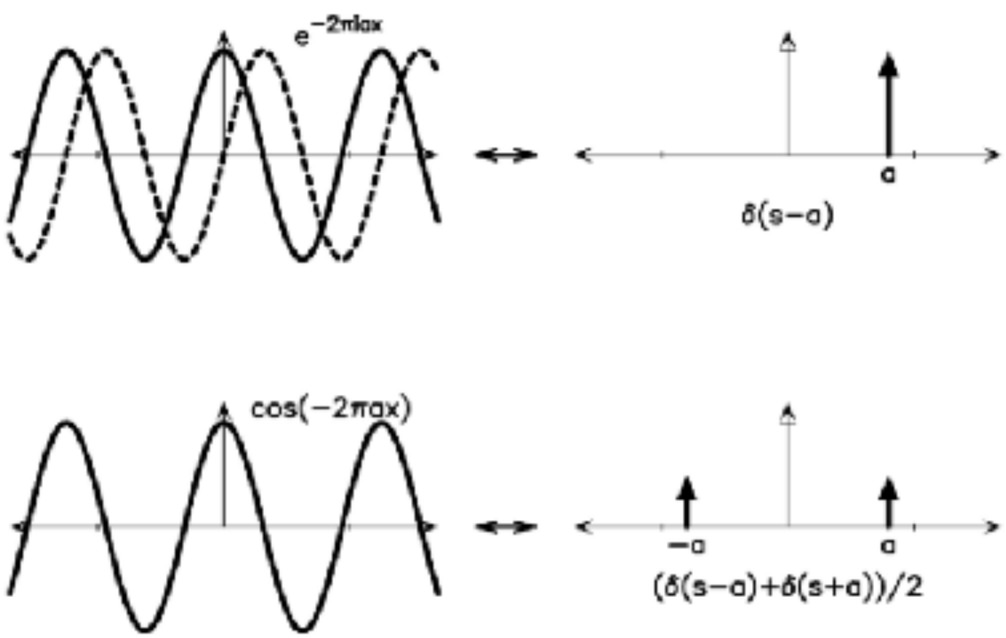

Fourier transform

$$\boxed{F(s) \equiv \int_{-\infty}^{\infty} f(x) \quad e^{-2\pi i s x} \, dx,}$$

$$\boxed{f(x) \equiv \int_{-\infty}^{\infty} F(s) \quad e^{2\pi i s x} \, ds,}$$

$$\boxed{f(x) + g(x) \Leftrightarrow F(s) + G(s).}$$

$$\boxed{af(x) \Leftrightarrow aF(s).}$$

$$\boxed{f(x-a) \Leftrightarrow e^{-2\pi i a s} F(s).}$$

$$\boxed{f(ax) \Leftrightarrow \frac{F(s/a)}{|a|}.}$$

$$\boxed{f(x)\cos(2\pi \nu x) \Leftrightarrow \frac{1}{2}F(s-\nu) + \frac{1}{2}F(s+\nu).}$$

$$\boxed{\frac{df}{dx} \Leftrightarrow i2\pi s F(s).}$$

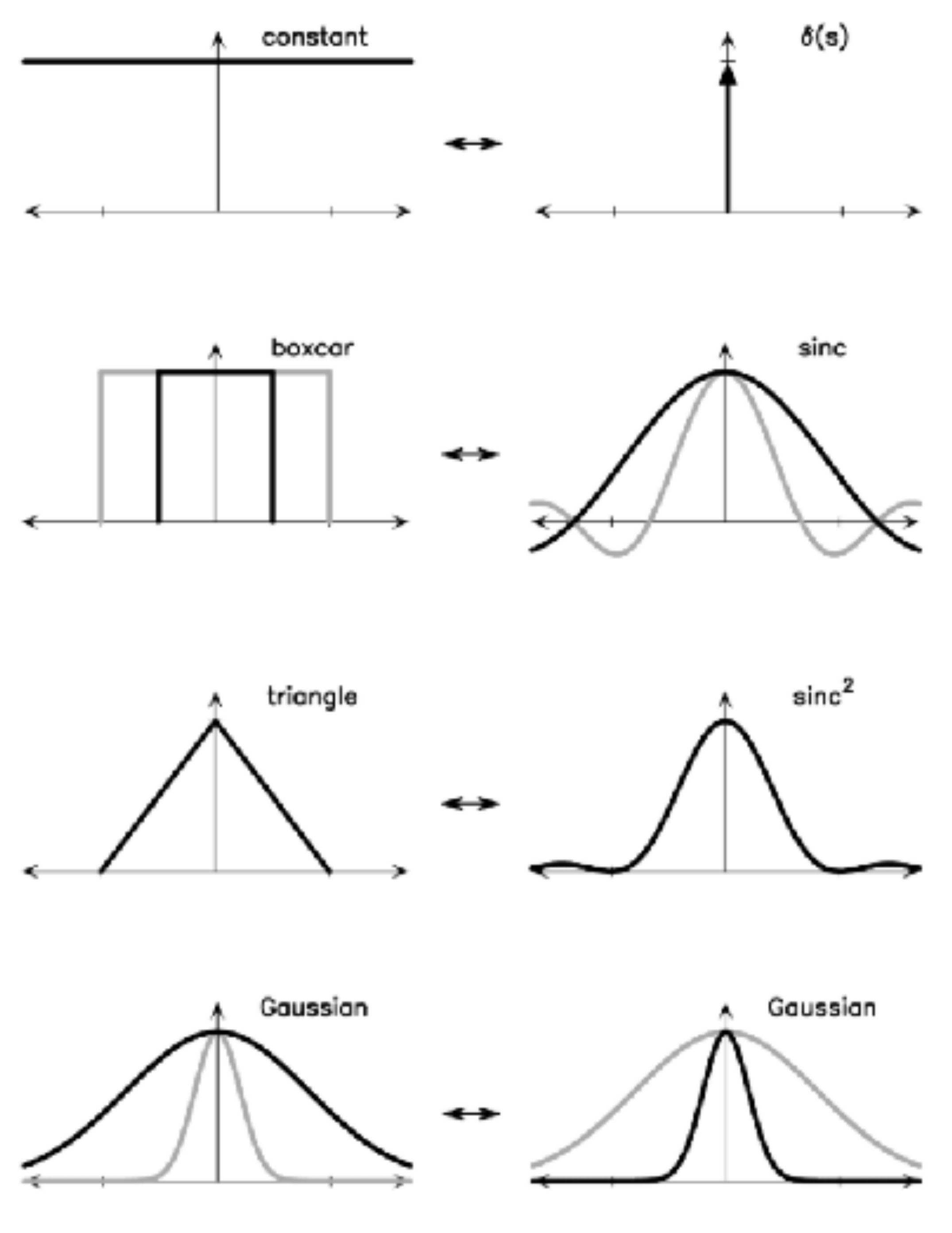

Convolution & Cross-correlation

- Convolution

$$h(x) = f * g \equiv \int_{-\infty}^{\infty} f(u)\, g(x-u)\ du.$$

$$\boxed{f * g \Leftrightarrow F \cdot G.}$$ Convolution theorem

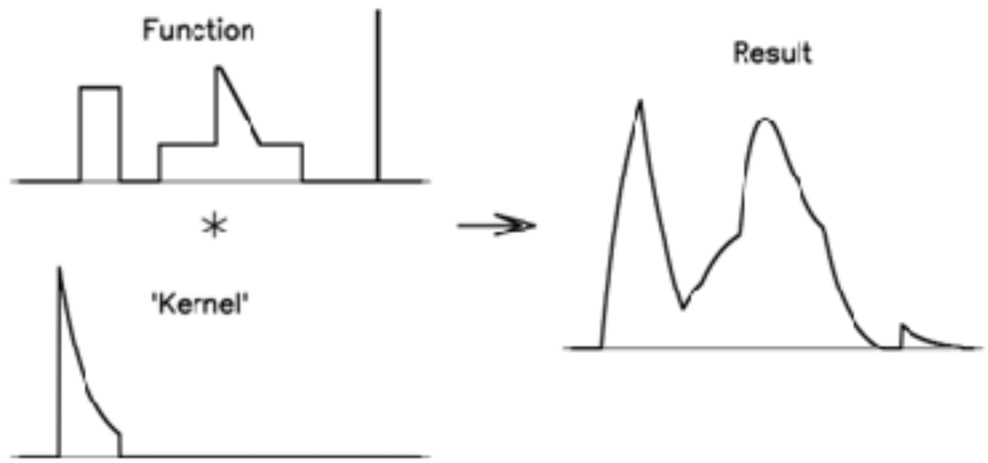

- Cross-correlation

$$f \star g \equiv \int_{-\infty}^{\infty} f(u)\, g(u-x)\ du.$$

$$\boxed{f \star g \Leftrightarrow \overline{F} \cdot G.}$$ Cross-correlation theorem

Auto-correlation

$$\boxed{f \star f \Leftrightarrow \overline{F} \cdot F = |F|^2.}$$

Wiener-Khinchin theorem

FOV & θ_s of interferometers

- Optical telescopes:
  detectors with millions pixels

- Radio single dish antennas:
  one or a small number of receivers
  (e.g., TRAO SEQUOIA with 16 pixels)

- Interferometers:
  e.g., ALMA 12 m antennas over 12 km in Band 6 (~1.2 mm)
  FOV ~ λ/D ~ 20”
  θ_s ~ λ/(longest baseline) ~ 0.02”
  ==> 10^6 “pixels”

Quasi-monochromatic 2-element interferometer

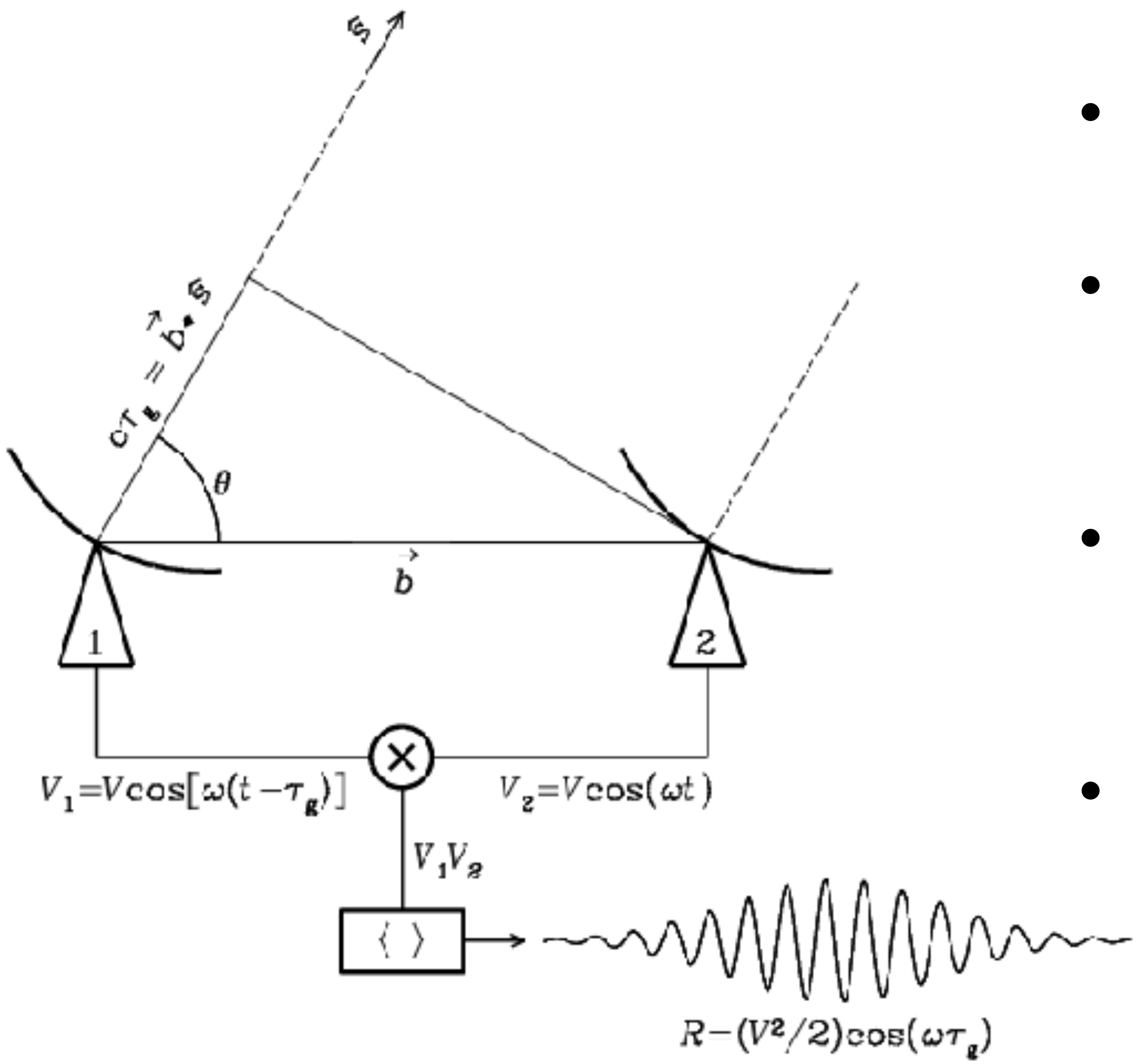

- "General" case!
- Quasi-monochromatic condition: $\Delta\nu \ll 1/\tau_g$
- **Correlator**: multiply and time-average
- **Geometric delay**: $\tau_g = \dfrac{\vec{b} \cdot \hat{s}}{c}$

Output of correlator

$$V_1 = V\cos[\omega(t-\tau_g)] \quad \text{and} \quad V_2 = V\cos(\omega t).$$

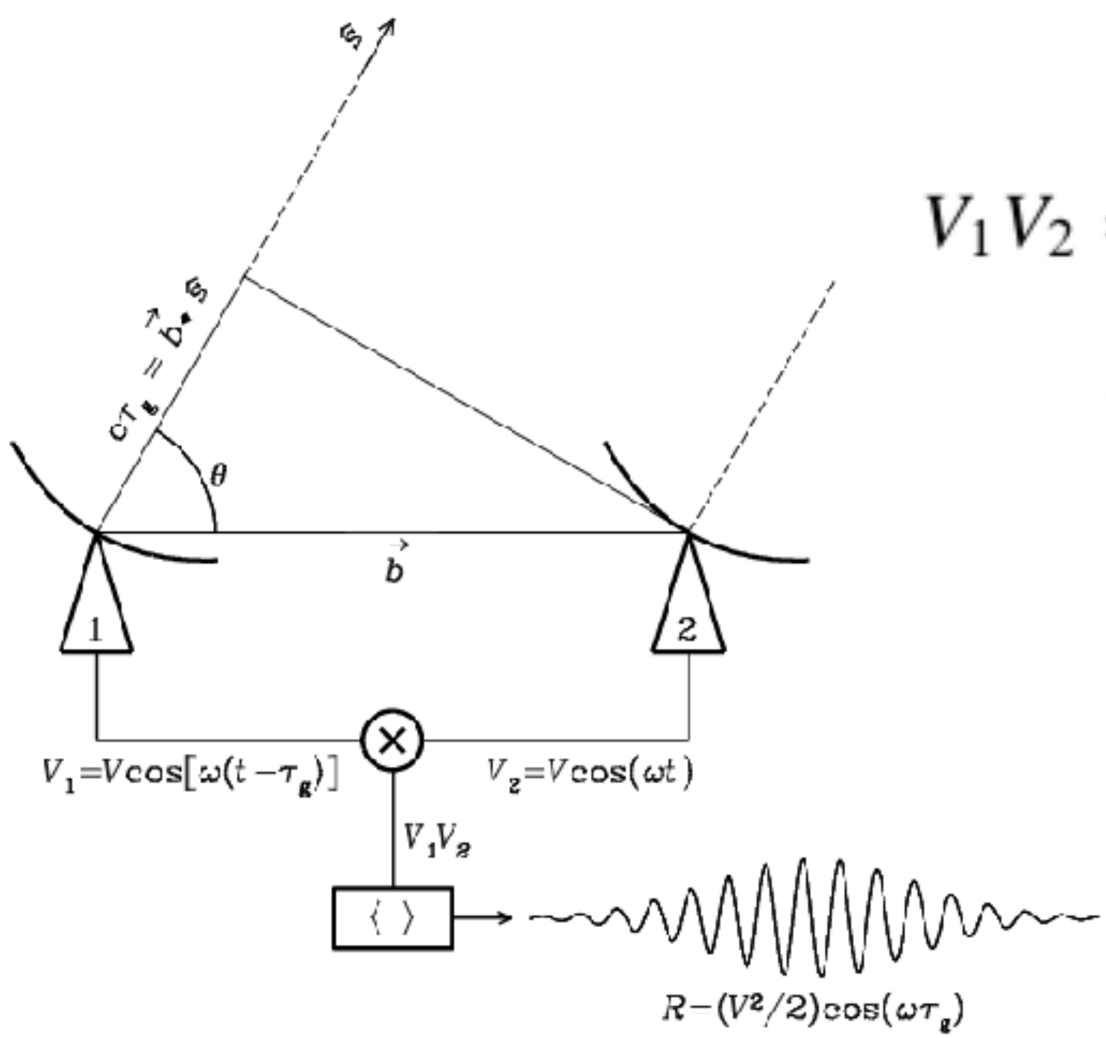

$$V_1V_2 = V^2\cos[\omega(t-\tau_g)]\cos(\omega t)$$
$$= \left(\frac{V^2}{2}\right)[\cos(2\omega t - \omega\tau_g) + \cos(\omega\tau_g)]$$

$\boxed{\cos x \cos y = [\cos(x+y) + \cos(x-y)]/2}$

$\boxed{\Delta t \gg (2\omega)^{-1}}$

$$\boxed{R = \langle V_1 V_2\rangle = \left(\frac{V^2}{2}\right)\cos(\omega\tau_g).}$$

Fringes

- Fringes: sinusoidal correlator output
- Fringe phase

$$\phi = \omega \tau_{\mathrm{g}} = \frac{\omega}{c} b \cos\theta$$

$$\left| \frac{d\phi}{d\theta} \right| = \frac{\omega}{c} b \sin\theta$$

$$= 2\pi \left(\frac{b \sin\theta}{\lambda} \right)$$

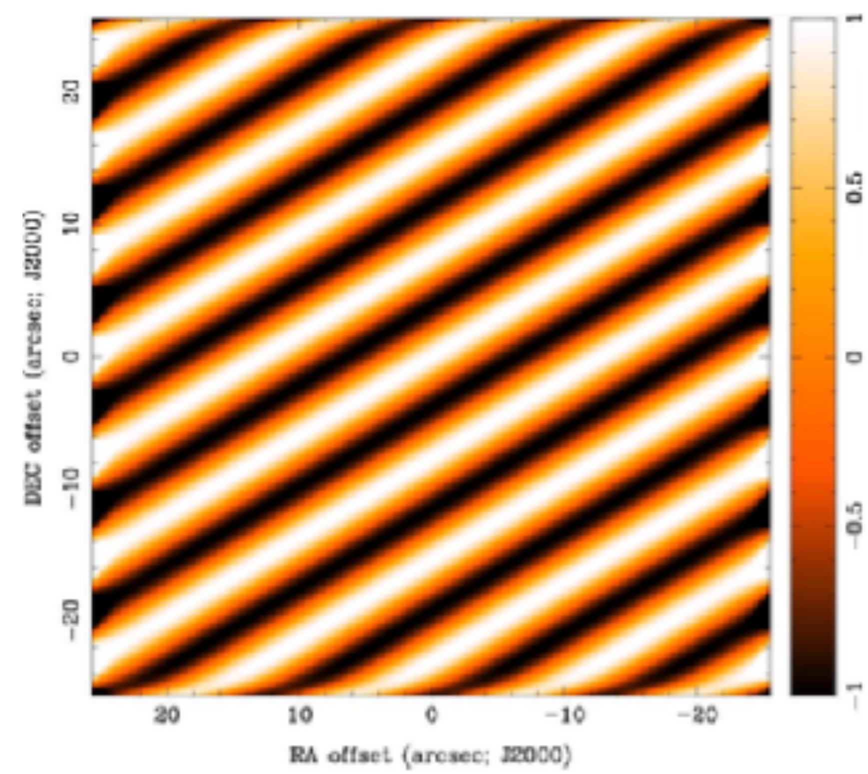

The **fringe period** $\Delta\phi = 2\pi$ corresponds to an angular shift $\Delta\theta = \lambda / (b \sin\theta)$.

Depending on projected baselines

Good image?

Sensitive Scales of Fringes

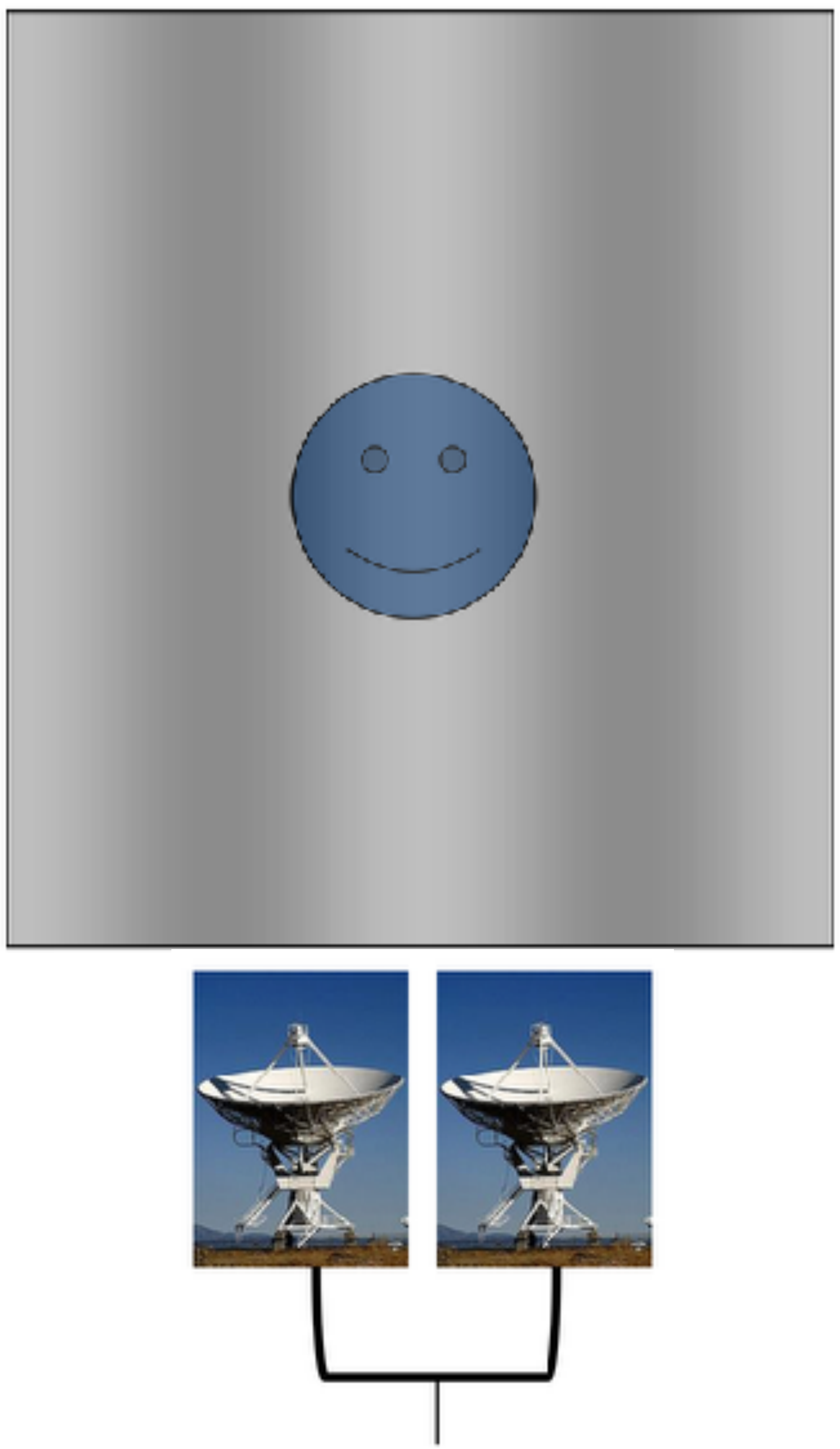

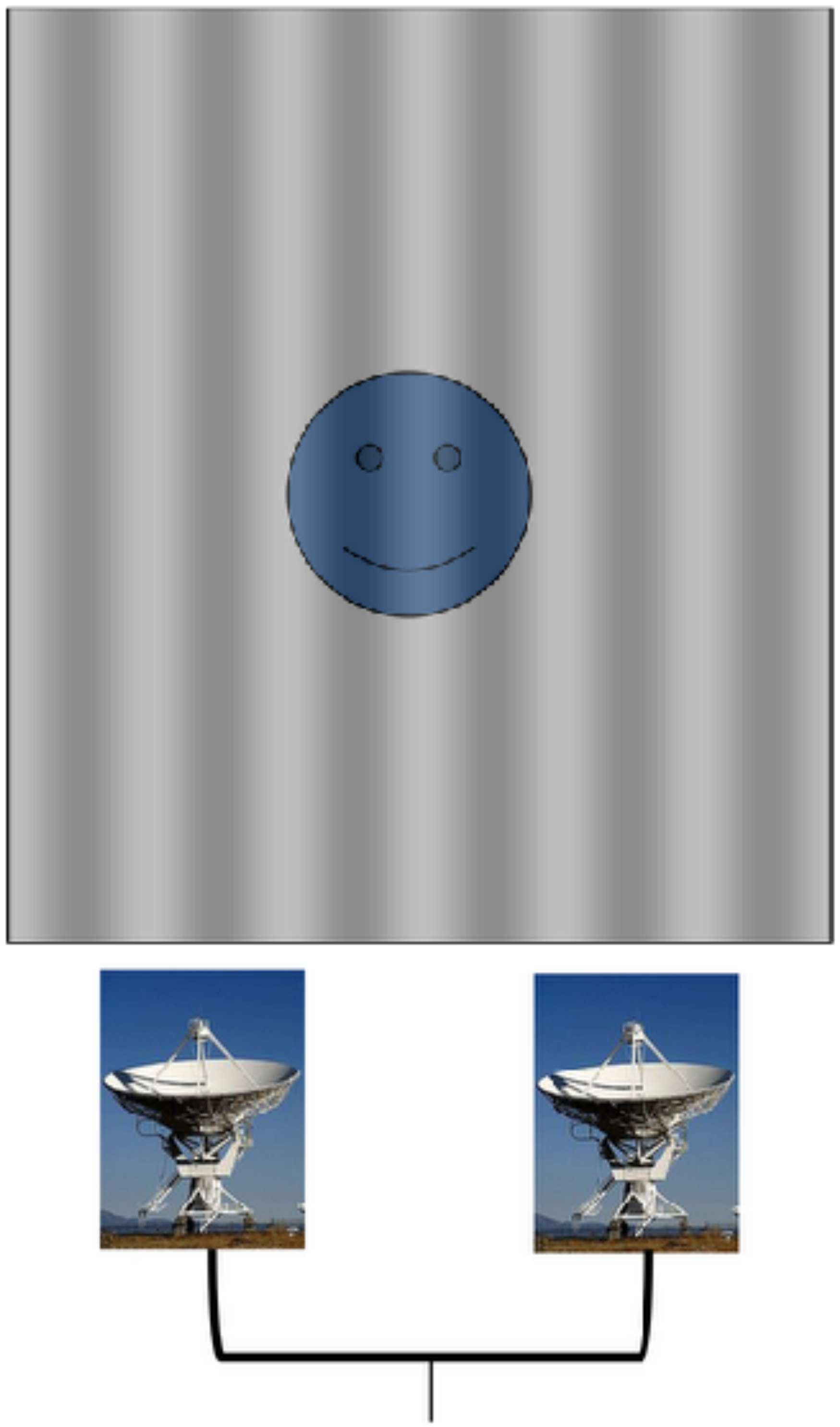

More antennas better image

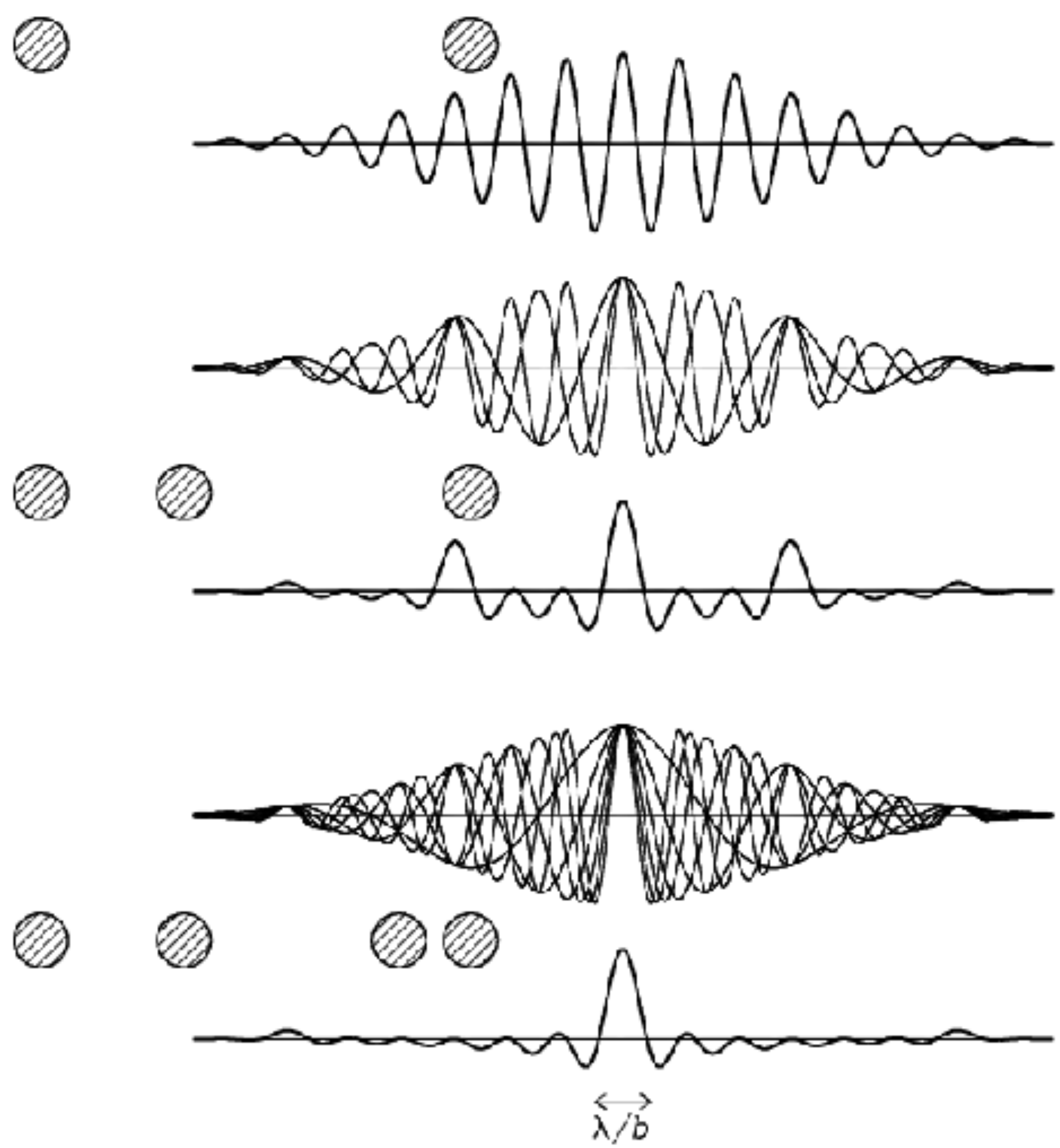

Complex correlator

- Slightly extended sources ($I = I_E + I_O$)
  - "cosine" correlator sensitive to even (inversion symmetric) structure
  - "sine" correlator sensitive to odd (anti-symmetric) structure

$$R_c = \int I(\hat{s}) \cos(2\pi\nu\vec{b}\cdot\hat{s}/c)d\Omega = \int I(\hat{s}) \cos(2\pi\vec{b}\cdot\hat{s}/\lambda)d\Omega$$

$$R_s = \int I(\hat{s}) \sin(2\pi\vec{b}\cdot\hat{s}/\lambda)d\Omega$$

- Complex correlator: combination of cosine and sine correlators
  cf. Euler's formula $\boxed{e^{i\phi} = \cos\phi + i\sin\phi}$

- **Complex visibility**

$$\mathscr{V} \equiv R_c - iR_s \qquad \mathscr{V} = Ae^{-i\phi}$$

$$A = (R_c^2 + R_s^2)^{1/2}$$

$$\phi = \tan^{-1}(R_s/R_c)$$

$$\boxed{\mathscr{V} = \int I(\hat{s}) \exp(-i2\pi\vec{b}\cdot\hat{s}/\lambda)\ d\Omega}$$

Bandwidth smearing

- Quasi-monochromatic interferometers
  => interferometers with finite bandwidths and integration times

$$\mathscr{V} = \int \left[\int_{\nu_c-\Delta\nu/2}^{\nu_c+\Delta\nu/2} I_\nu(\hat{s}) \exp(-i2\pi\vec{b}\cdot\hat{s}/\lambda)\ d\nu \right] d\Omega$$

$$= \int \left[\int_{\nu_c-\Delta\nu/2}^{\nu_c+\Delta\nu/2} I_\nu(\hat{s}) \exp(-i2\pi\nu\tau_g)\ d\nu \right] d\Omega.$$

$$\mathscr{V} \approx \int I_\nu(\hat{s})\ \mathrm{sinc}\ (\Delta\nu\,\tau_g)\ \exp(-i2\pi\nu_c\tau_g)d\Omega.$$

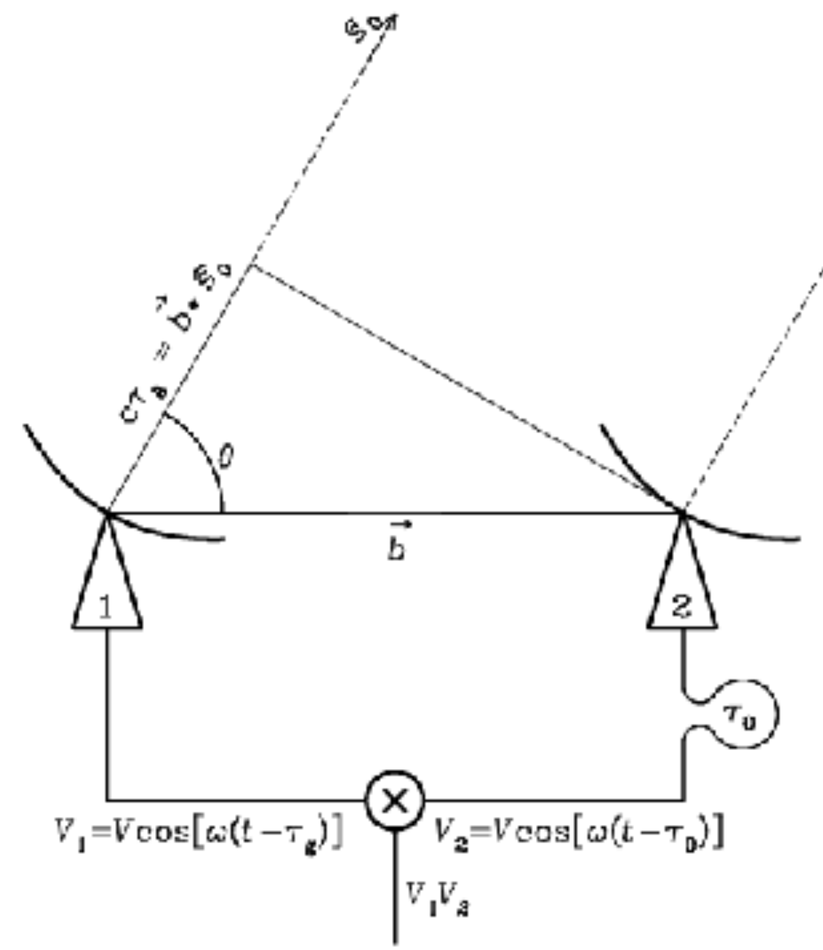

- Instrumental delay τ_0
  to minimize the attenuation

$|\tau_0 - \tau_g| \ll (\Delta$

$c\tau_g = \vec{b}\cdot\vec{s} = b\,c$

$$\Delta\nu \ll \frac{\nu\theta_s}{\Delta\theta} = \frac{1.5\times10^9\ \mathrm{Hz}\cdot 4\ \ \mathrm{arcsec}}{900\ \ \mathrm{arcsec}} \approx 7\ \ \mathrm{MHz}.$$

$$\boxed{\Delta\nu \ll \nu\frac{\theta_s}{\Delta\theta}}$$

Integration time smearing

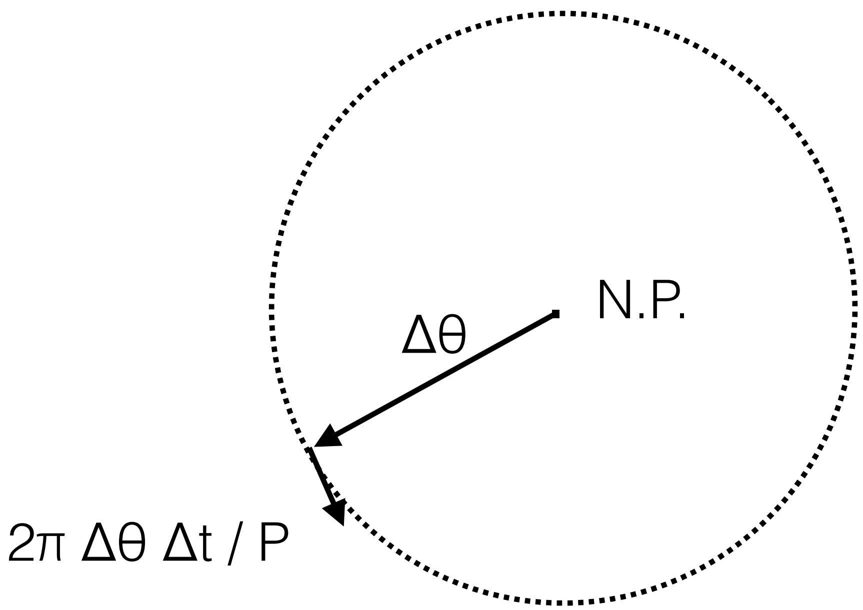

$$\boxed{P \approx 23^{\mathrm{h}}56^{\mathrm{m}}04^{\mathrm{s}} \approx 86164}$$

$$\frac{2\pi \Delta\theta \Delta t}{P} \ll \theta_s$$

$$\boxed{\Delta t \ll \frac{\theta_s}{\Delta\theta} \cdot 1.37 \times 10^4 \ \mathrm{s}}$$

$$\boxed{\Delta t \ll \frac{\theta_s}{\Delta\theta} \cdot 1.37 \times 10^4 \ \mathrm{s} = \frac{4 \ \mathrm{arcsec}}{900 \ \mathrm{arcsec}} \cdot 1.37 \times 10^4 \ \mathrm{s} \approx 60 \ \mathrm{s}.}$$

Visibility

- Now, assuming an interferometer with a negligible bandwidth attenuation
- Visibility: data of interferometers
  (Fourier transform of an image)

Steering antenna with an instrumental delay

$$\tau = \tau_g - \tau_i$$

Phase center s_0

$$\hat{s} = \hat{s}_0 + \hat{\sigma}$$

$$\mathscr{V} \approx \int I_\nu(\hat{s})\, \mathrm{sinc}\,(\Delta\nu\, \tau_g)\, \exp(-i2\pi\nu_c\tau_g) d\Omega.$$

$$V \approx \int A(\hat{s}) I_\nu(\hat{s}) \exp(-i2\pi\nu\tau) d\Omega$$

$$= \int A(\hat{s}) I_\nu(\hat{s}) \exp[-i2\pi\nu\left(\frac{\vec{b}\cdot\hat{s}}{c} - \tau_i\right)] d\Omega$$

$$= \exp[-i2\pi\nu(\frac{\vec{b}\cdot\hat{s_0}}{c} - \tau_i)] \int A(\hat{s}) I_\nu(\hat{s}) \exp[-i2\pi\nu\left(\frac{\vec{b}\cdot\hat{\sigma}}{c}\right)] d\Omega$$

$$\boxed{V = \int A(\hat{s}) I_\nu(\hat{s}) \exp[-i2\pi\nu\left(\frac{\vec{b}\cdot\hat{\sigma}}{c}\right)] d\Omega}$$

Visibility

- Now, assuming an interferometer with a negligible bandwidth attenuation
- Visibility: data of interferometers
  (Fourier transform of an image)

$$\mathscr{V} \approx \int I_\nu(\hat{s})\, \mathrm{sinc}\,(\Delta\nu\, \tau_g) \exp(-i2\pi\nu_c\tau_g) d\Omega.$$

$$V \approx \int A(\hat{s}) I_\nu(\hat{s}) \exp(-i2\pi\nu\tau) d\Omega$$

$$= \int A(\hat{s}) I_\nu(\hat{s}) \exp[-i2\pi\nu\Big(\frac{\vec{b}\cdot\hat{s}}{c} - \tau_i$$

$$= \exp[-i2\pi\nu(\frac{\vec{b}\cdot\hat{s_0}}{c} - \tau_i)] \int A(\hat{s}) I_\nu($$

$$\boxed{V = \int A(\hat{s}) I_\nu(\hat{s}) \exp[-i2\pi\nu\Big(\frac{\vec{b}\cdot\hat{\sigma}}{c}\Big)] d\Omega}$$

Steering antenna with an instrumental delay

$$\tau = \tau_g - \tau_i$$

Phase center s_0

$$\hat{s} = \hat{s_0} + \hat{\sigma}$$

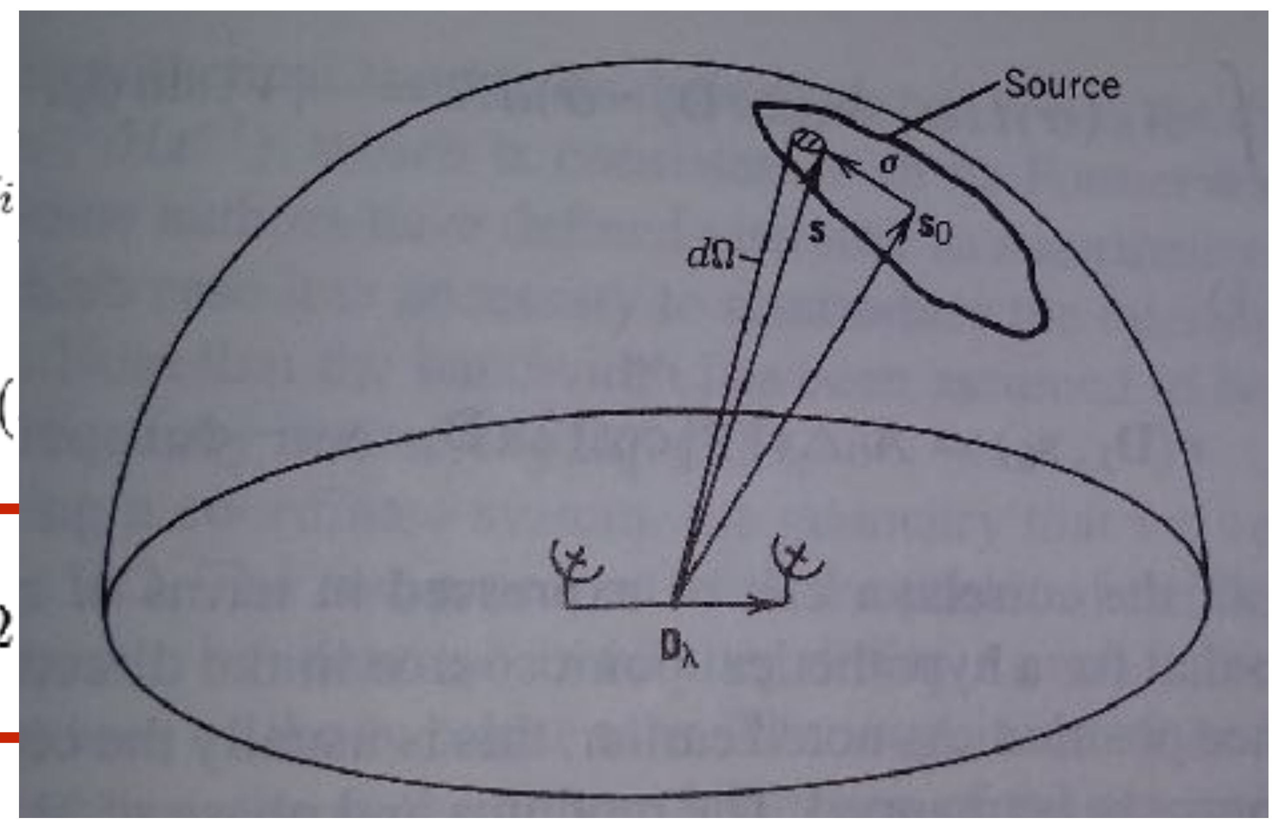

Interferometers in 3D

$$V = \int A(\hat{s}) I_\nu(\hat{s}) \exp[-i2\pi\nu\left(\frac{\vec{b}\cdot\hat{\sigma}}{c}\right)] d\Omega$$

$$\boxed{\begin{aligned} 2\pi\nu\frac{\vec{b}}{c} &= 2\pi\frac{\vec{b}}{\lambda} = 2\pi(u,v,w) \\ \hat{\sigma} &= (l,m,n) \\ d\Omega &= \frac{dl\,dm}{\sqrt{1-l^2-m^2}} \end{aligned}}$$

$$V(u,v,w) = \int\int \frac{A(l,m)I(l,m)}{\sqrt{1-l^2-m^2}} \exp[-i2\pi(ul+vm+w\sqrt{1-l^2-m^2})]\, dl\, dm$$

$$\boxed{\sqrt{1-l^2-m^2} \approx 1}$$

$$V(u,v,w) = \exp(-i2\pi w) \int\int A(l,m)I(l,m) \exp[-i2\pi(ul+vm)]\, dl\, dm$$

Interferomete

$$V = \int A(\hat{s}) I_\nu(\hat{s}) \exp[-i2\pi\nu\left(\frac{\vec{b}\cdot\hat{\sigma}}{c}\right)$$

$$2\pi\nu\frac{\vec{b}}{c} = 2\pi\frac{\vec{b}}{\lambda} = 2\pi(u, v, w)$$

$$\hat{\sigma} = (l, m, n)$$

$$d\Omega = \frac{dl\, dm}{\sqrt{1 - l^2 - m^2}}$$

$$V(u, v, w) = \int\int \frac{A(l, m) I(l, m)}{\sqrt{1 - l^2 - m^2}} \exp[-i2\pi(ul$$

$$\boxed{\sqrt{1 - l^2 - m^2} \approx 1}$$

$$V(u, v, w) = \exp(-i2\pi w) \int\int A(l, m) I(l, m)$$

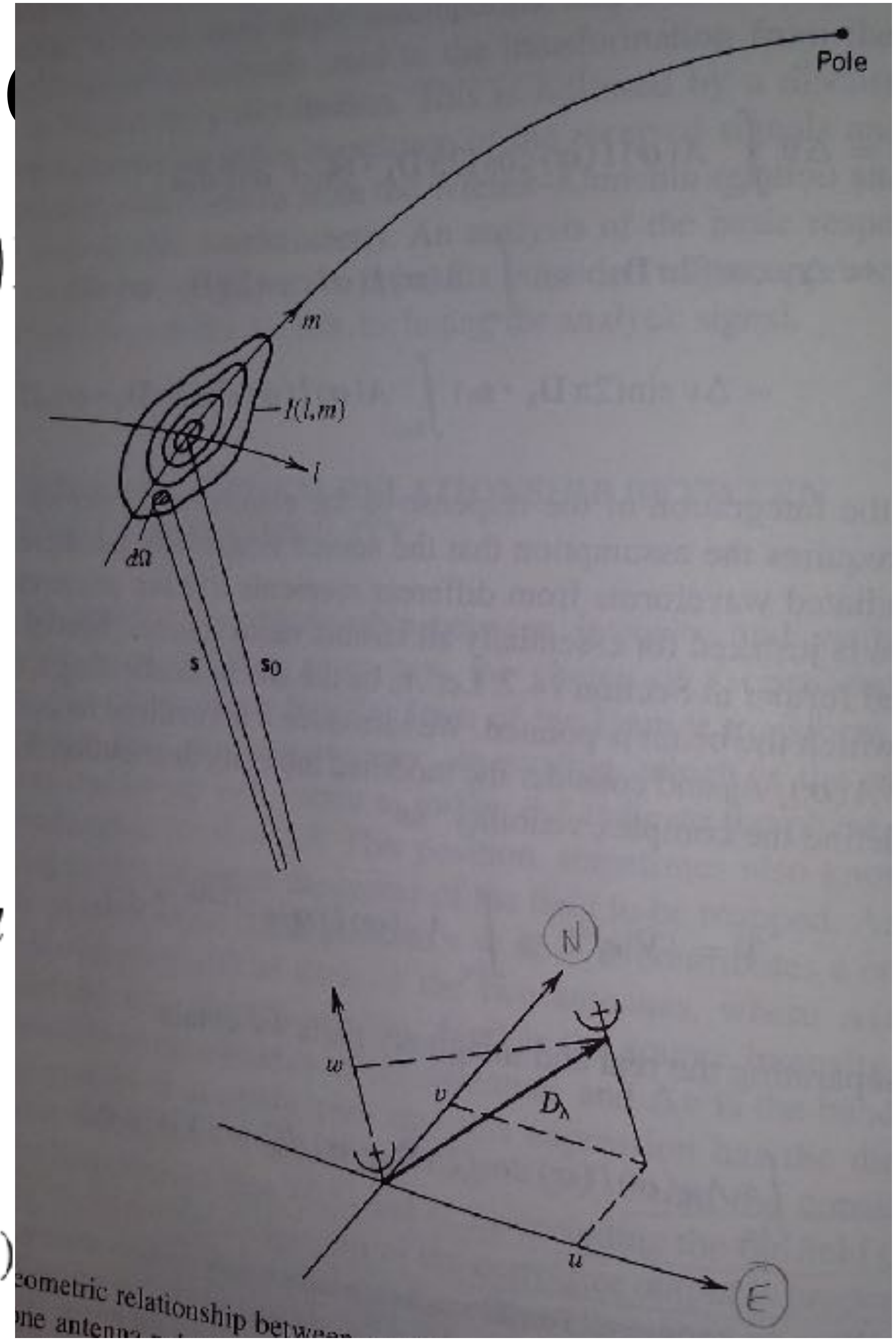

Visibility and Image

- (Inverse) Fourier transformation

On w = 0 plane:

$$V(u,v) = \int\int A(l,m)I(l,m)\exp[-i2\pi(ul+vm)]\,dl\,dm$$

$$\boxed{\begin{aligned} V(u,v) &\rightleftharpoons A(l,m)I(l,m) \\ S(u,v)V(u,v) &\rightleftharpoons FT^{-1}[S(u,v)] * FT^{-1}[V(u,v)] \\ S(u,v)V(u,v) &\rightleftharpoons B_D(l,m) * [A(l,m)I(l,m)] \end{aligned}}$$

Sensitivity

- A single antenna

$$\sigma_S = \frac{2kT_s}{A_e(\Delta\nu\,\tau)^{1/2}}$$

- A two-element interferometer

$$\sigma_S = \frac{2^{1/2}kT_s}{A_e(\Delta\nu\,\tau)^{1/2}}$$

- A N-element interferometer: N(N-1)/2 independent paris

$$\boxed{\sigma_S = \frac{2kT_s}{A_e[N(N-1)\,\Delta\nu\,\tau]^{1/2}}}$$

Interferometric observations

- Calibrators
  Flux (also called amplitude) calibrator
  Bandpass calibrator
  Phase calibrator

- A typical sequence
  Flux cal. —> Bandpass cal. —> Phase cal. and science target cycles (e.g., 10 min period) —> Last phase cal.

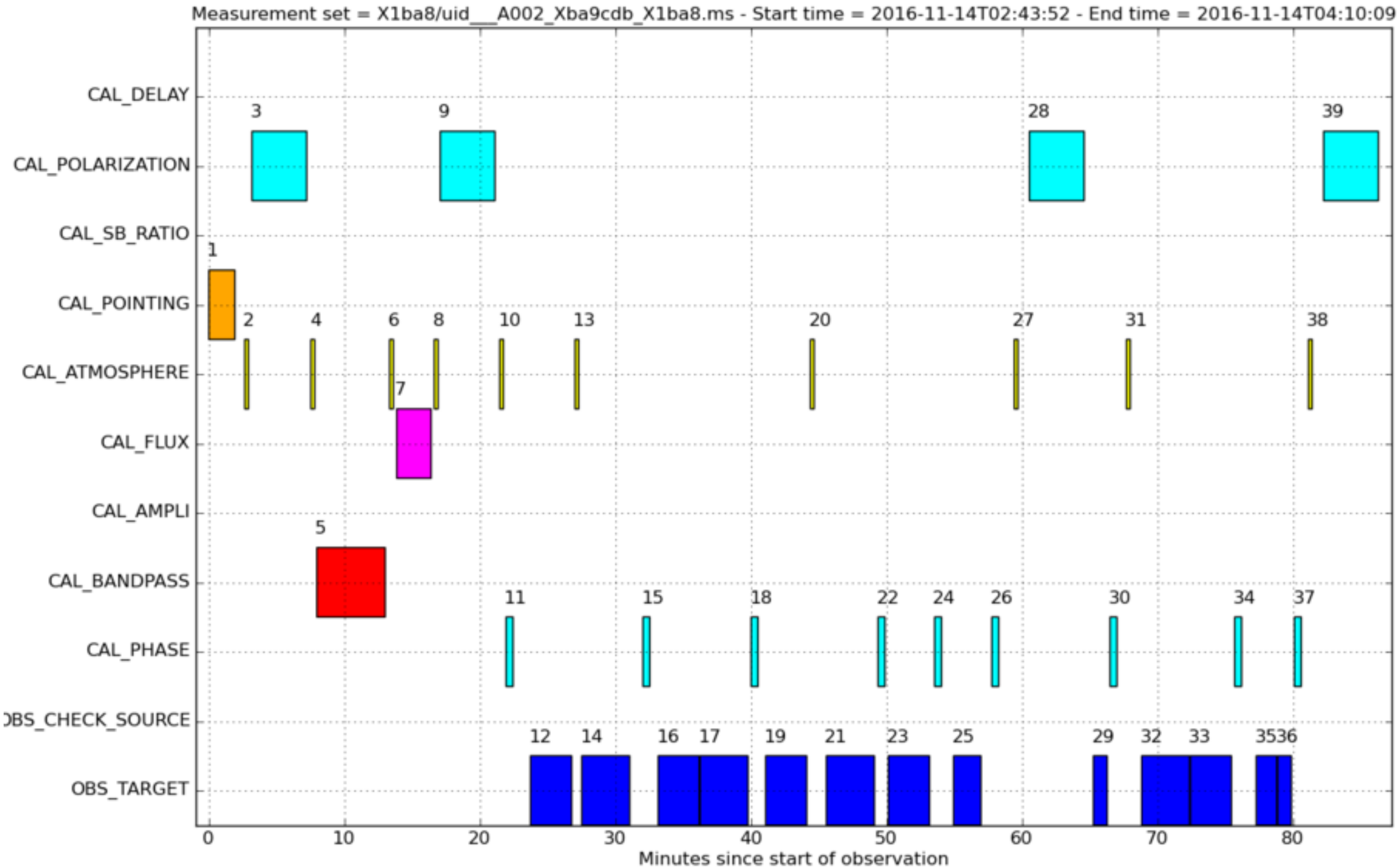

Observing Schedule

From raw data to image

- ALMA provides images ready for sciences and reduction scripts!

- Calibration: to have all antennas phased up
  - Bandpass calibration
  - Flux (amplitude) calibration
  - Phase calibration

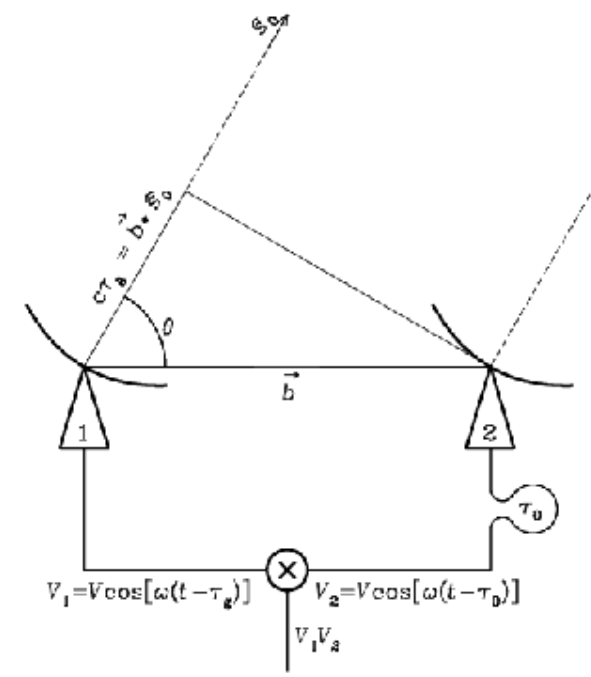

- Imaging: from calibrated visibilities to images
  - Inverse Fourier transform
  - Deconvolution
  - Primary beam correction

$$\boxed{S(u,v)V(u,v) \quad \rightleftharpoons \quad B_D(l,m) * [A(l,m)I(l,m)]}$$

Take-home messages

- Interferometry samples Fourier components of sky brightness: visibilities
- Images are made by Fourier transforming sampled visibilities
  - images are not unique
  - limited scales of detected structures due to missing visibilities

$$\boxed{S(u,v)V(u,v) \quad \rightleftharpoons \quad B_D(l,m) * [A(l,m)I(l,m)]}$$

Slides captured from

Imaging and Deconvolution

15th Synthesis Imaging Workshop

David J. Wilner (CfA)

Visibility and Sky Brightness

- *V(u,v), the complex visibility function, is the 2D Fourier transform of T(l,m), the sky brightness distribution (for incoherent source, small field of view, far field, etc.)*
  [for derivation from van Cittert-Zernike theorem, see TMS Ch. 14]

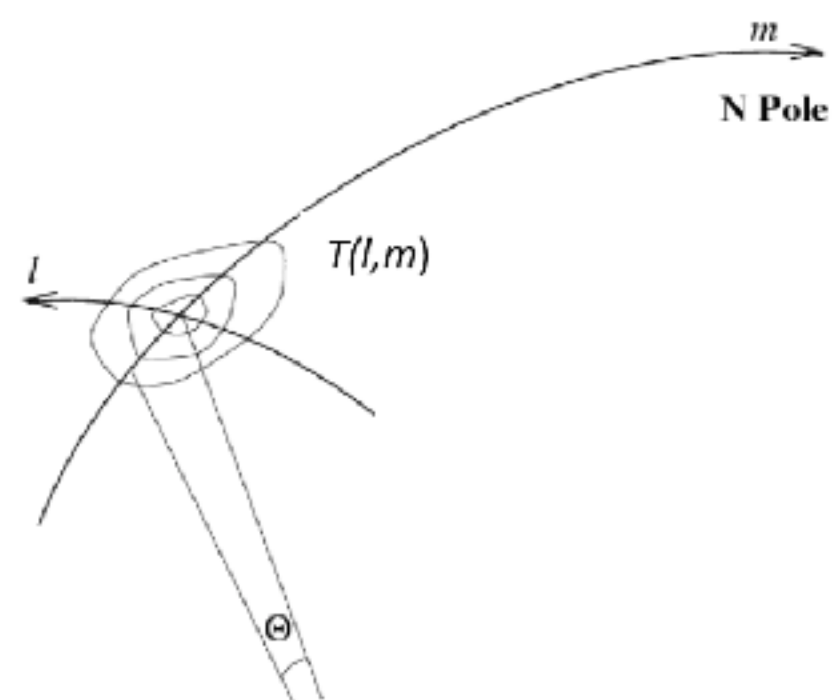

- mathematically

$$V(u,v) = \int\int T(l,m) e^{-i2\pi(ul+vm)} dl dm$$

$$T(l,m) = \int\int V(u,v) e^{i2\pi(ul+vm)} du dv$$

u,v are E-W, N-S spatial frequencies [wavelengths]

l,m are E-W, N-S angles in the tangent plane [radians]

(recall $e^{ix} = \cos x + i \sin x$)

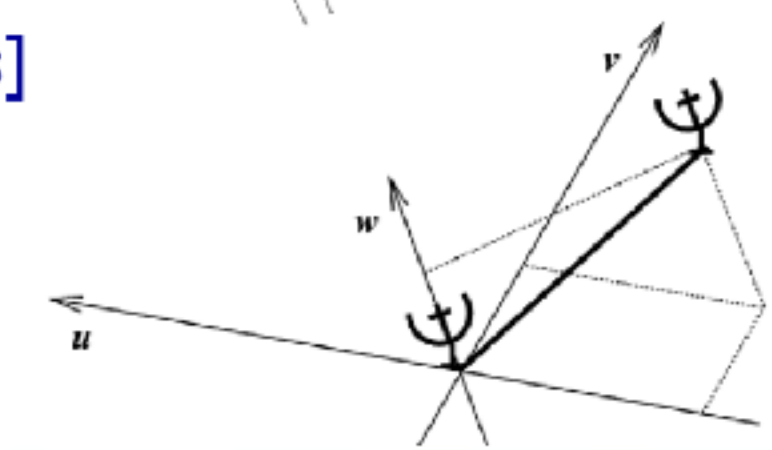

$$V(u,v) \xrightarrow{\mathcal{F}} T(l,m)$$

Visibilities

- each *V(u,v)* is a complex quantity
  - expressed as *(real, imaginary)* or *(amplitude, phase)*

T(l,m)

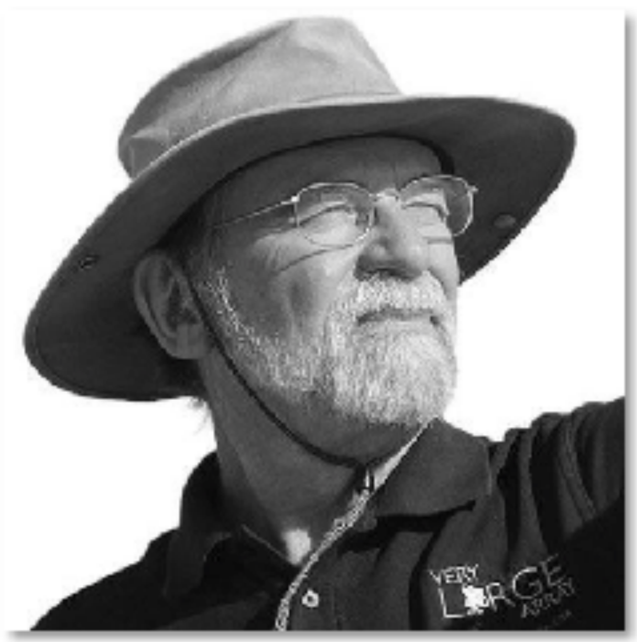

$\xrightarrow{\mathcal{F}}$

V(u,v) amplitude

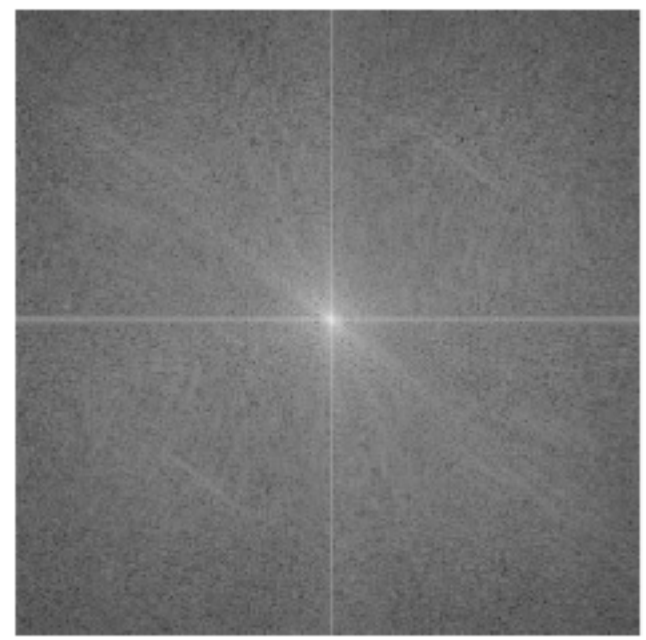

V(u,v) phase

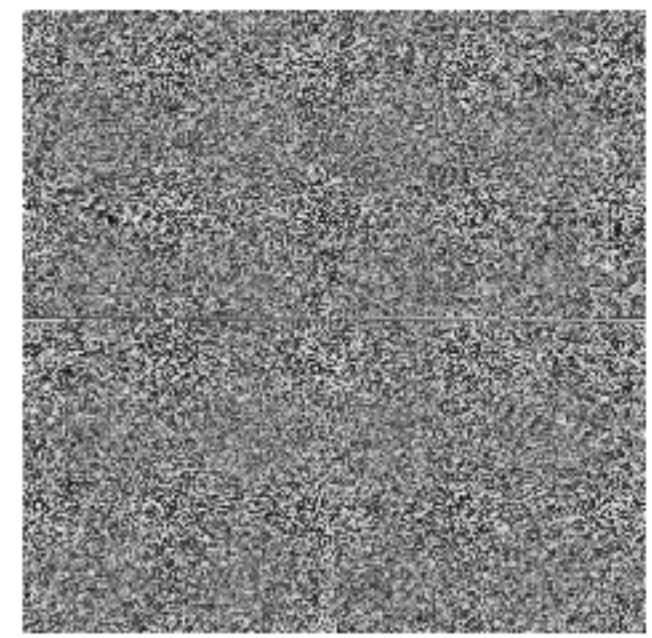

- each *V(u,v)* contains information on *T(l,m) everywhere*, not just at a given *(l,m)* coordinate or within a particular subregion

Example 2D Fourier Transforms

T(l,m) *V(u,v) amplitude*

δ function 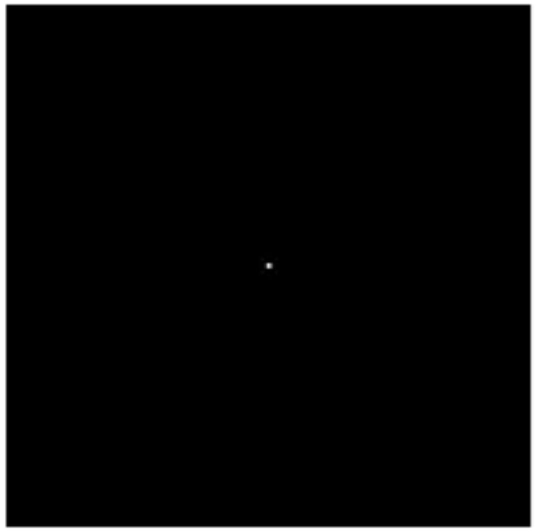 $\xrightarrow{\mathcal{F}}$ 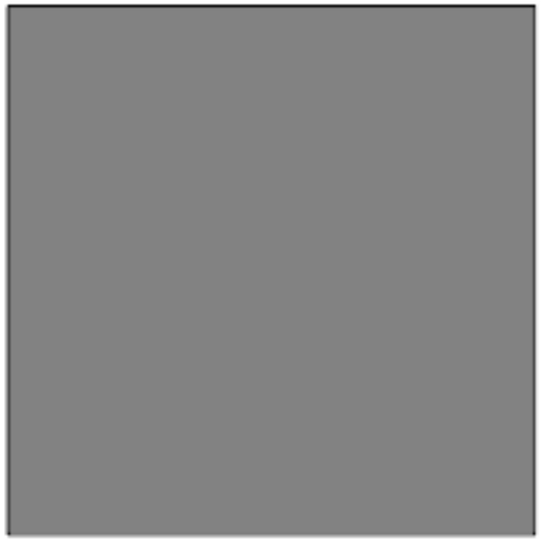 constant

elliptical Gaussian 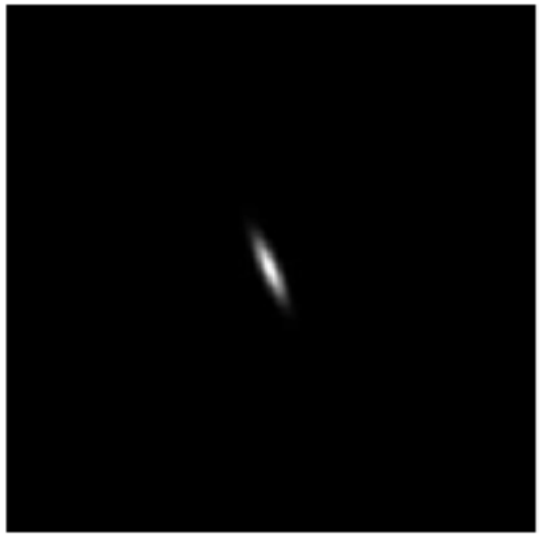 $\xrightarrow{\mathcal{F}}$  elliptical Gaussian

narrow features transform into wide features (and vice-versa)

Example 2D Fourier Transforms

T(l,m) *V(u,v) amplitude*

uniform disk

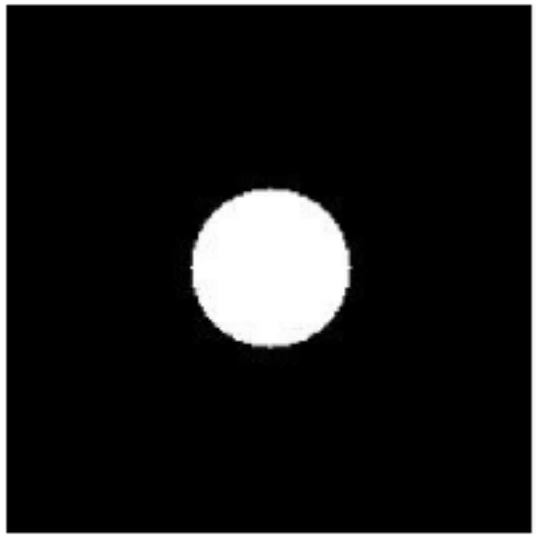

$\xrightarrow{\mathcal{F}}$

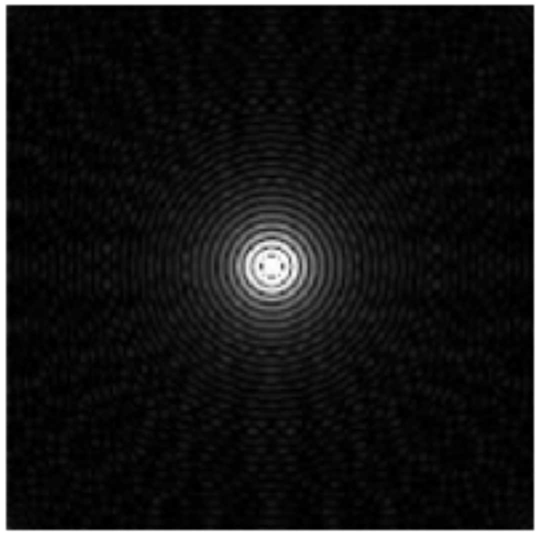

Bessel function

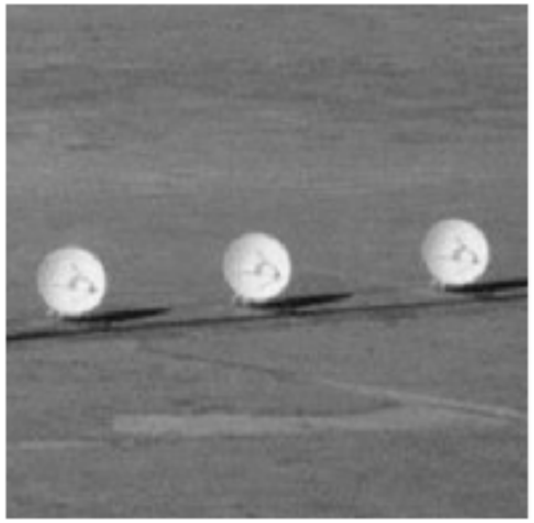

$\xrightarrow{\mathcal{F}}$

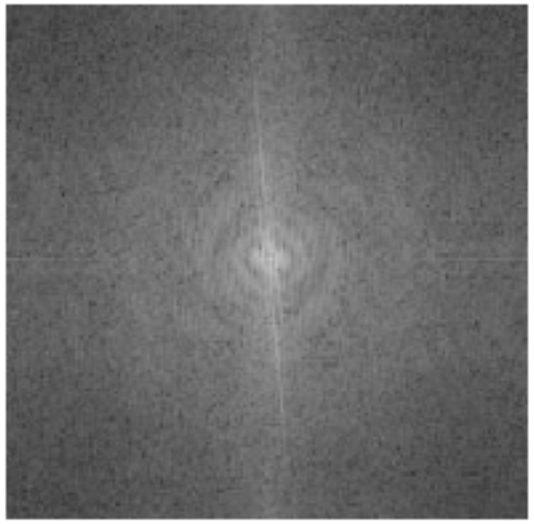

sharp edges result in many high spatial frequencies

Amplitude and Phase

- amplitude tells "how much" of a certain spatial frequency
- phase tells "where" this spatial frequency component is located

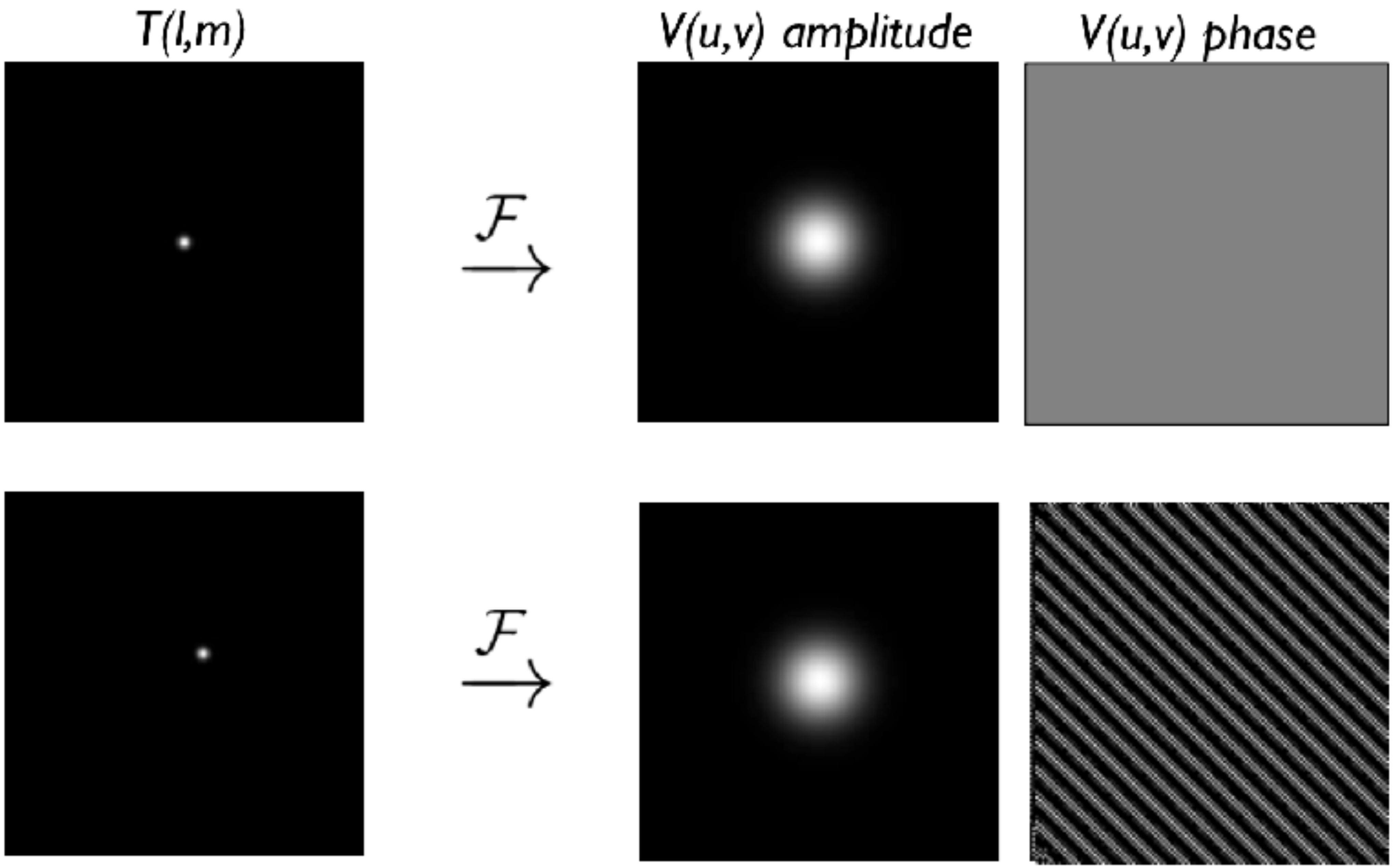

The Visibility Concept

$$V(u,v) = \int\int T(l,m) e^{-i2\pi(ul+vm)} dl dm$$

- visibility as a function of baseline coordinates *(u,v)* is the Fourier transform of the sky brightness distribution as a function of the sky coordinates *(l,m)*

- *V(u=0,v=0)* is the integral of *T(l,m)dldm* = total flux density

- since *T(l,m)* is real, $V(-u,-v) = V^*(u,v)$
  - *V(u,v)* is Hermitian
  - get two visibilities for one measurement

Small Source, Short Baseline

$$V(u,v) = \int\int T(l,m)e^{-i2\pi(ul+vm)}dldm$$

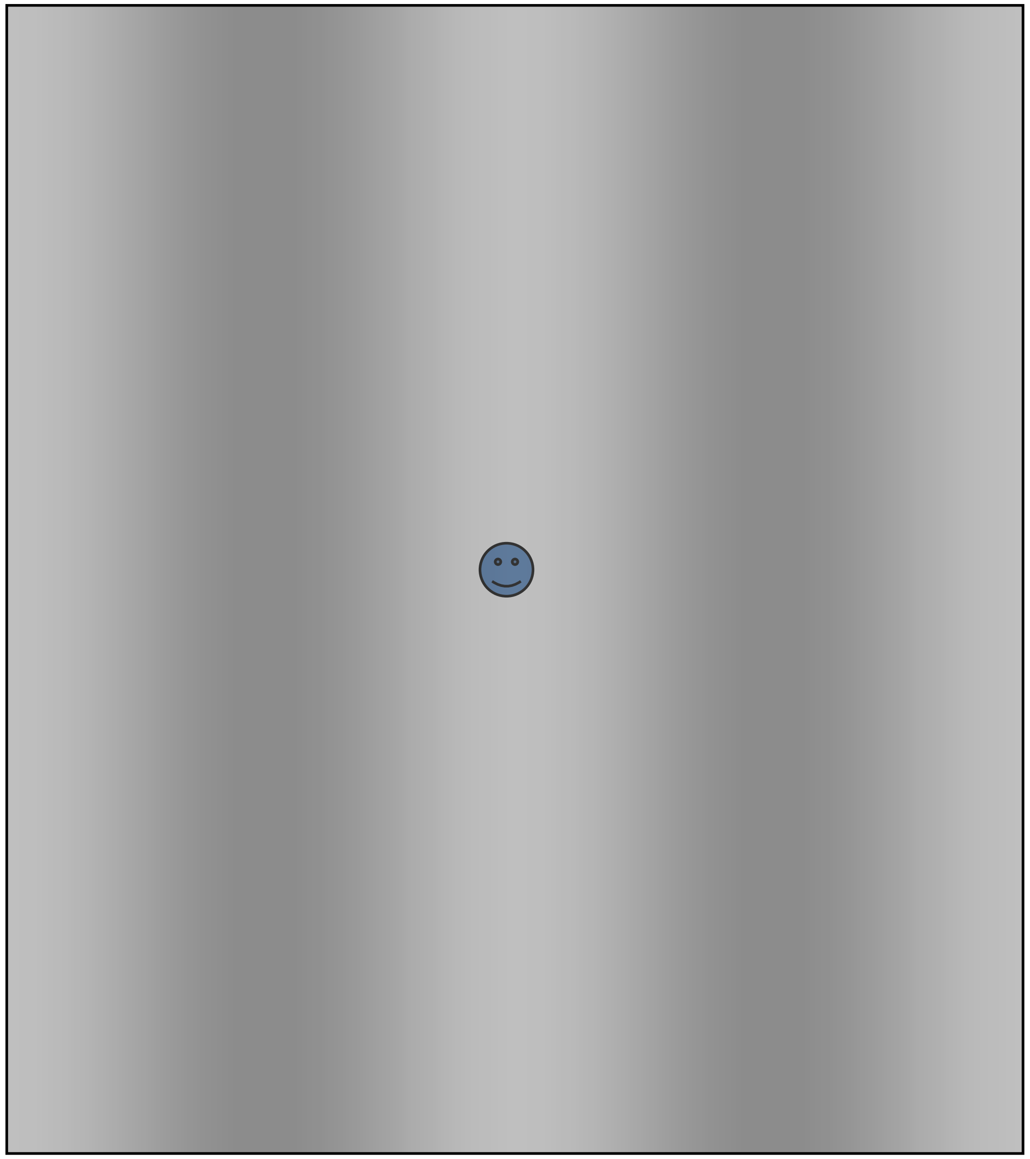

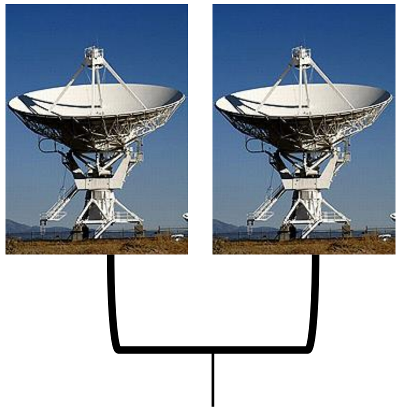

Small Source, Short Baseline

$$V(u,v) = \int\int T(l,m) e^{-i2\pi(ul+vm)} dl dm$$

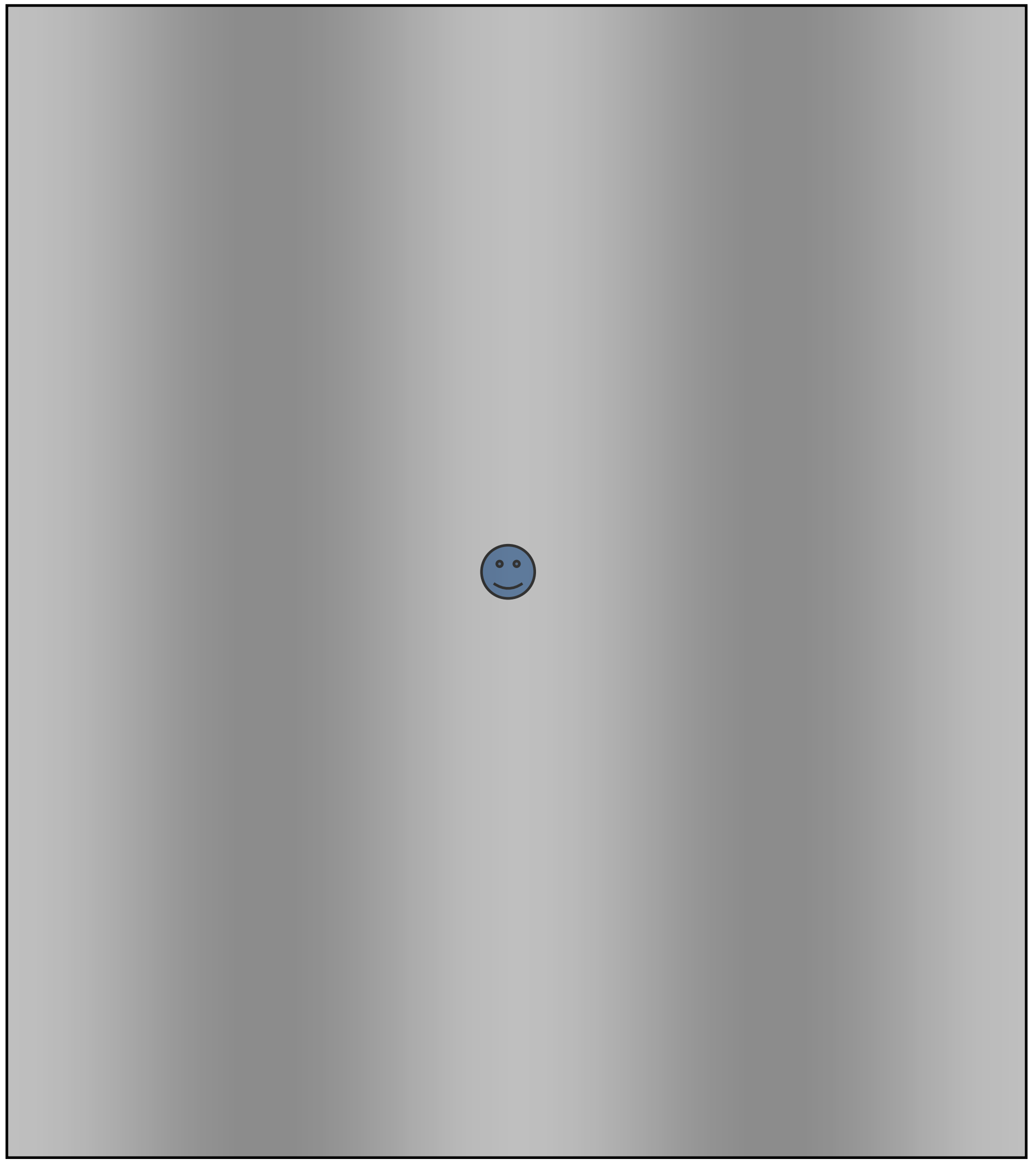

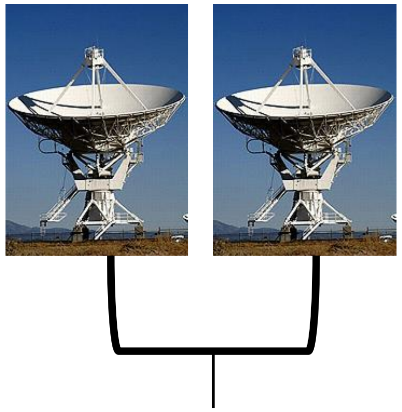

Small Source, Long Baseline

$$V(u,v) = \int\int T(l,m) e^{-i2\pi(ul+vm)} dl dm$$

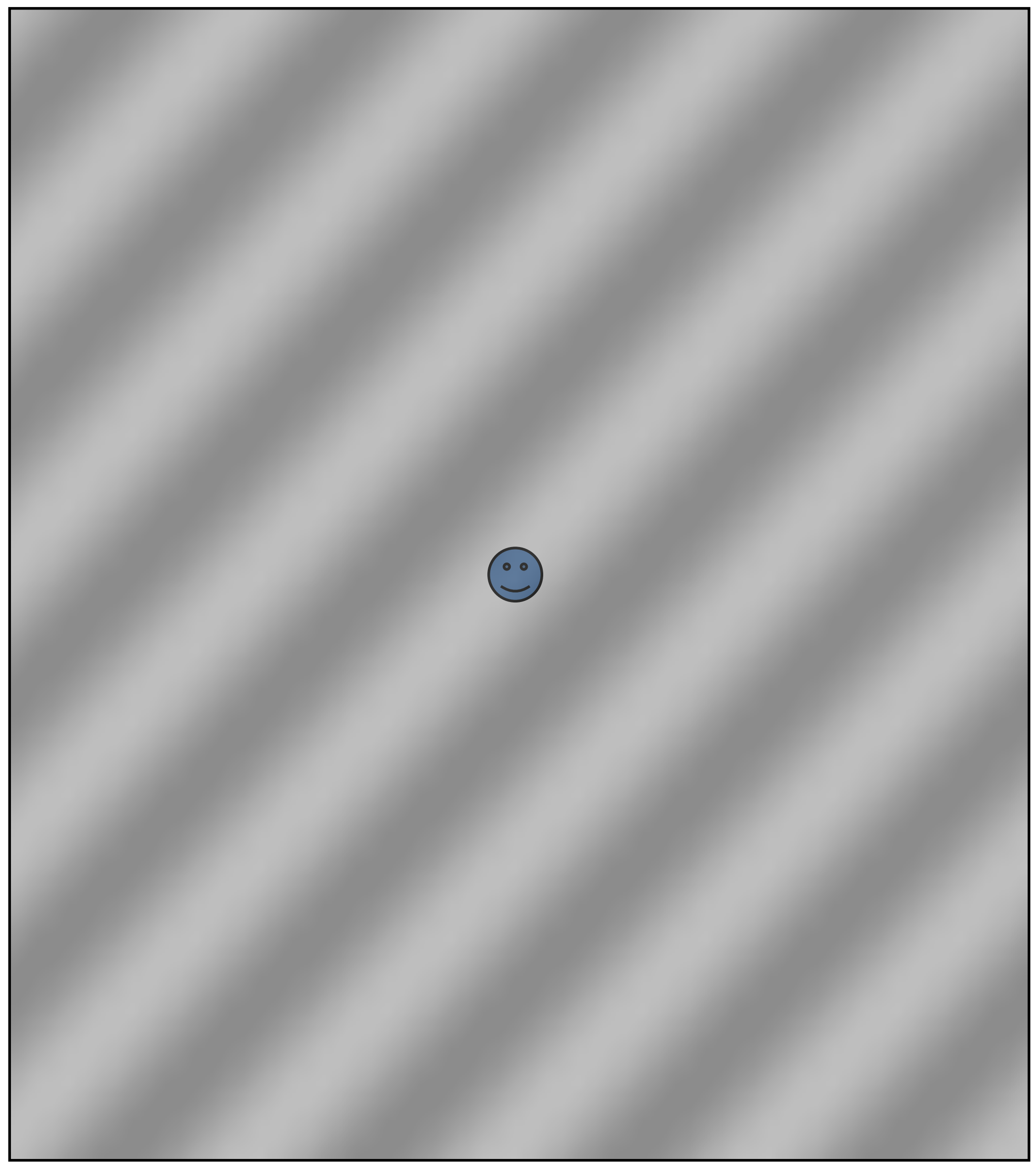

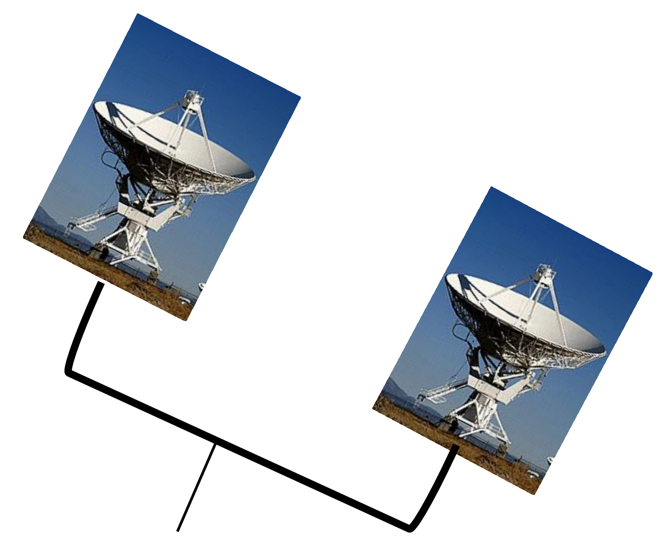

Large Source, Short Baseline

$$V(u,v) = \int\int T(l,m) e^{-i2\pi(ul+vm)} dl dm$$

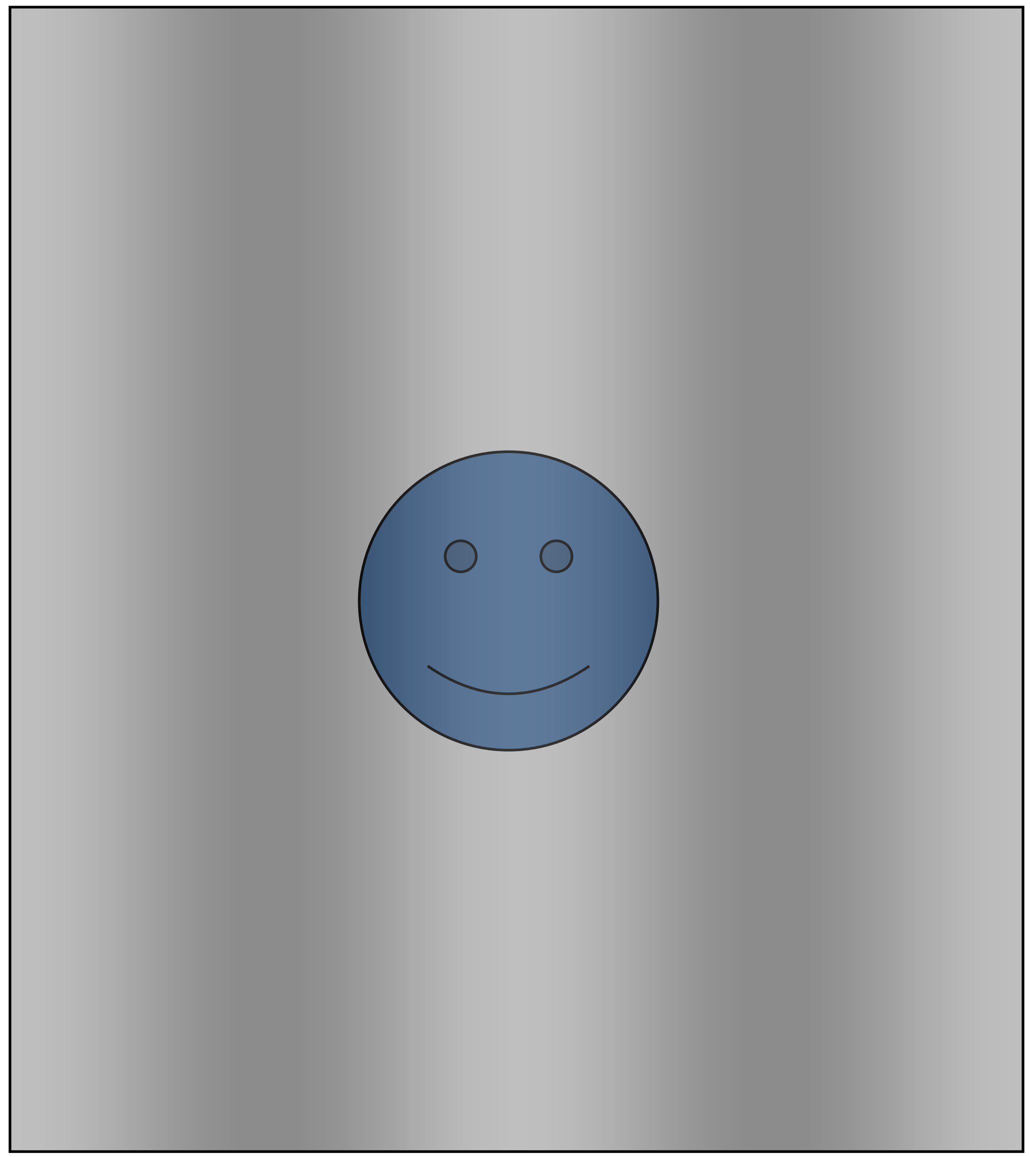

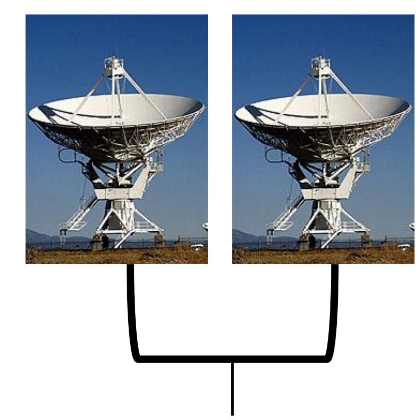

Large Source, Long Baseline

$$V(u,v) = \int\int T(l,m)e^{-i2\pi(ul+vm)}dldm$$

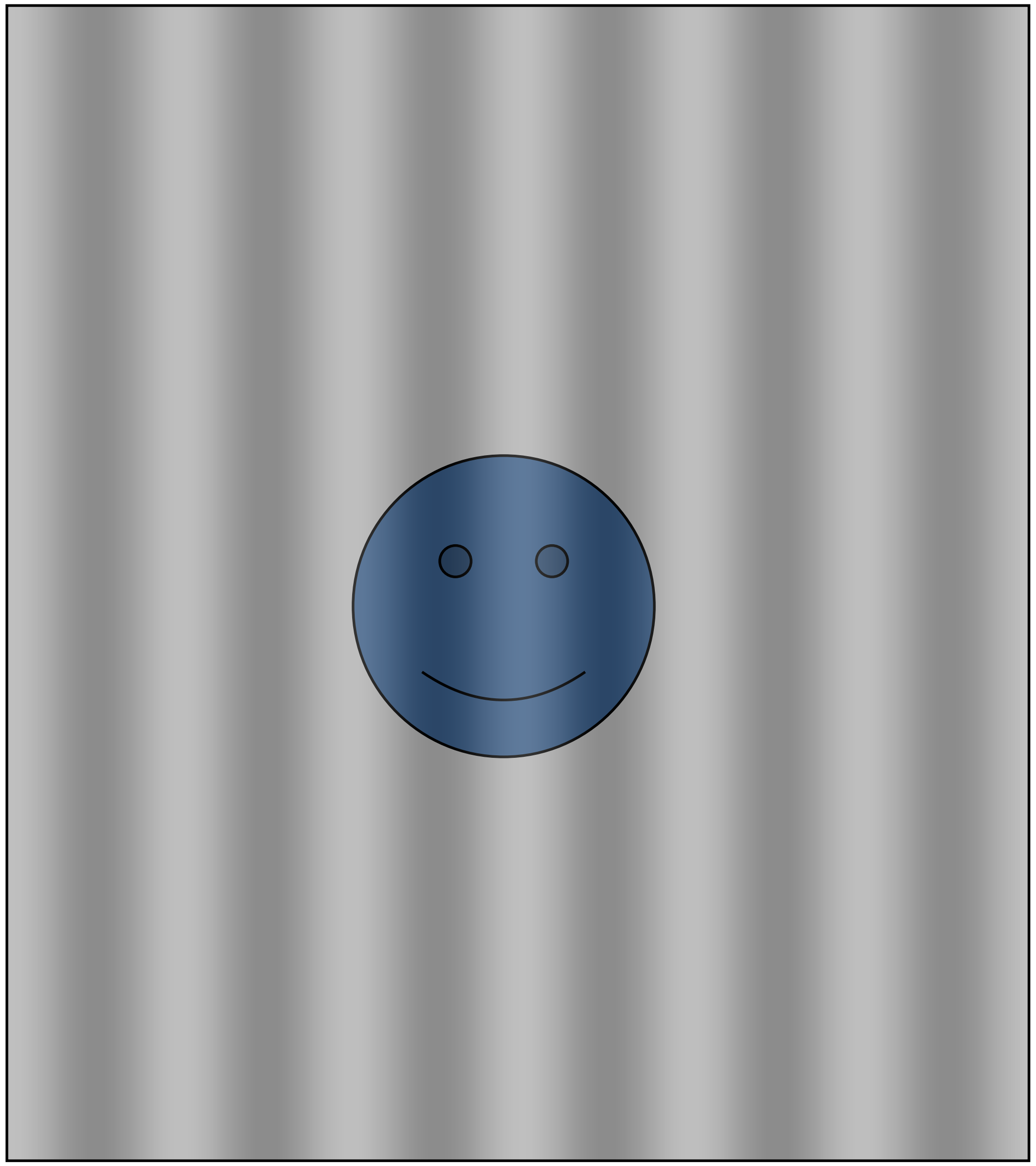

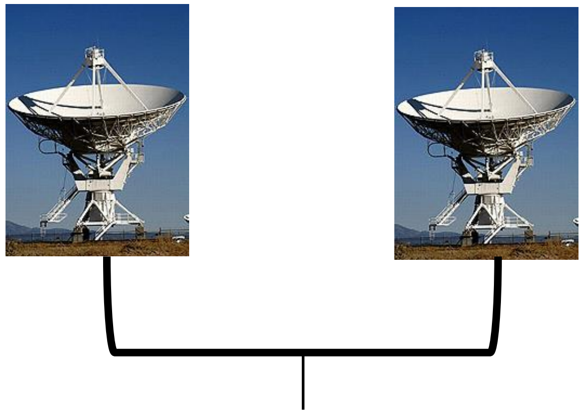

Large Source, Long Baseline

$$V(u,v) = \int\int T(l,m) e^{-i2\pi(ul+vm)} dl dm$$

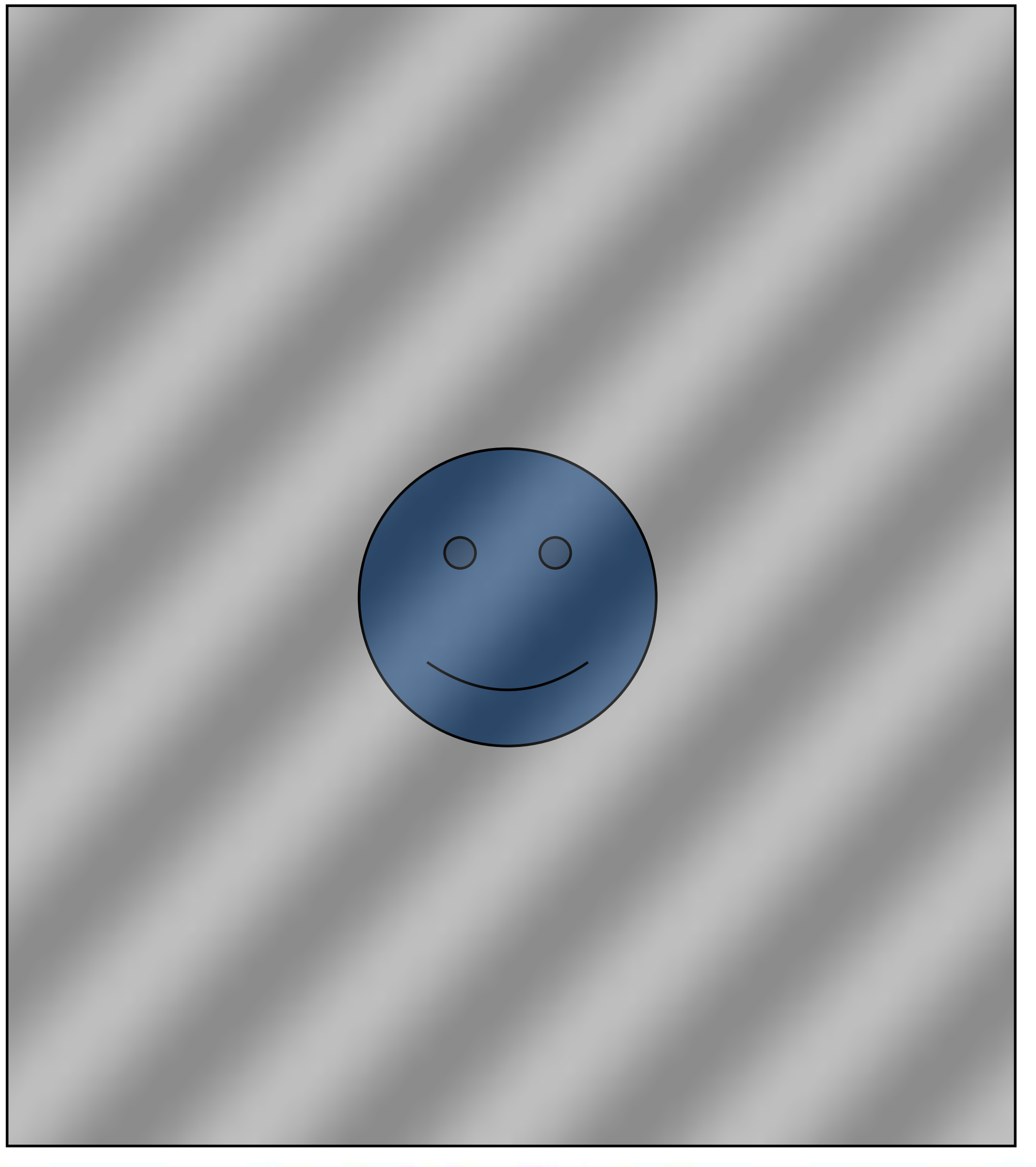

Aperture Synthesis Basics

- idea: sample *V(u,v)* at enough *(u,v)* points using distributed small aperture antennas to synthesize a large aperture antenna of size (u_{max}, v_{max})

- one pair of antennas = one baseline
  = two *(u,v)* samples at a time
- N antennas = N(N-1) samples at a time
- use Earth rotation to fill in *(u,v)* plane over time
  (Sir Martin Ryle, 1974 Nobel Prize in Physics)
- reconfigure physical layout of N antennas for more samples
- observe at multiple wavelengths for more *(u,v)* plane coverage, for source spectra amenable to simple characterization ("multi-frequency synthesis")

- if source is variable in time, then be careful

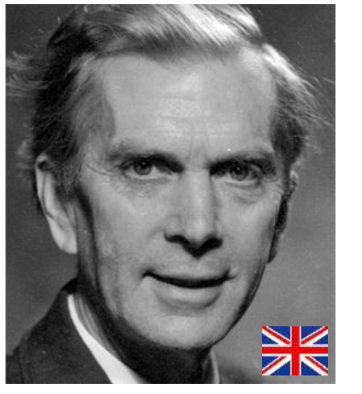

Sir Martin Ryle
1918-1984

A few Aperture Synthesis Telescopes for Observations at Millimeter Wavelengths

Example of (u,v) Plane Sampling

2 Antennas, 1 Min

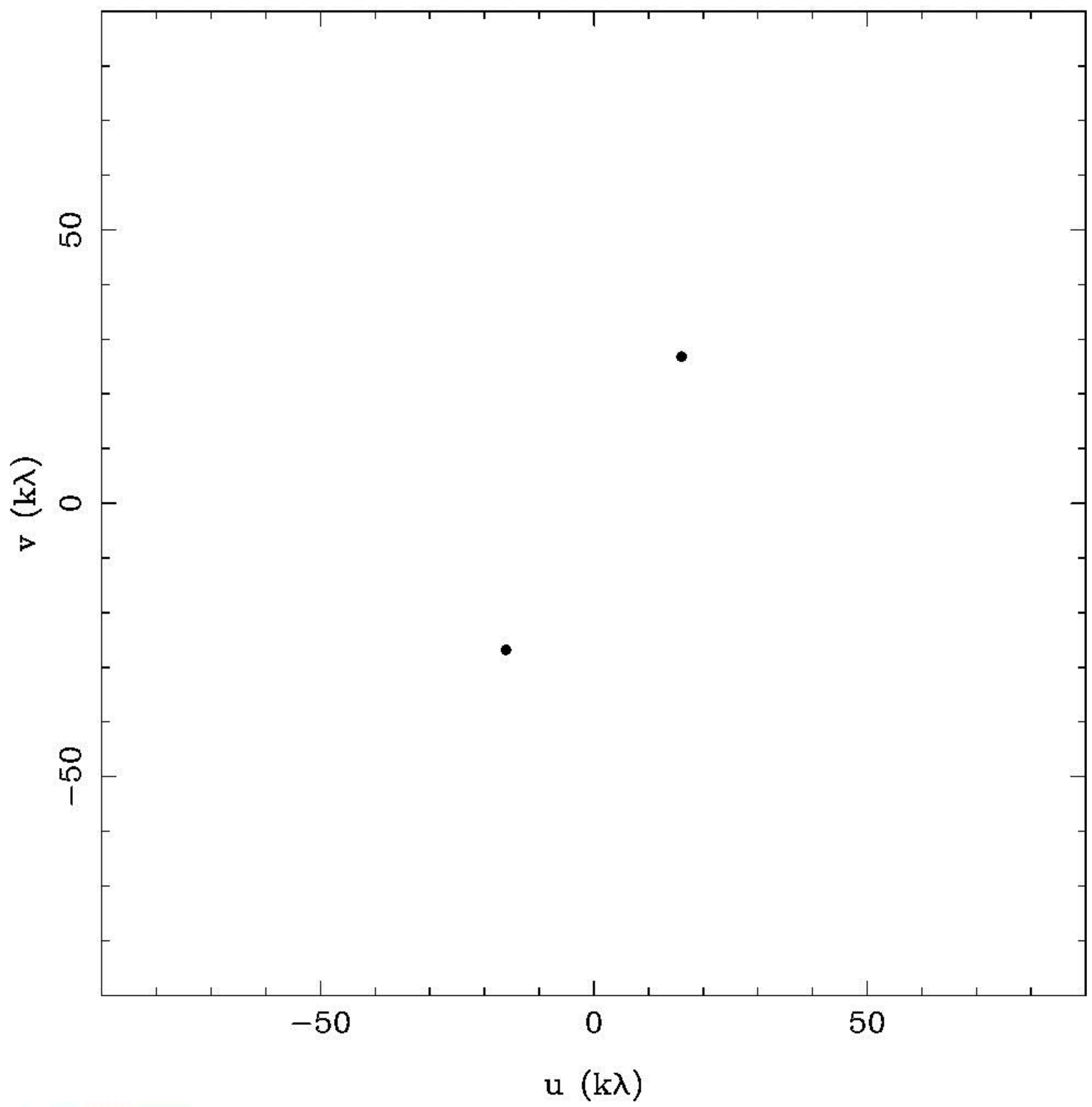

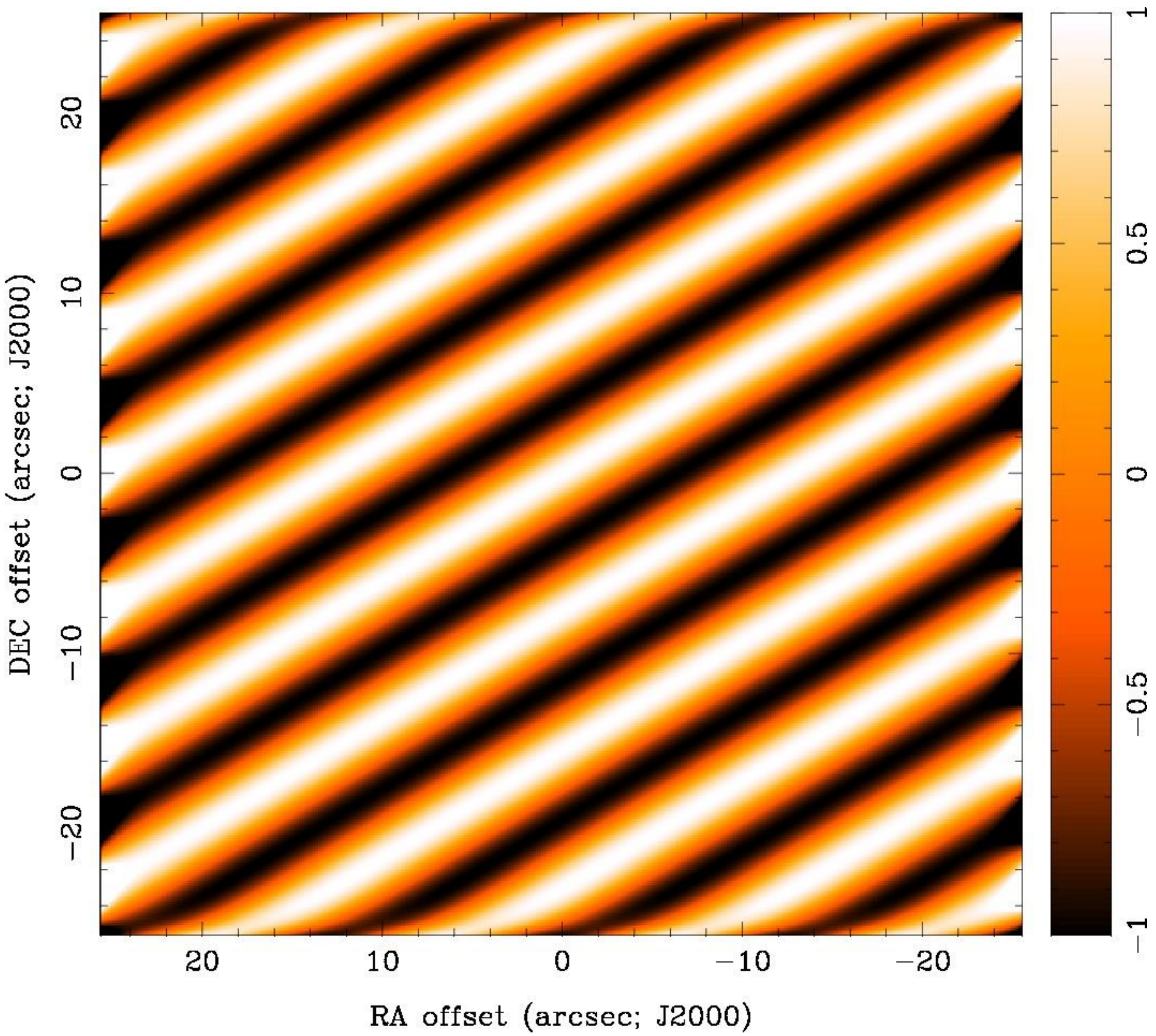

Example of (u,v) Plane Sampling

3 Antennas, 1 Min

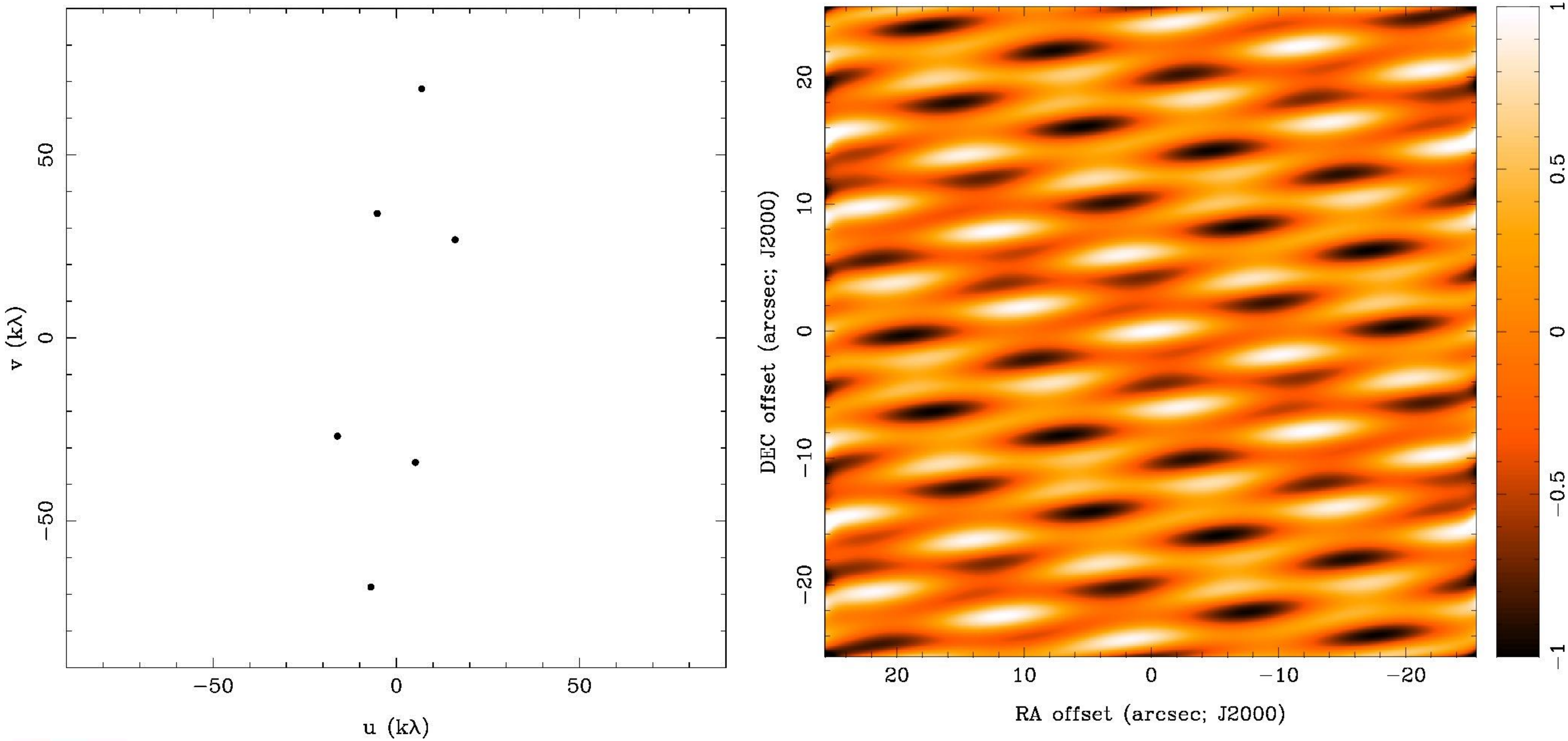

Example of (u,v) Plane Sampling

4 Antennas, 1 Min

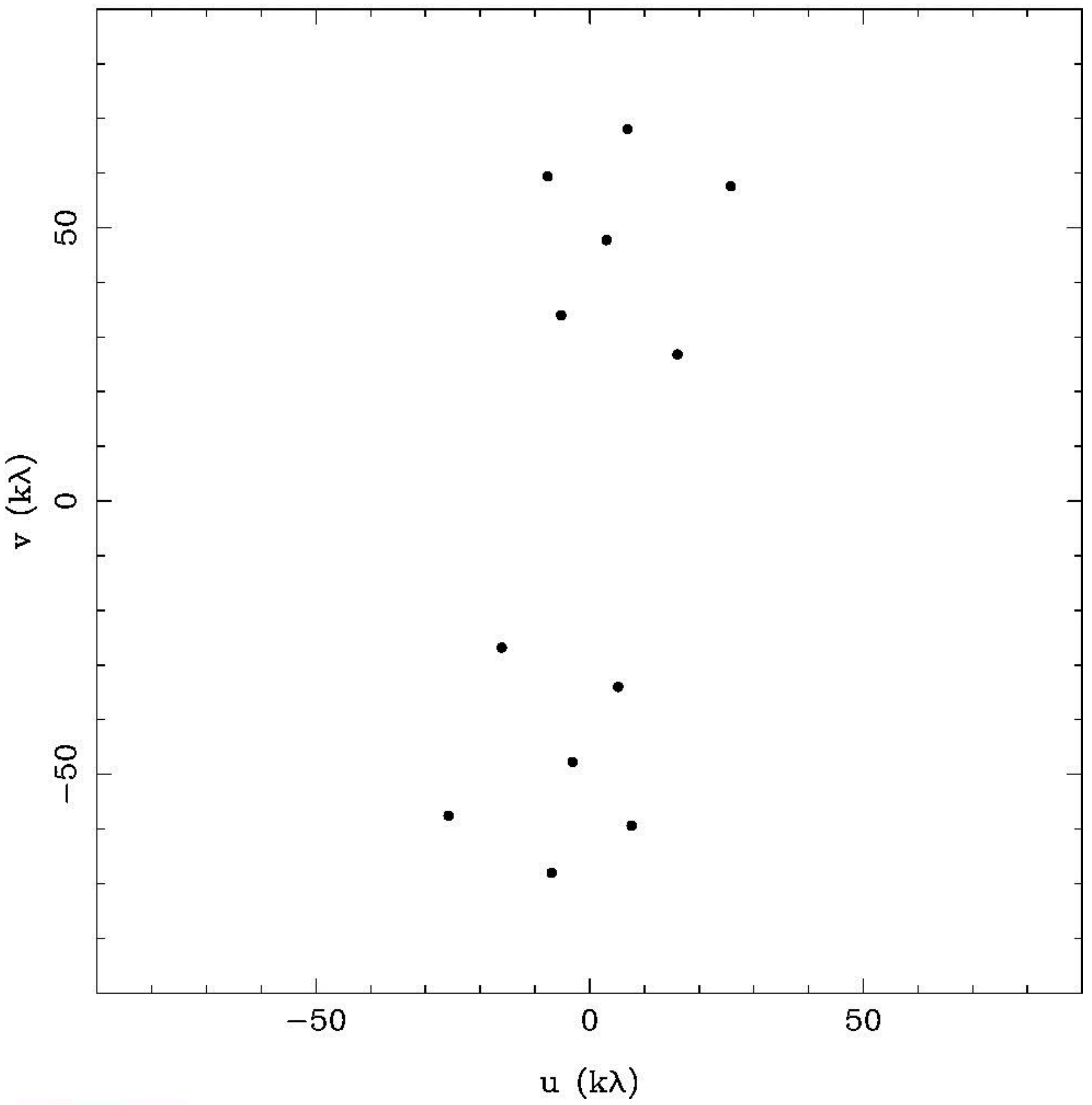

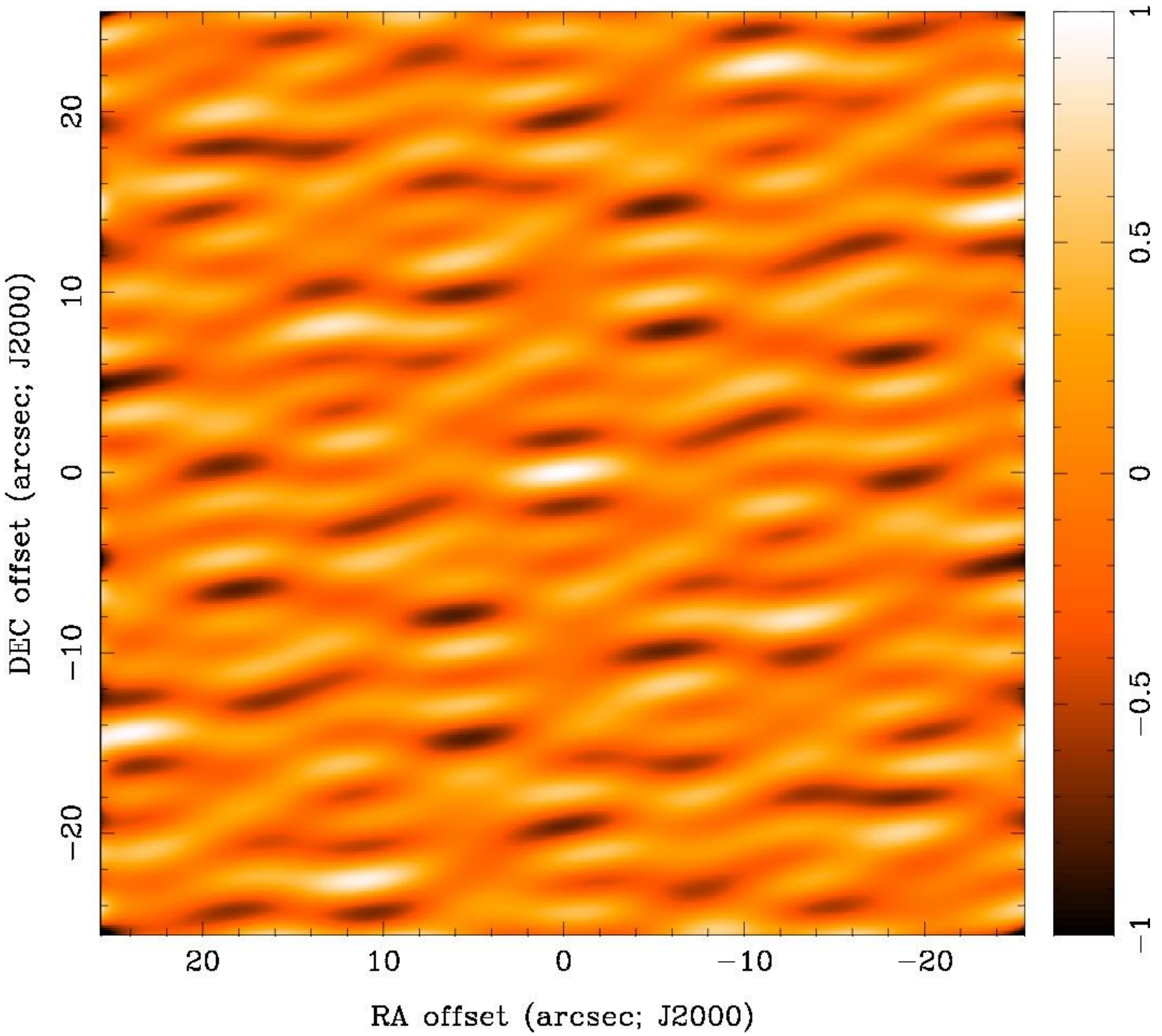

Example of (u,v) Plane Sampling

7 Antennas, 1 Min

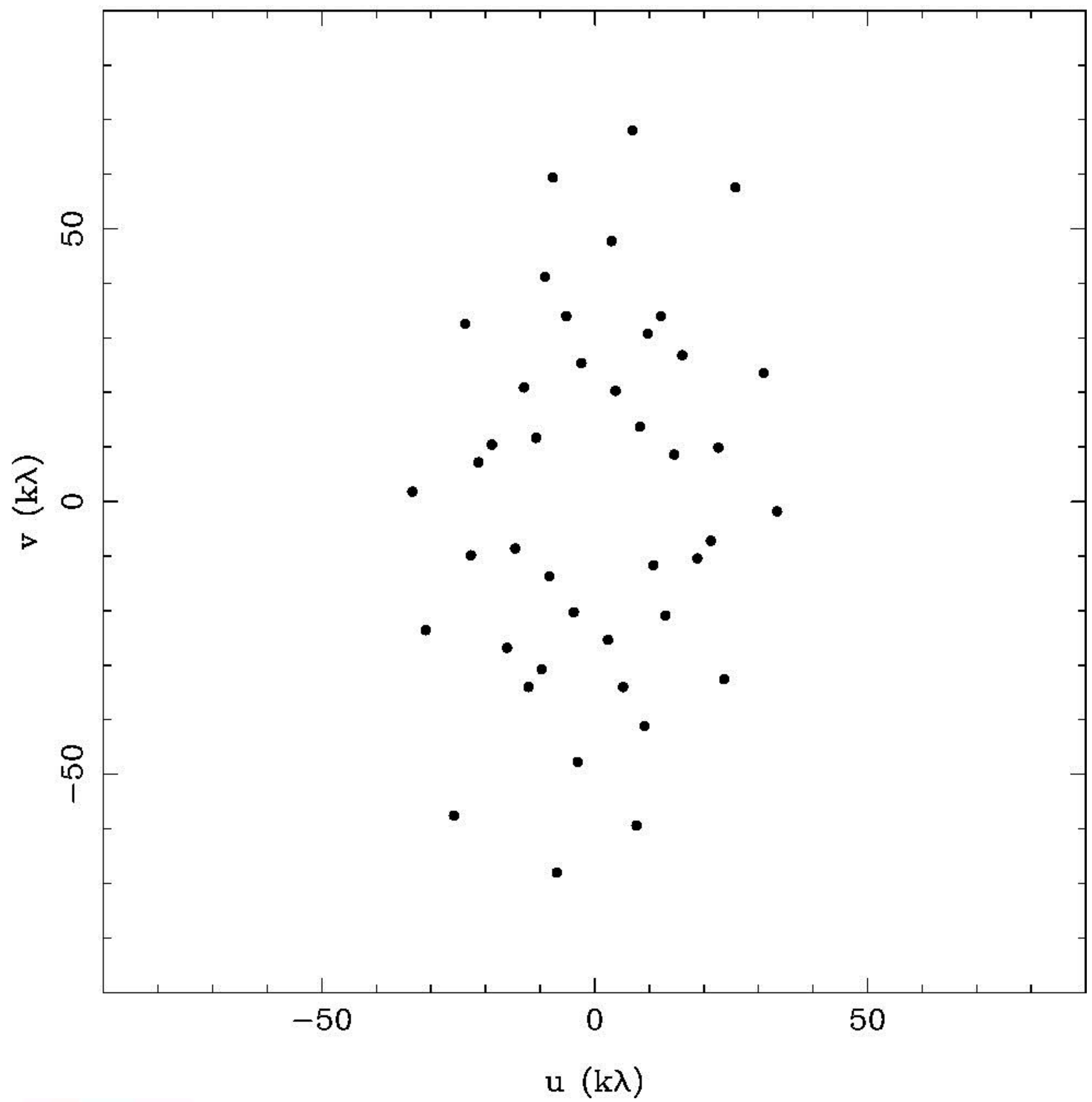

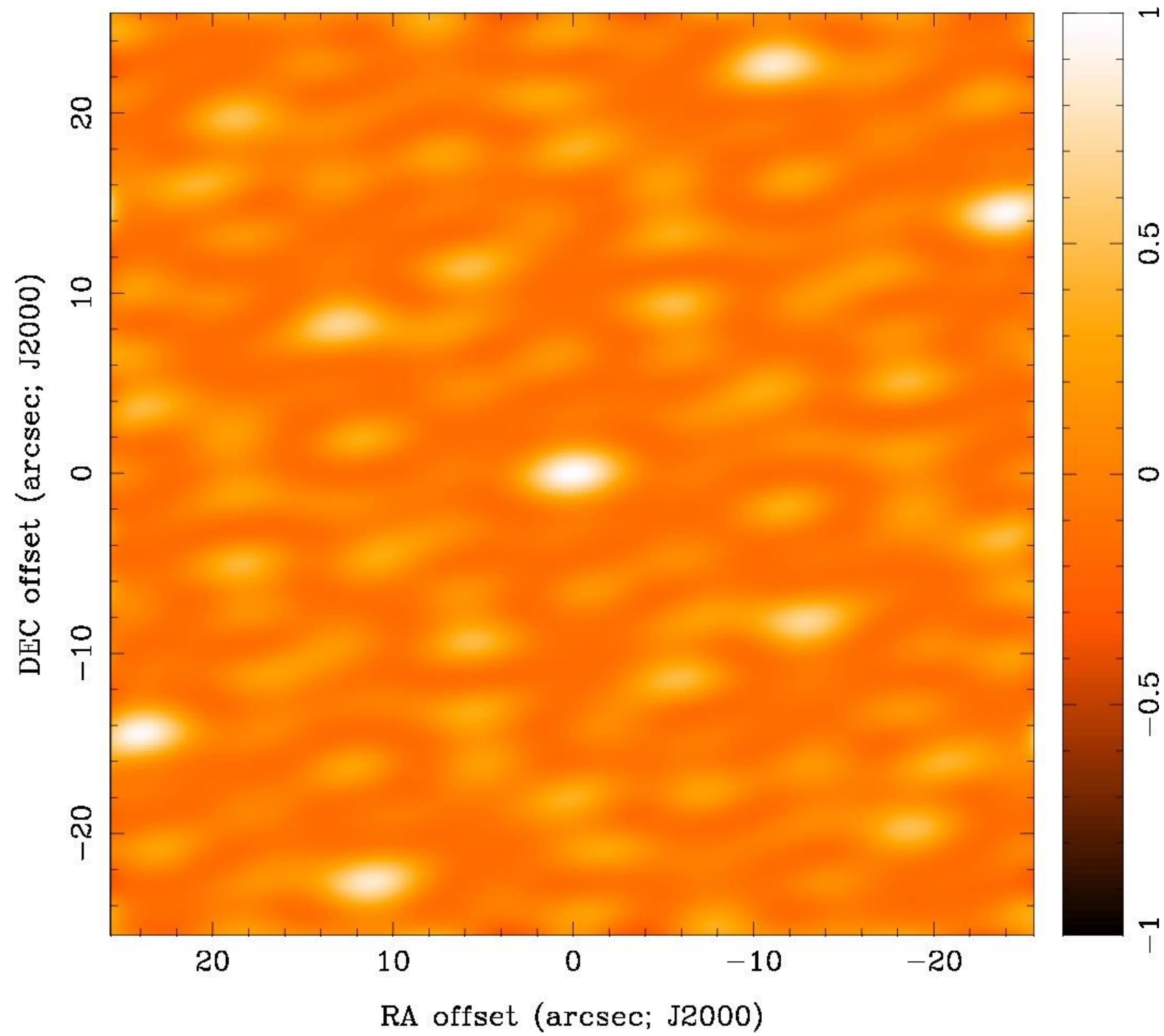

Example of (u,v) Plane Sampling

7 Antennas, 10 min

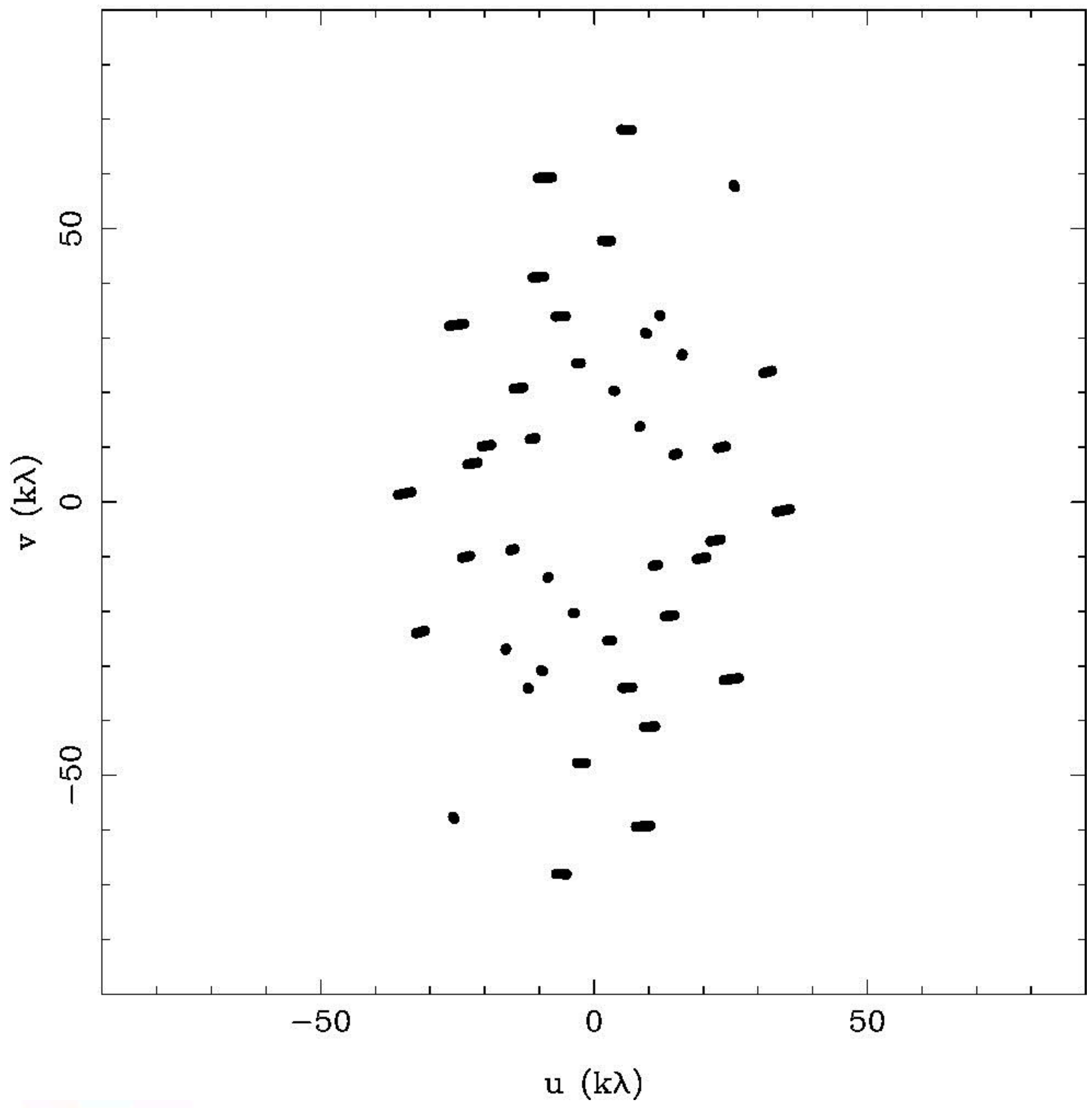

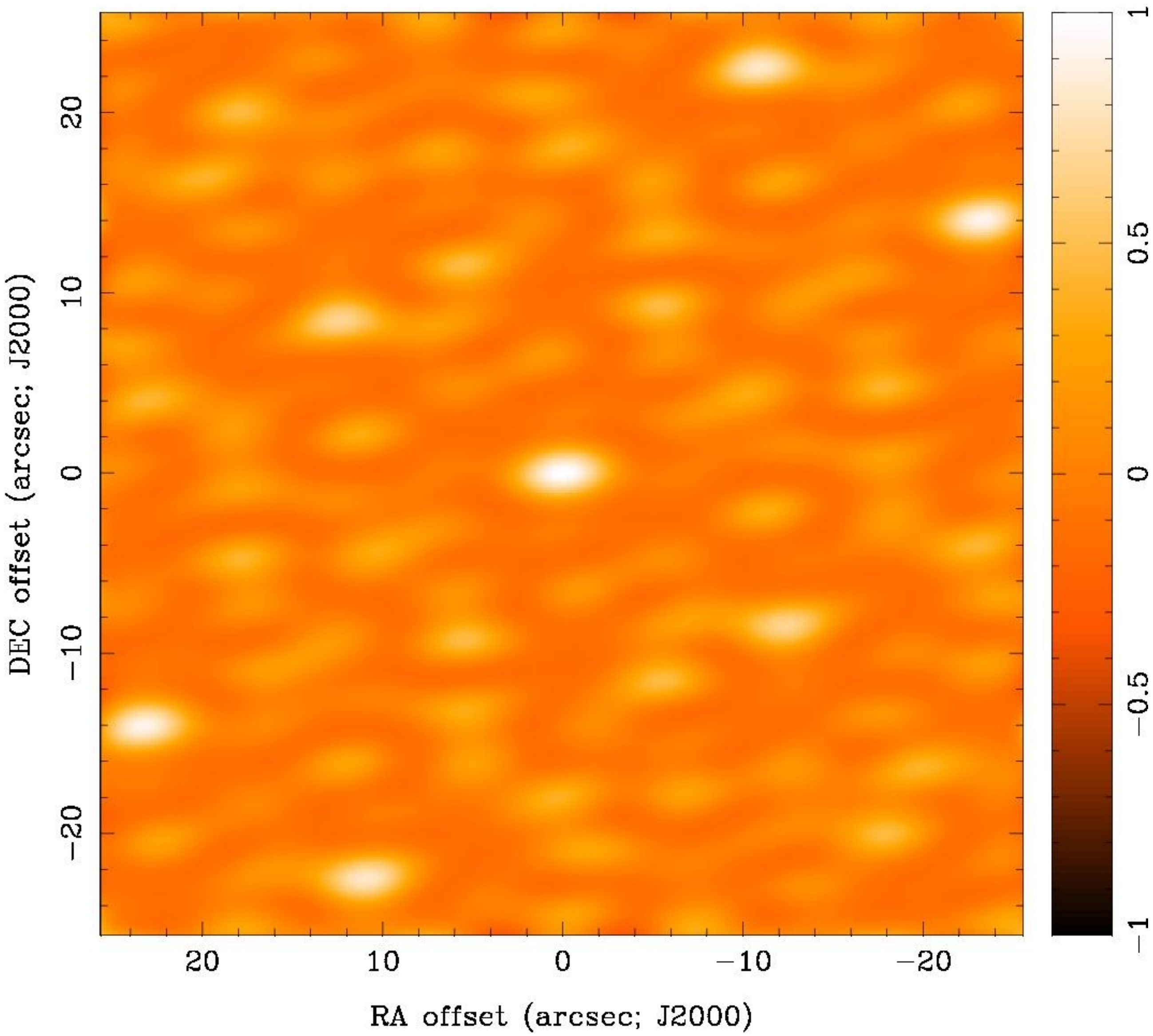

Example of (u,v) Plane Sampling

7 Antennas, 1 hour

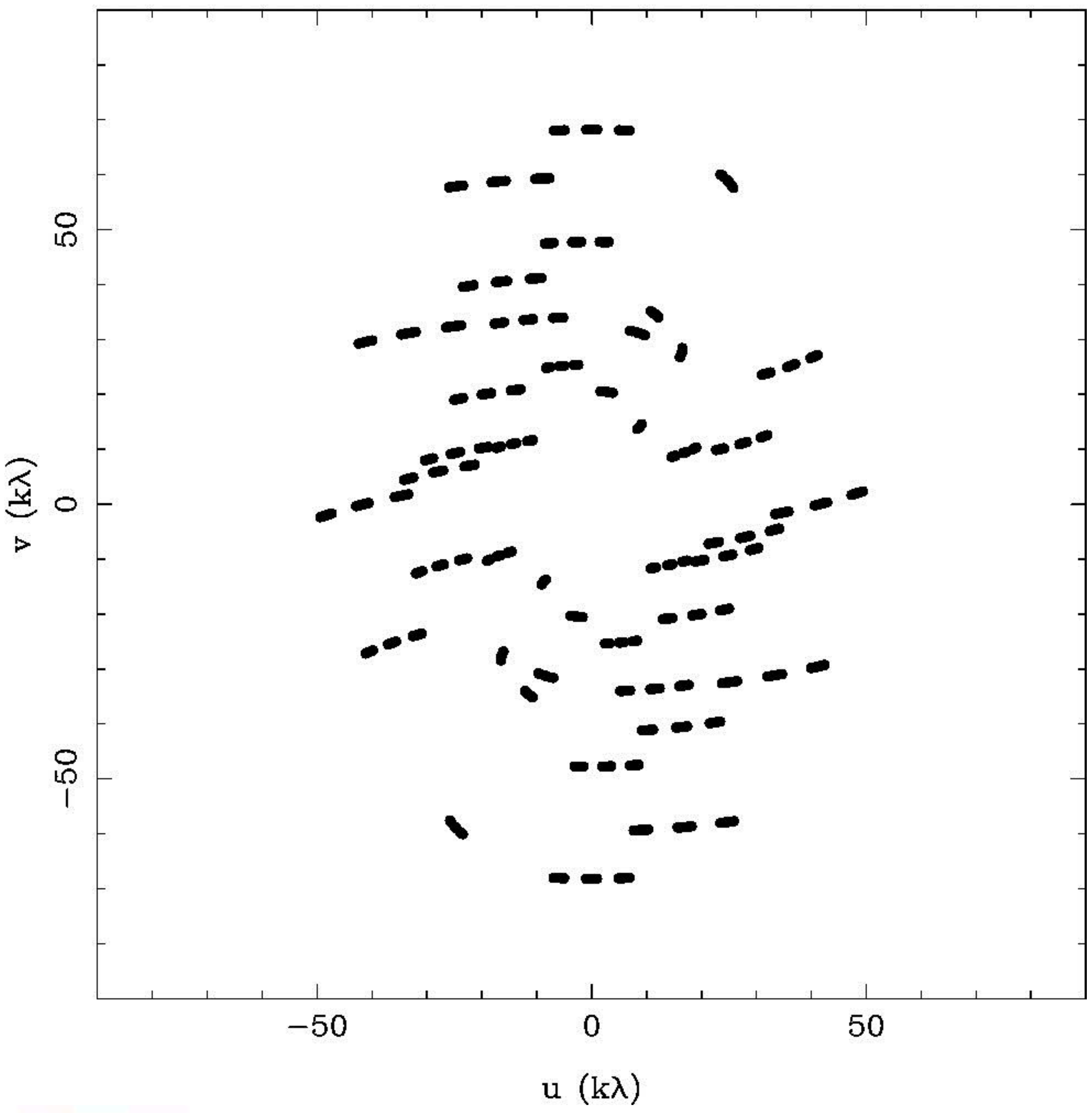

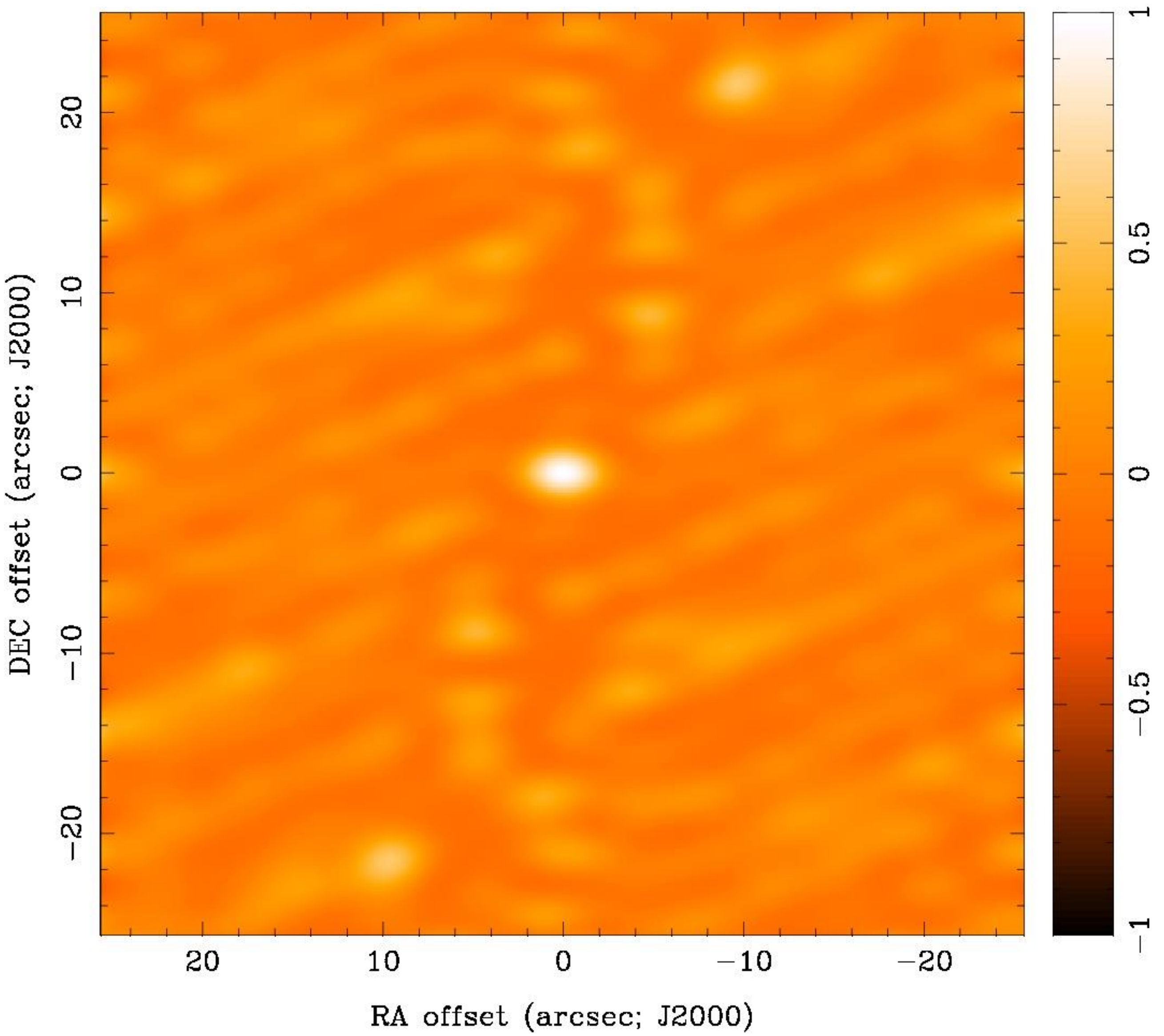

Example of (u,v) Plane Sampling

7 Antennas, 3 hours

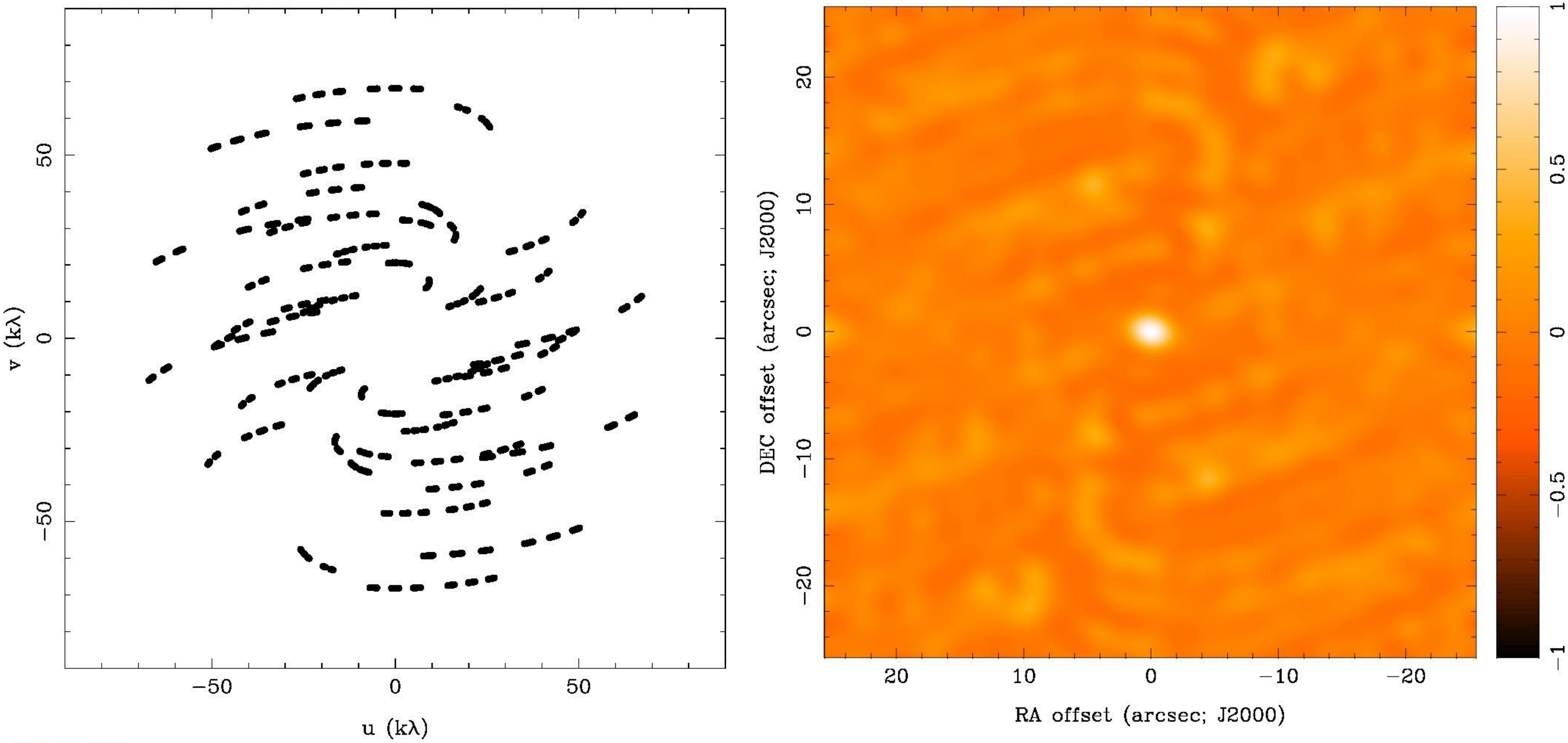

Example of (u,v) Plane Sampling

7 Antennas, 8 hours

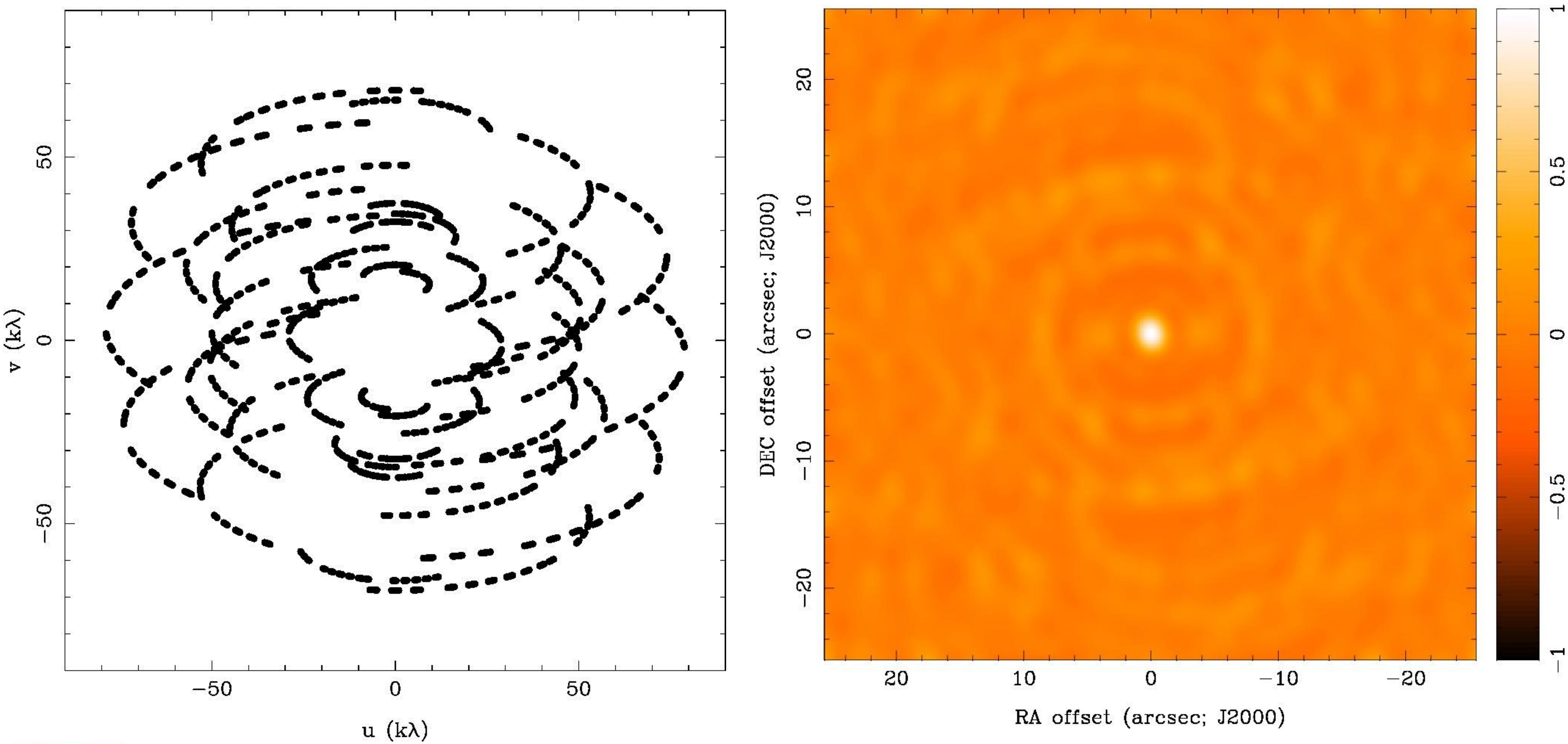

Example of (u,v) Plane Sampling

COM configurations of 7 SMA antennas, ν = 345 GHz, dec = +22 deg

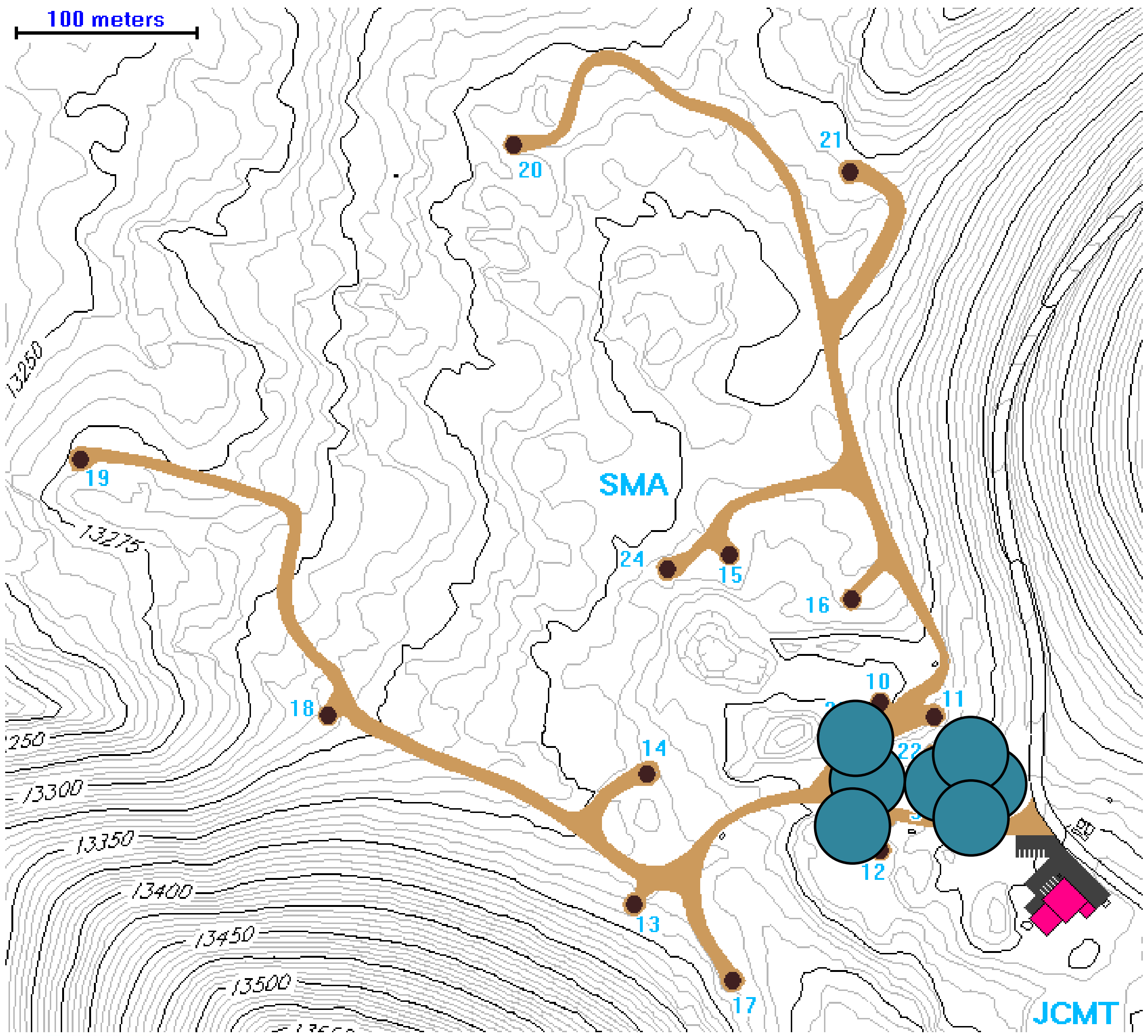

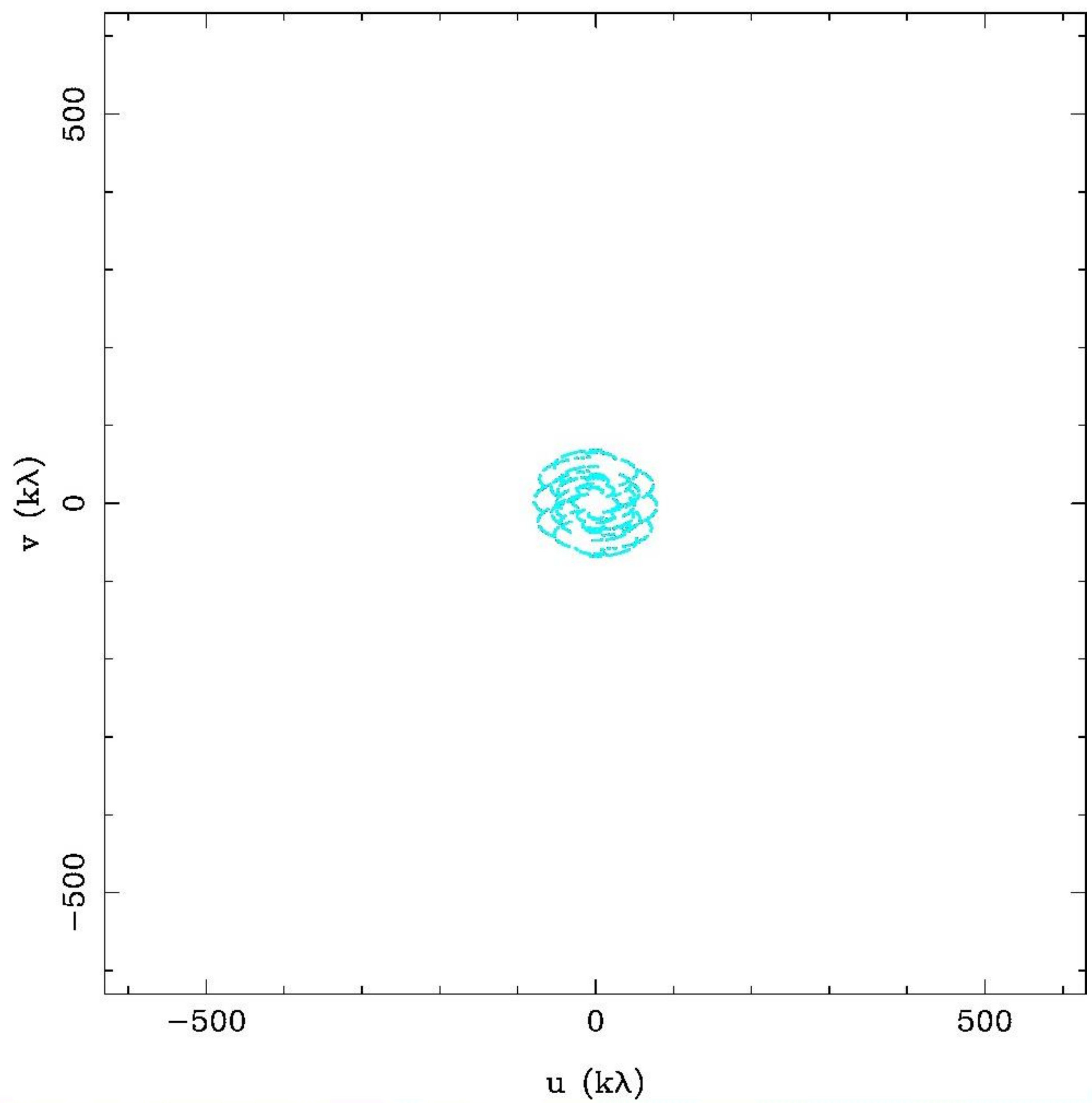

Example of (u,v) Plane Sampling

EXT configurations of 7 SMA antennas, ν = 345 GHz, dec = +22 deg

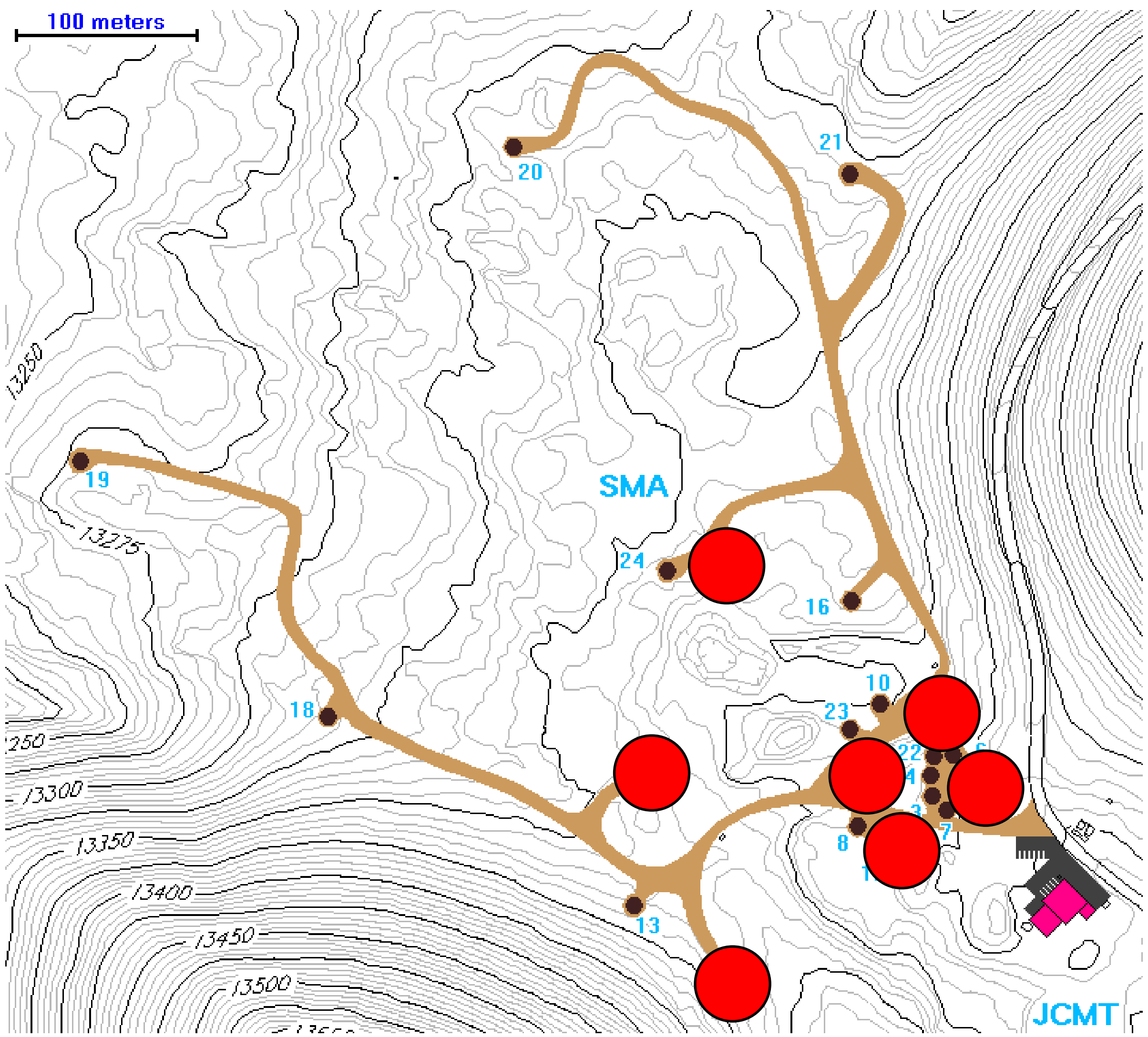

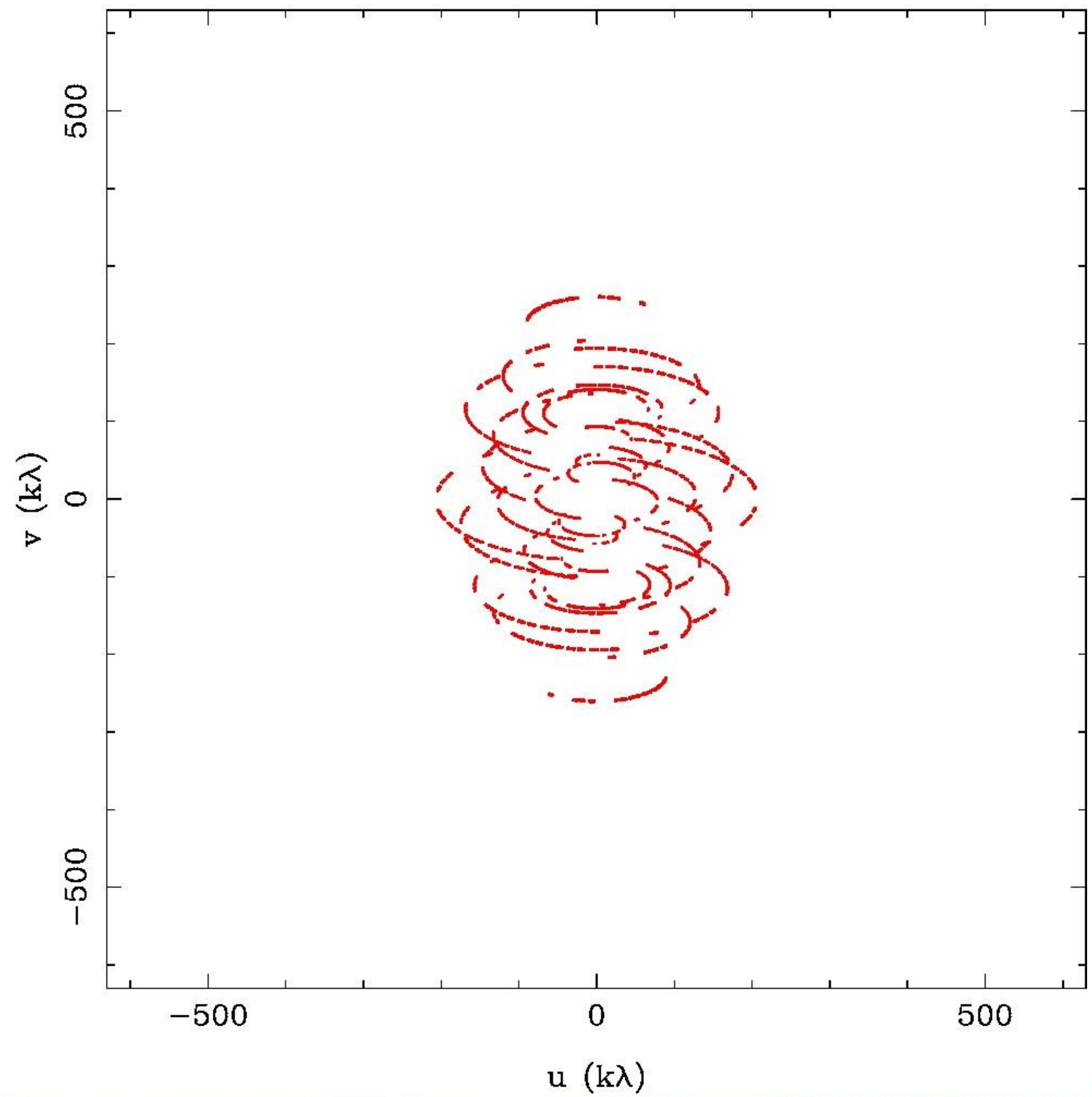

Example of (u,v) Plane Sampling

VEX configuration of 6 SMA antennas, ν = 345 GHz, dec = +22 deg

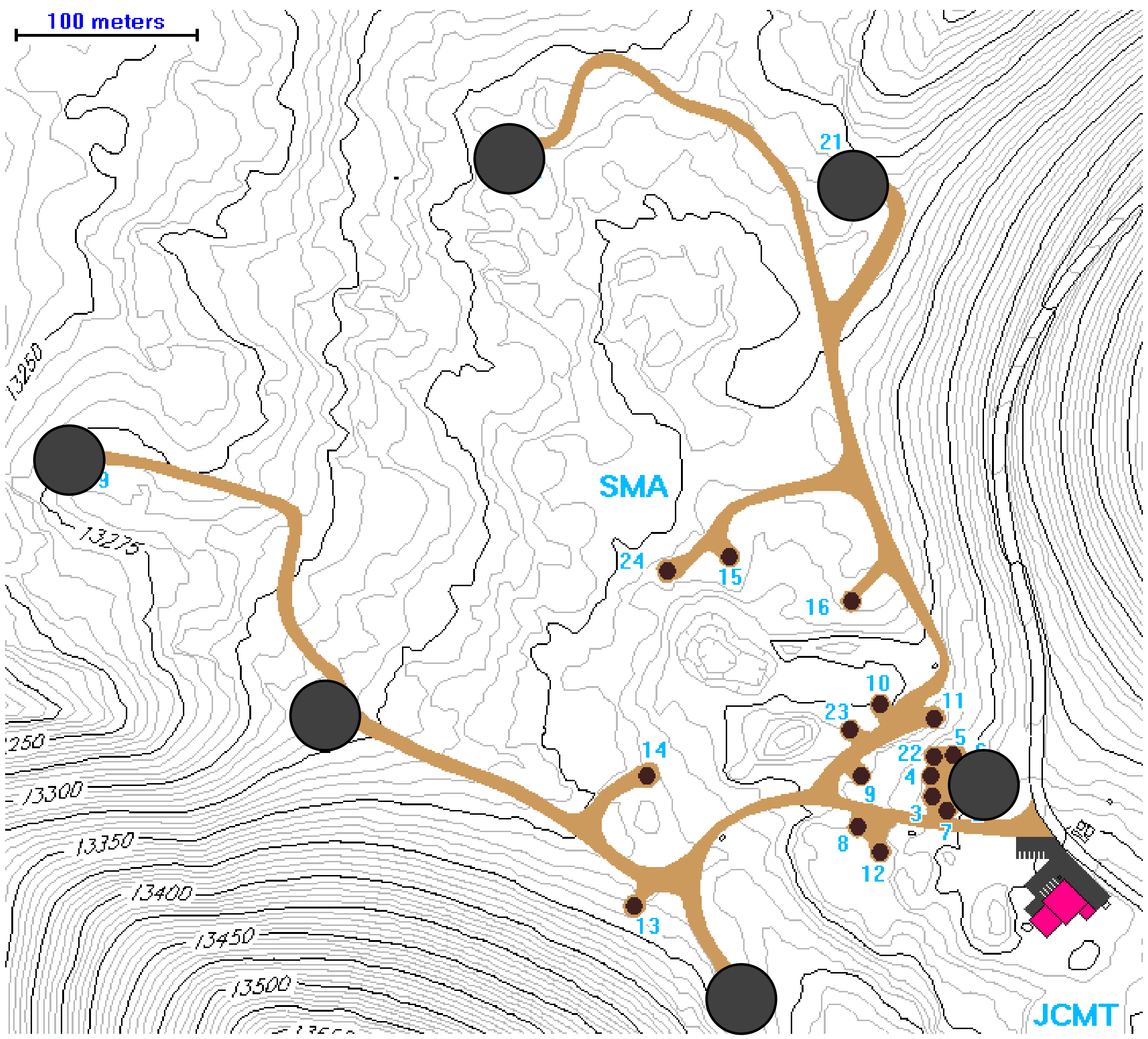

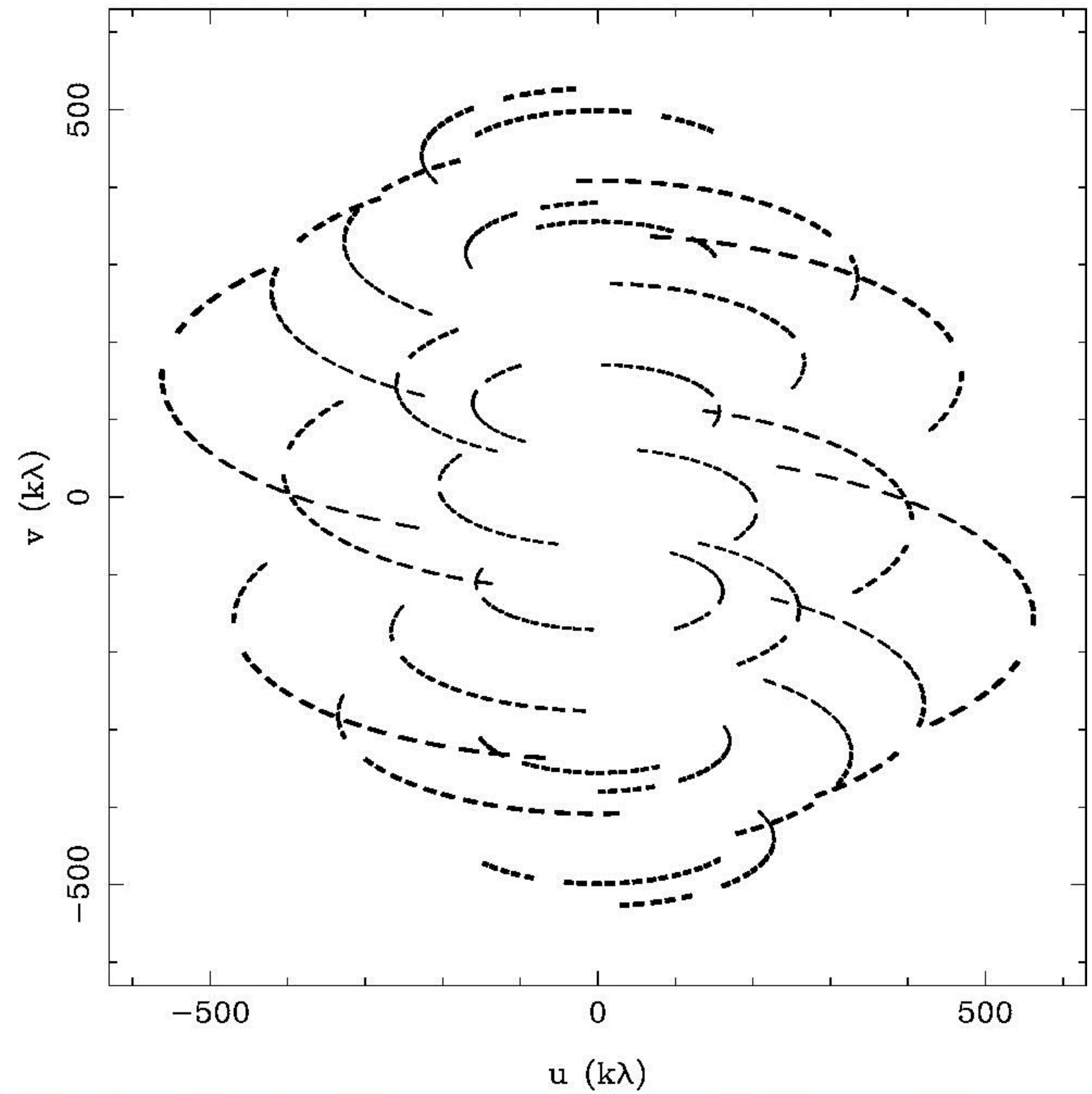

Implications of (u,v) Plane Sampling

samples of *V(u,v)* are limited by number of antennas and by Earth-sky geometry

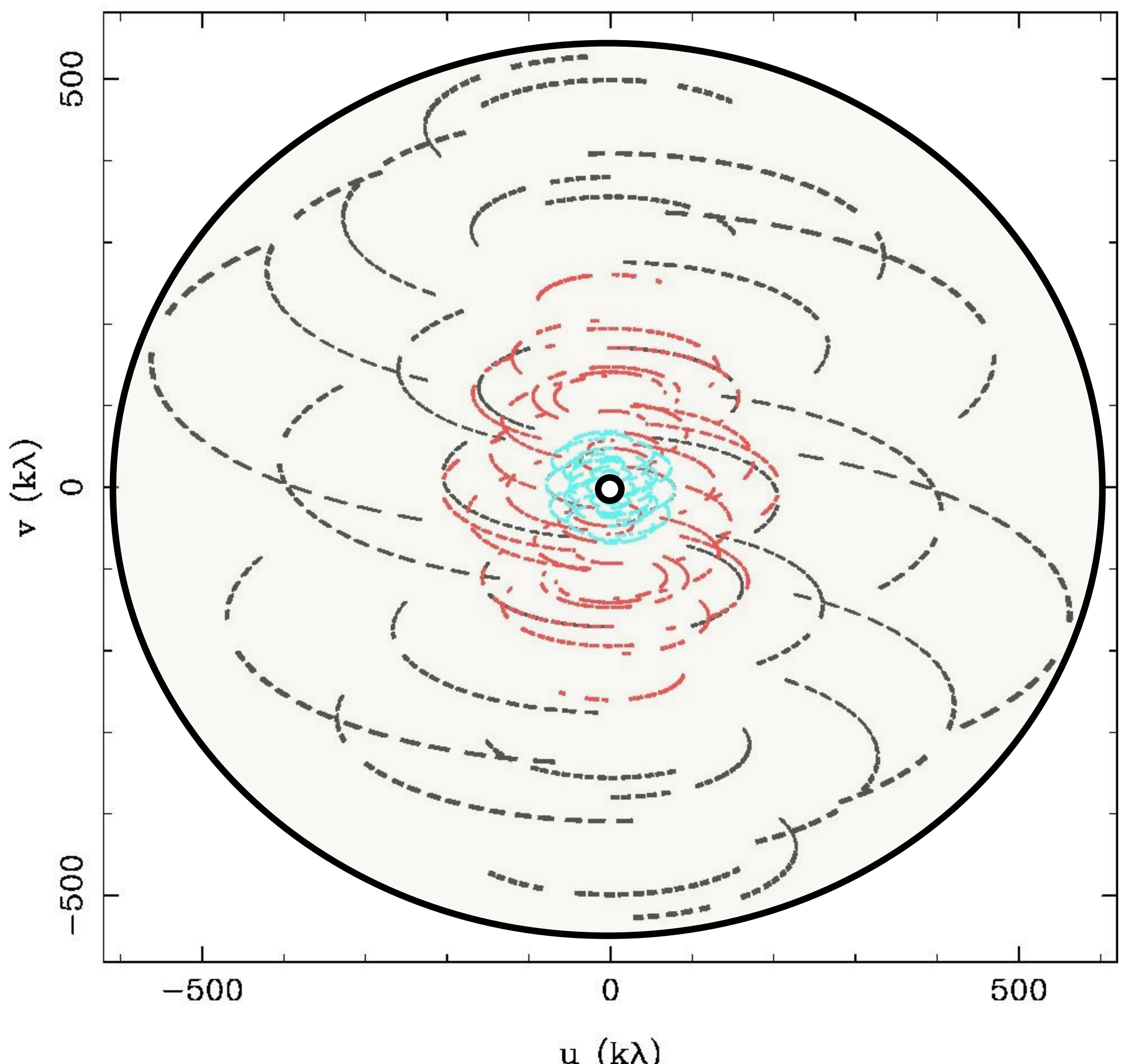

- *outer boundary*
  - no information on smaller scales
  - resolution limit
- *inner hole*
  - no information on larger scales
  - extended structures invisible
- *irregular coverage between boundaries*
  - sampling theorem violated
  - information missing

Inner and Outer (u,v) Boundaries

V(u,v) amplitude

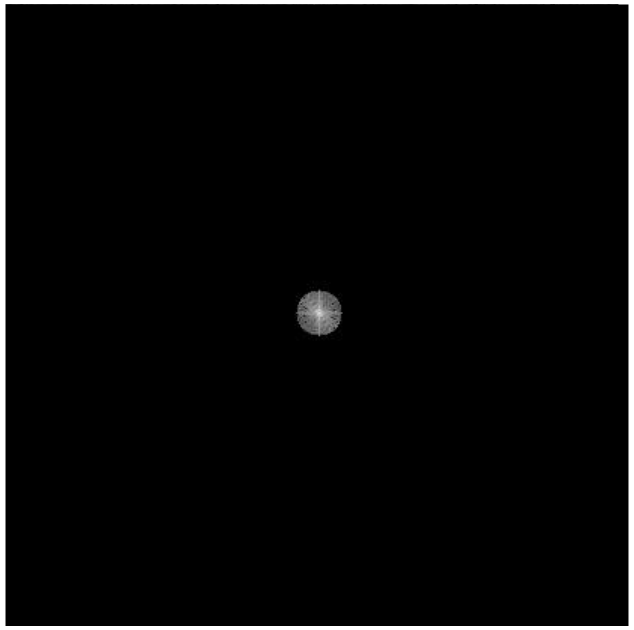

V(u,v) phase

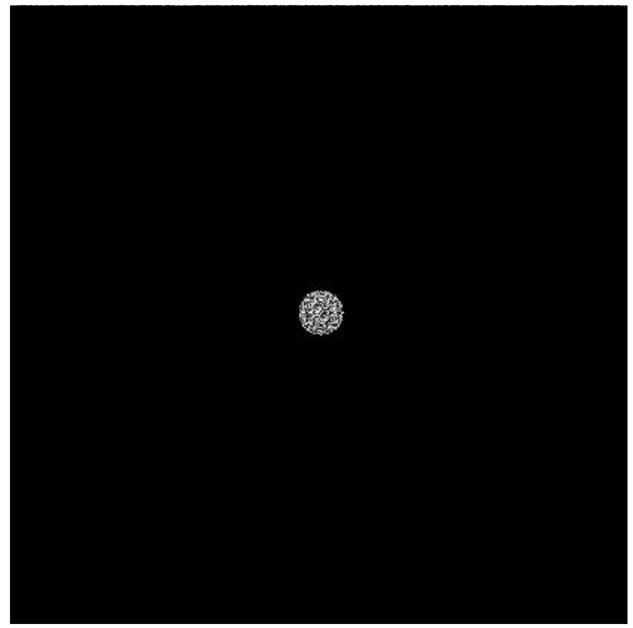

$\xrightarrow{\mathcal{F}}$

T(l,m)

V(u,v) amplitude

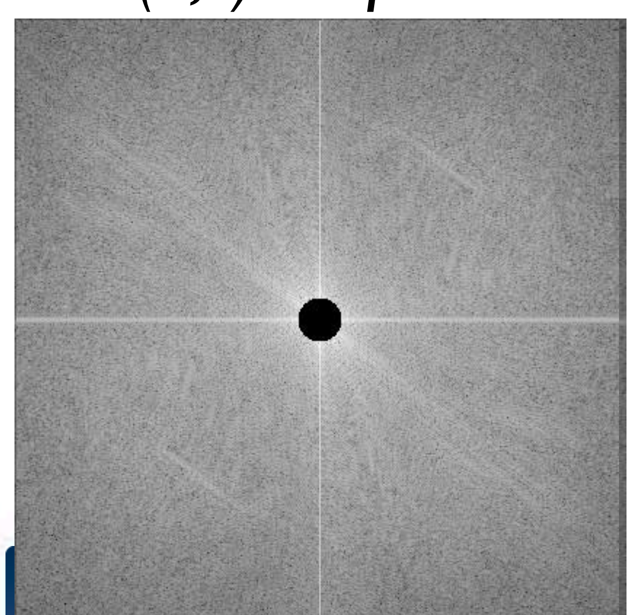

V(u,v) phase

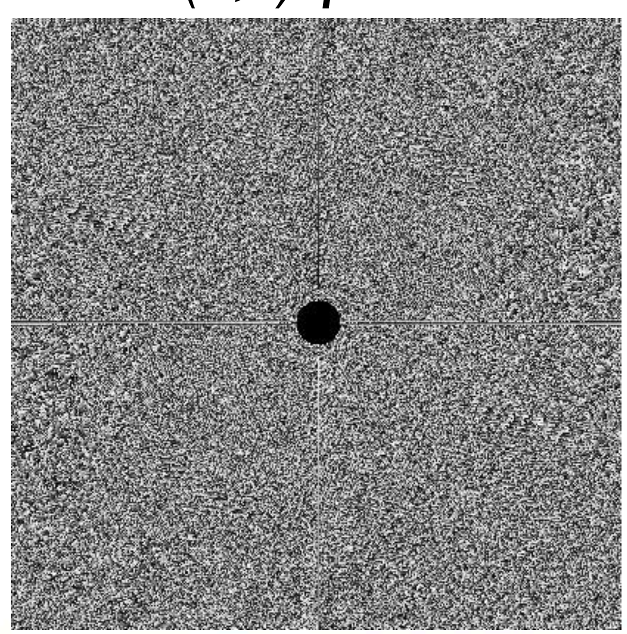

$\xrightarrow{\mathcal{F}}$

T(l,m)

Formal Description of Imaging

$$V(u,v) \xrightarrow{\mathcal{F}} T(l,m)$$

- sample Fourier domain at discrete points $$S(u,v) = \sum_{k=1}^{M} \delta(u-u_k, v-v_k)$$
- Fourier transform sampled visibility function $$V(u,v)S(u,v) \xrightarrow{\mathcal{F}} T^D(l,m)$$
- apply the convolution theorem $$T(l,m) * s(l,m) = T^D(l,m)$$
  where the Fourier transform of the sampling pattern
  $s(l,m) \xrightarrow{\mathcal{F}} S(u,v)$ is the "point spread function"

the Fourier transform of the sampled visibilities yields the true sky brightness convolved with the point spread function

radio jargon: the "dirty image" is the true image convolved with the "dirty beam"

Dirty Beam and Dirty Image

S(u,v)

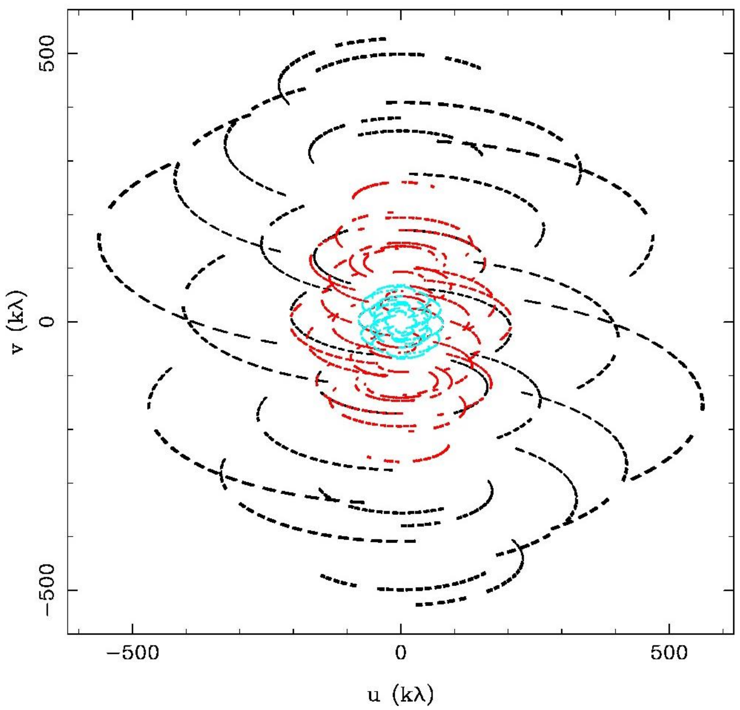

$\xrightarrow{\mathcal{F}}$

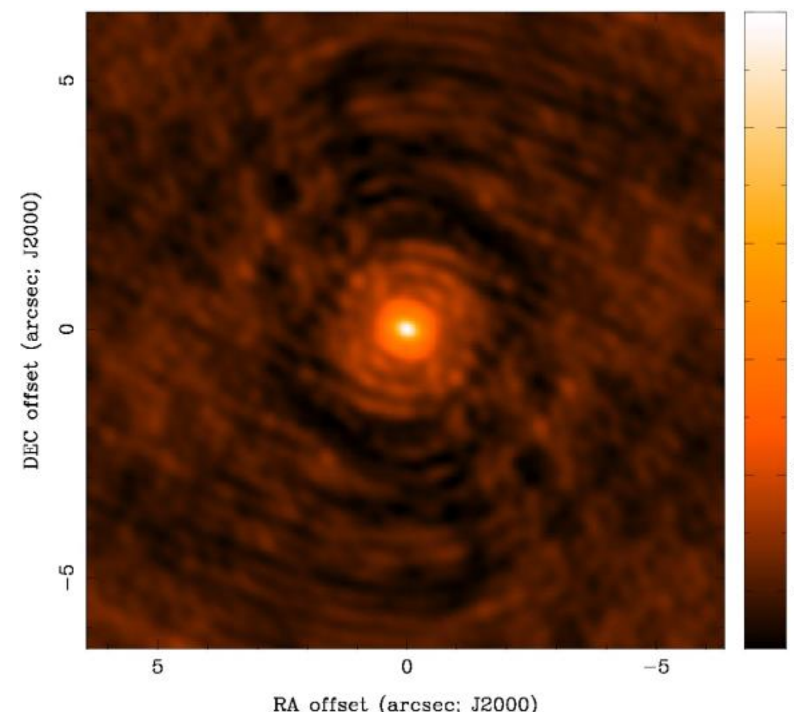

s(l,m)
"dirty beam"

$*$

T(l,m)

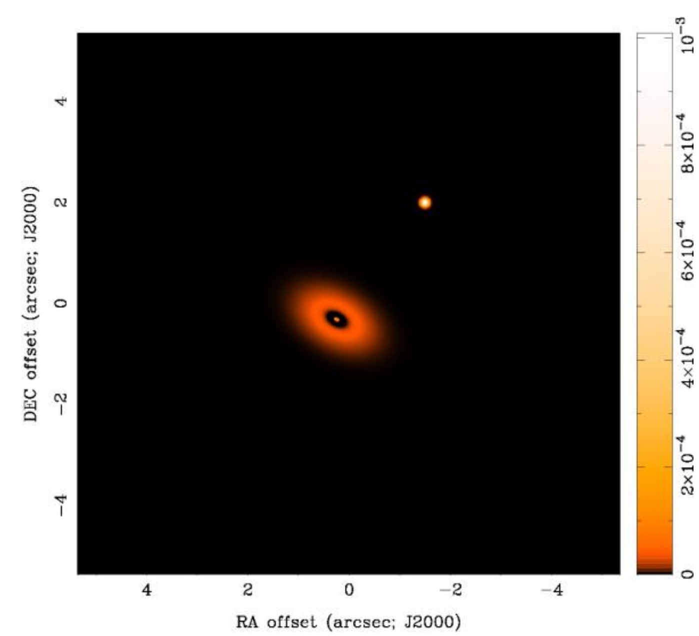

$\leftarrow$

T^D(l,m)
"dirty image"

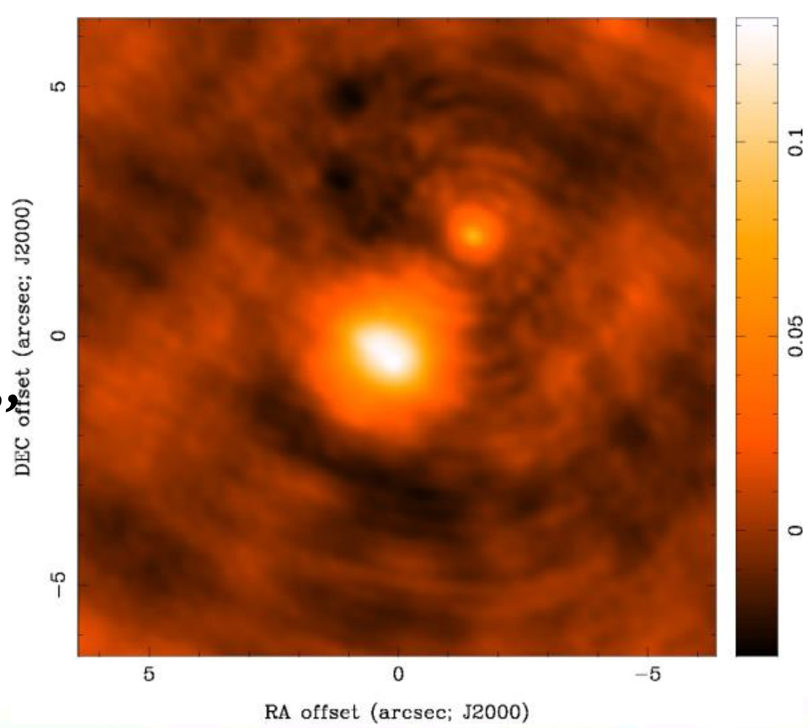

Imaging Decisions: Visibility Weighting

- introduce weighting function $W(u,v)$
  - modifies sampling function
  - $S(u,v) \rightarrow S(u,v)W(u,v)$
  - changes $s(l,m)$, the dirty beam
  - CASA `clean` "weighting"

- "natural" weighting
  - $W(u,v) = 1/\sigma^2$ in occupied cells, where σ^2 is the noise variance
  - maximizes point source sensitivity
  - lowest rms in image
  - generally gives more weight to short baselines, so the angular resolution is degraded

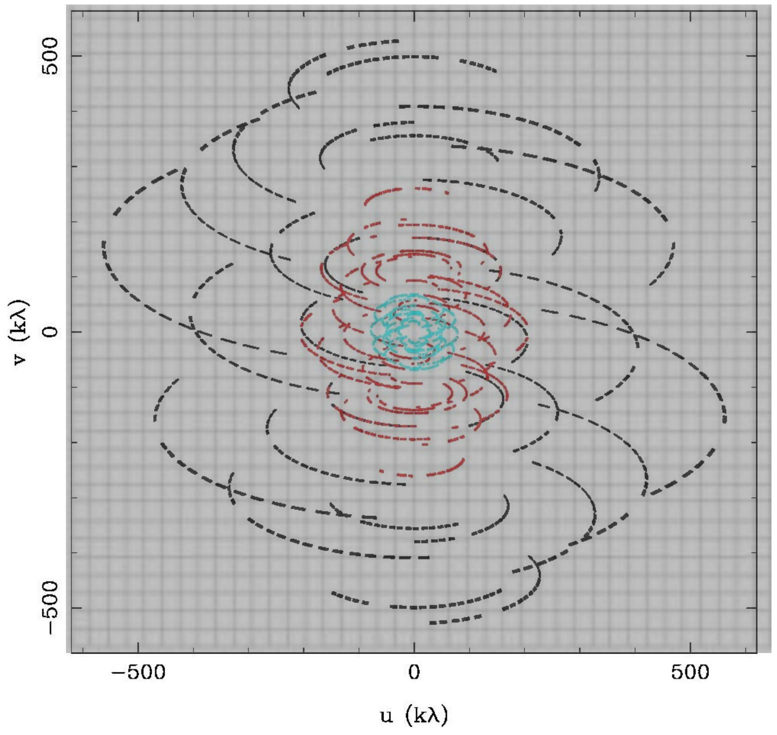

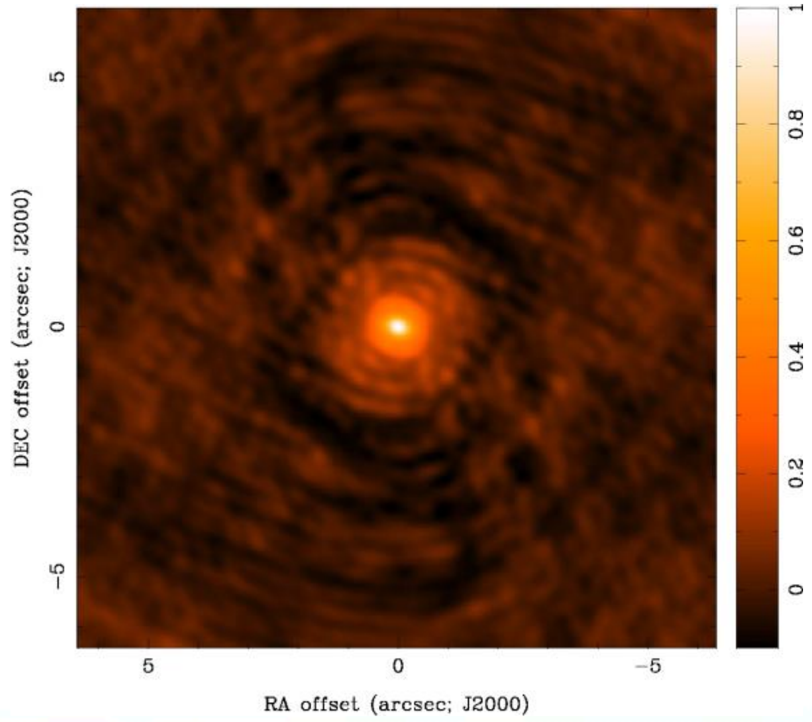

Imaging Decisions: Visibility Weighting

- "uniform" weighting
  - *W(u,v)* inversely proportional to local density of *(u,v)* samples
  - weight for occupied cell = const
  - fills *(u,v)* plane more uniformly and dirty beam sidelobes are lower
  - gives more weight to long baselines, so angular resolution is enhanced
  - downweights some data, so point source sensitivity is degraded

  - n.b. can be trouble with sparse *(u,v)* coverage: cells with few samples have same weight as cells with many

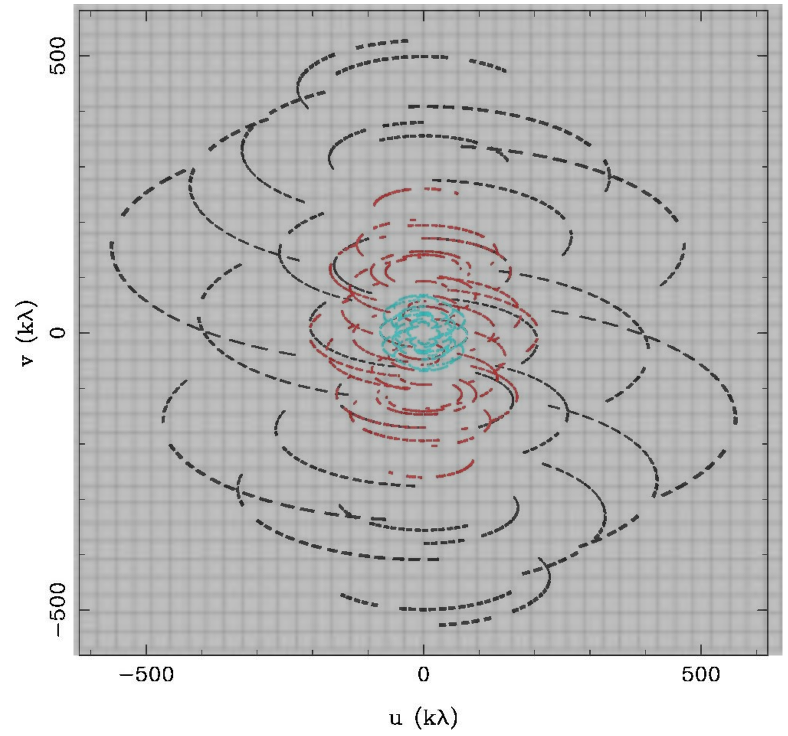

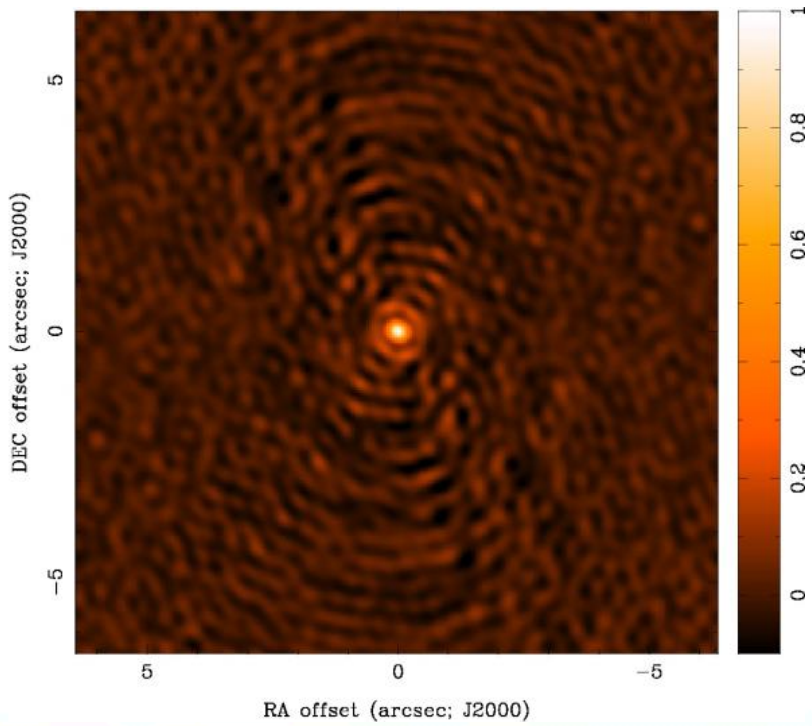

Imaging Decisions: Visibility Weighting

- "robust" (or "Briggs") weighting
  - variant of uniform weighting that avoids giving too much weight to cells with low natural weight
  - software implementations differ
  - e.g. $$W(u,v) = \frac{1}{\sqrt{1 + S_N^2 / S_{thresh}^2}}$$

    S_N is cell natural weight

    S_{thresh} is a threshold

    high threshold $\rightarrow$ natural weight

    low threshold $\rightarrow$ uniform weight
- *an adjustable parameter allows for continuous variation between maximum point source sensitivity and resolution*

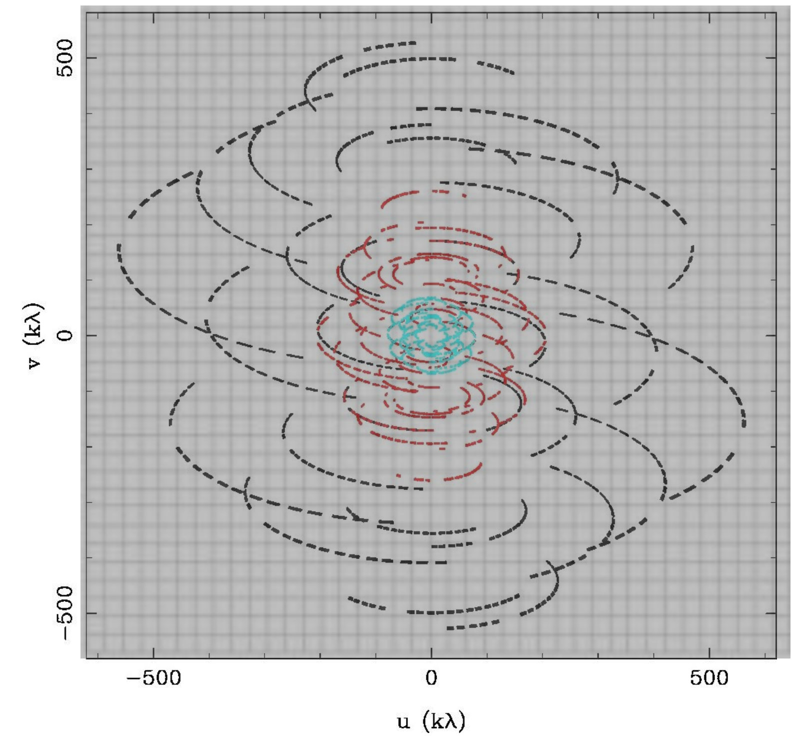

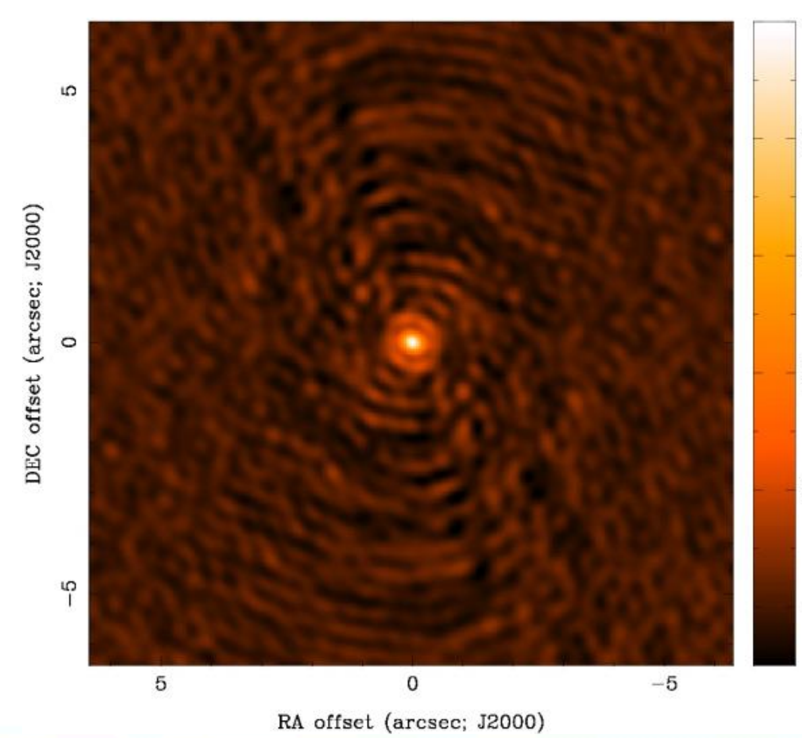

ALMA C40-4 Configuration Resolution?

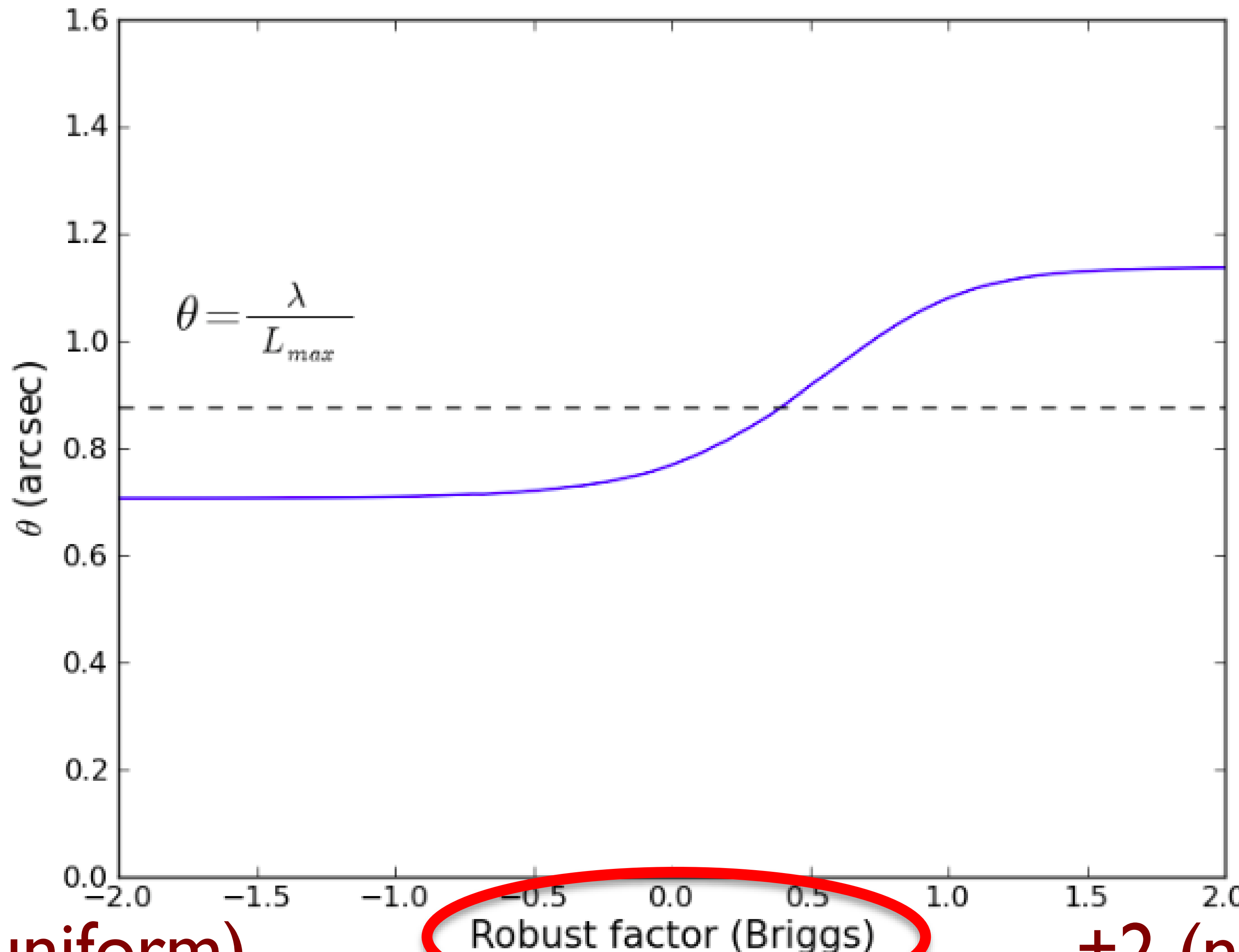

CASA `clean`

-2 (uniform)

+2 (natural)

Figure 7.6: Angular resolution achieved using different values of the CASA *robust* parameter for a 1-hour observation at 100 GHz and a declination of -23 deg in the C40-4 configuration. Note that $robust = -2$ is close to uniform weighting and $robust = 2$ is close to natural weighting. The dotted line corresponds to $\frac{\lambda}{L_{max}}$.

ALMA Cycle 4 Technical Handbook

Imaging Decisions: Visibility Weighting

- uvtaper
  - apodize *(u,v)* sampling by a Gaussian

$$W(u,v) = \exp\left(-\frac{(u^2+v^2)}{t^2}\right)$$

    t = adjustable tapering parameter
  - like convolving image by a Gaussian
  - gives more weight to short baselines, degrades angular resolution
  - downweights data at long baselines, so point source sensitivity degraded
  - may improve sensitivity to extended structure sampled by short baselines
  - limits to usefulness

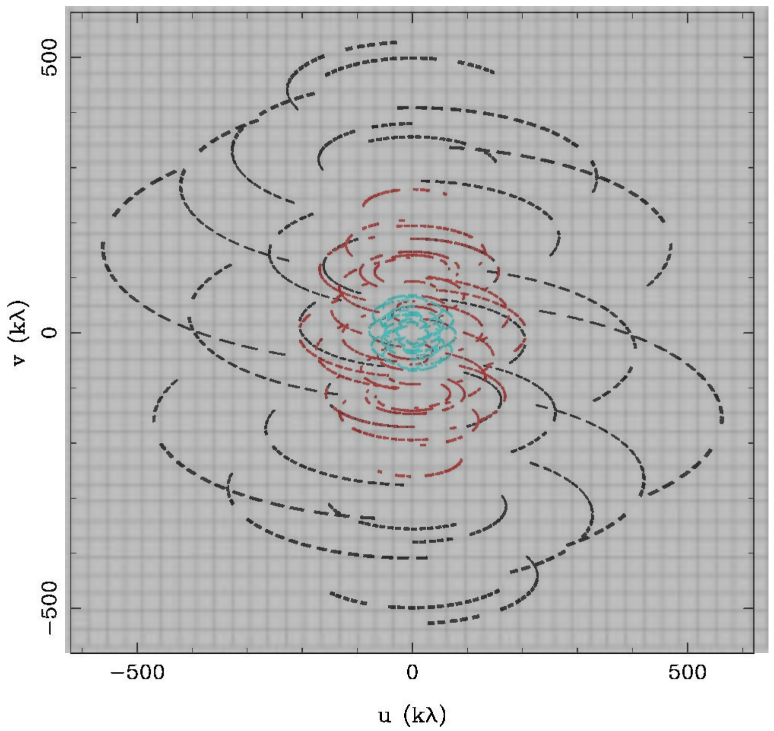

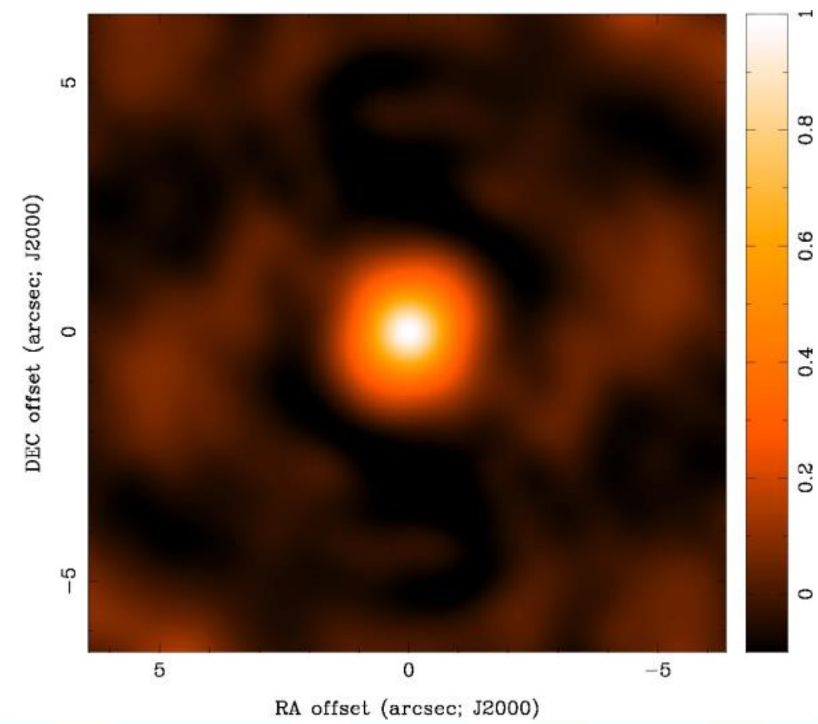

Visibility Weighting and Image Noise

natural
0.59x0.50

rms=1.0

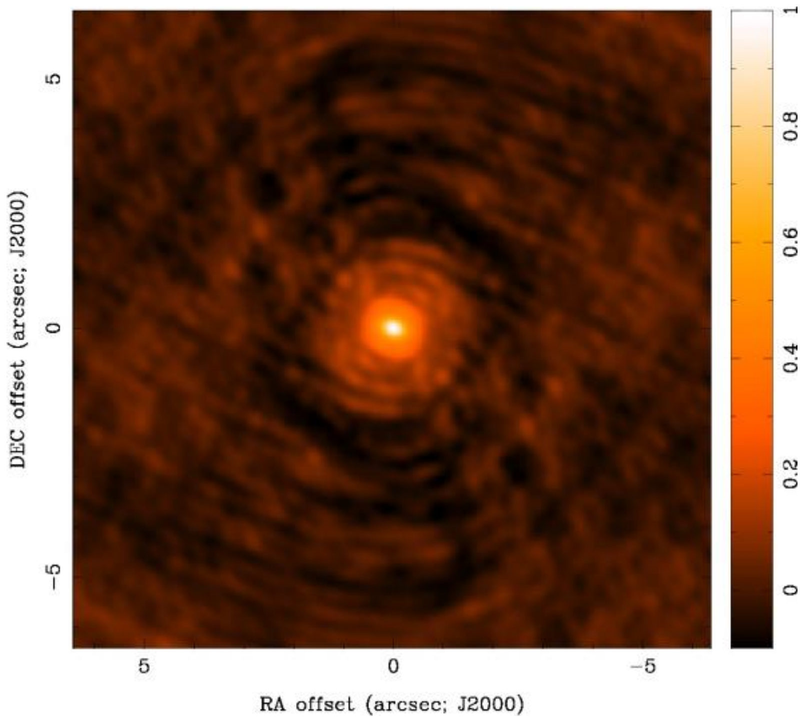

robust=0
0.40x0.34

rms=1.3

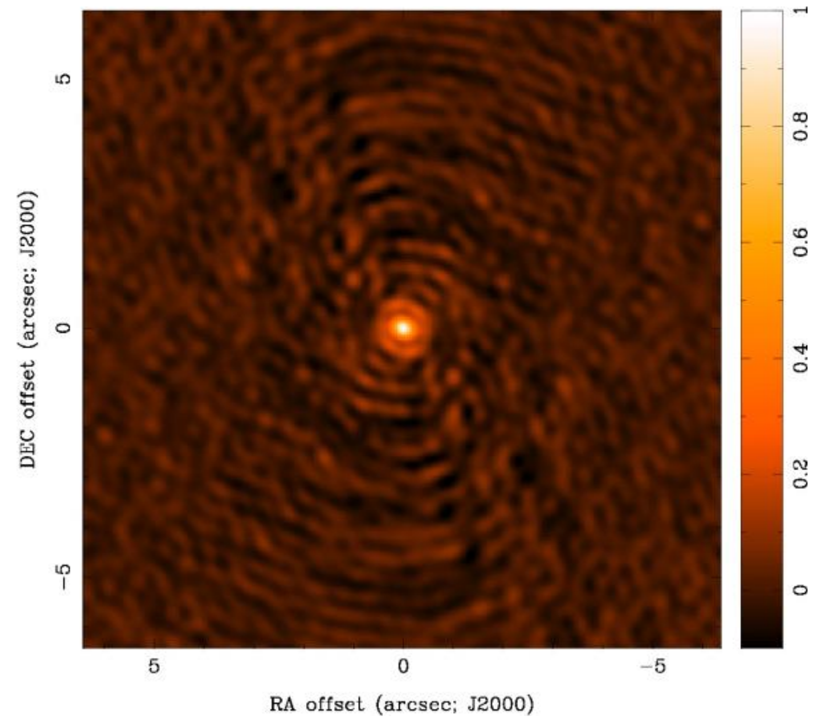

uniform
0.35x0.30

rms=2.1

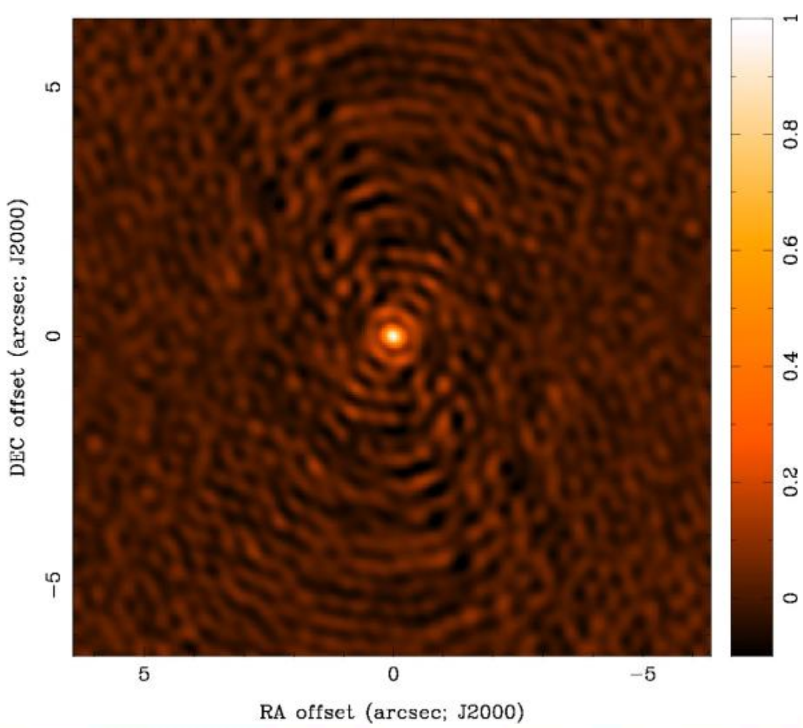

robust=0
+ taper to
0.59x0.50

rms=1.2

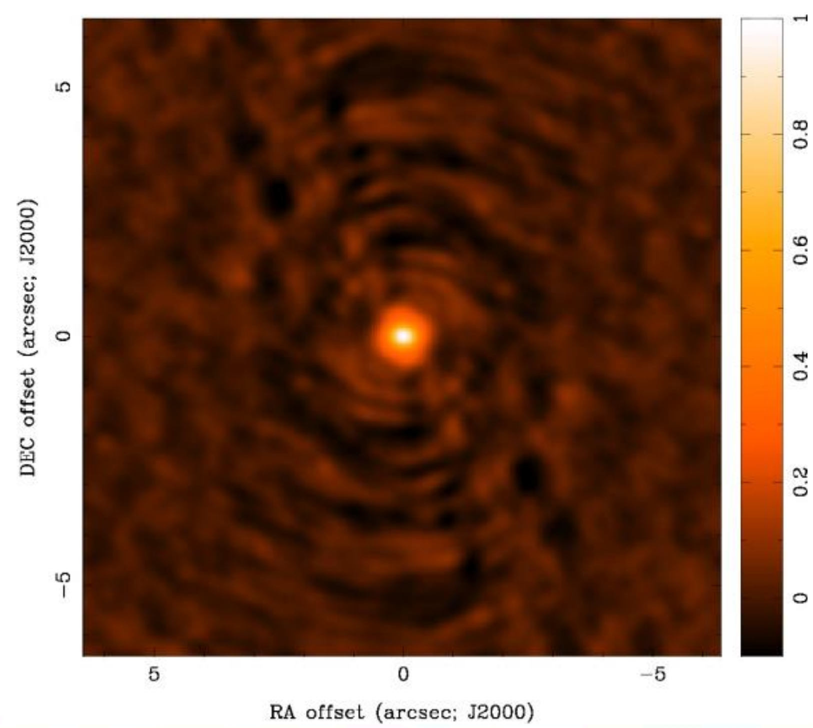

Deconvolution Algorithms

- use non-linear techniques to interpolate/extrapolate samples of *V(u,v)* into unsampled regions of the *(u,v)* plane
- aim to find a sensible model of *T(l,m)* compatible with data
- requires *a priori* assumptions about *T(l.m)* to pick plausible "invisible" distributions to fill unsampled parts of *(u,v)* plane

- "clean" is by far the dominant deconvolution algorithm in radio astronomy

- a very active research area, e.g. compressed sensing,

Classic Högbom (1974) clean Algorithm

- *a priori* assumption: *T(l,m)* is a collection of point sources

initialize a *clean component* list

initialize a *residual image* = dirty image

1. identify the highest peak in the *residual image* as a point source
2. subtract a scaled dirty beam *s(l,m)* x "loop gain" from this peak
3. add this point source location and amplitude to the *clean component* list
4. goto step 1 (an iteration) unless stopping criterion reached

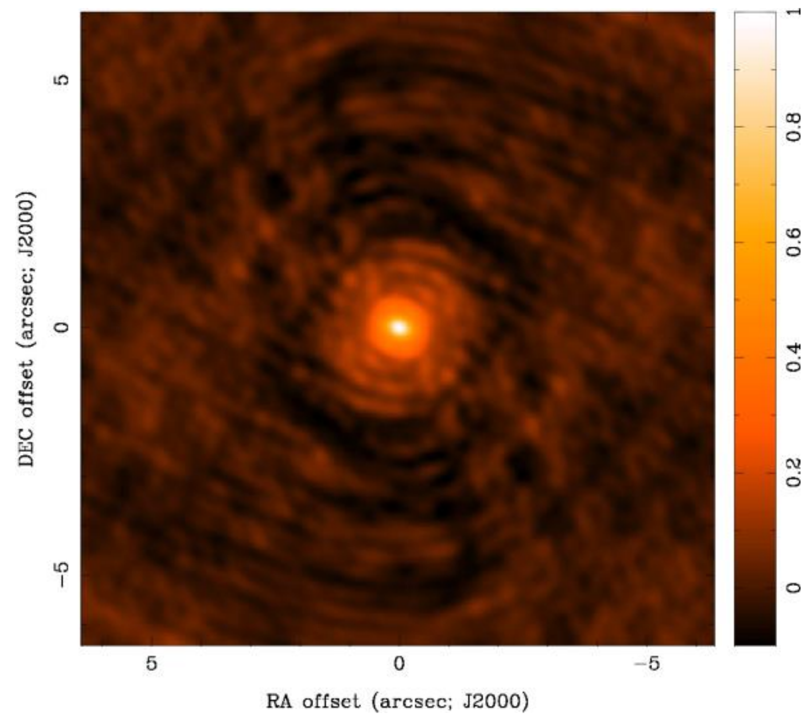

s(l,m)

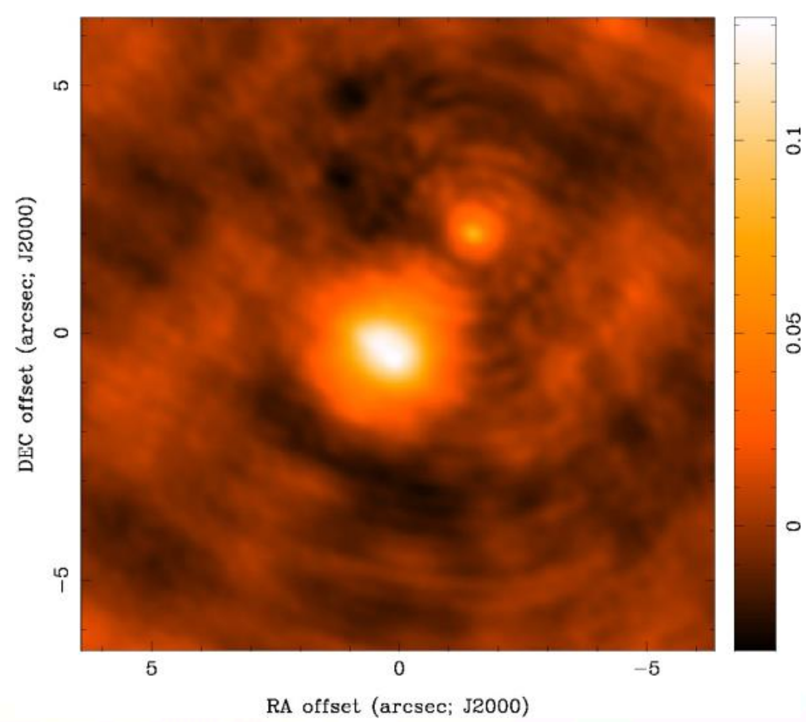

$T^D(l,m)$

Classic Högbom (1974) clean Algorithm

- stopping criterion
  - *residual map* maximum < threshold = multiple of rms , e.g. 2 x rms (if noise limited)
  - *residual map* maximum < threshold = fraction of dirty map maximum (if dynamic range limited)
- loop gain parameter
  - good results for g=0.1 (CASA `clean` default)
  - lower values can work better for smoother emission
- finite support
  - easy to include *a priori* information about where in dirty map to search for *clean components* (CASA `clean` "mask")
  - very useful but potentially dangerous

Classic Högbom (1974) clean Algorithm

- last step is to create a final "restored" image
  - make a model image with all point source *clean components*
  - convolve point source model image with a "clean beam", an elliptical Gaussian fit to the main lobe of the dirty beam
  - add back *residual map* with noise and structure below the threshold
- restored image is an estimate of the true sky brightness $T(l,m)$
  - units of the restored image are (mostly) Jy per clean beam area = intensity, or brightness temperature

- Schwarz (1978) showed that clean is equivalent to a least squares fit of sinusoids to visibilities in the case of no noise

clean example

initialize

$T^D(l,m)$

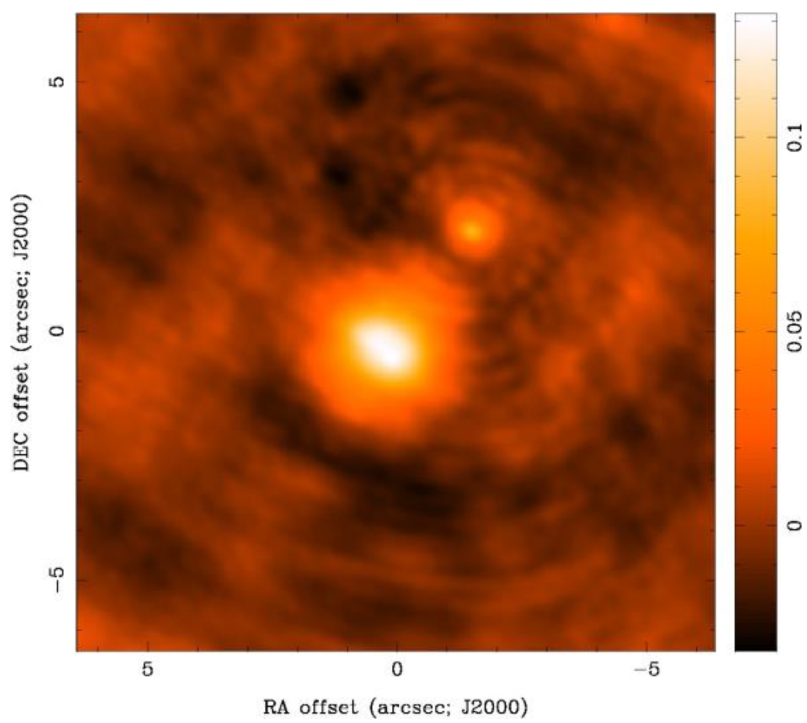

0 clean components

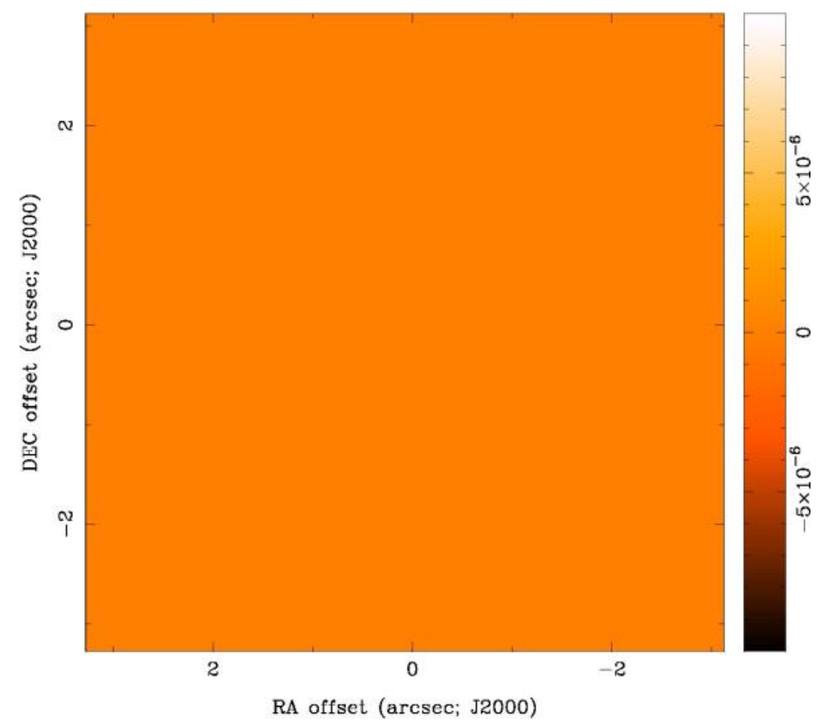

residual map

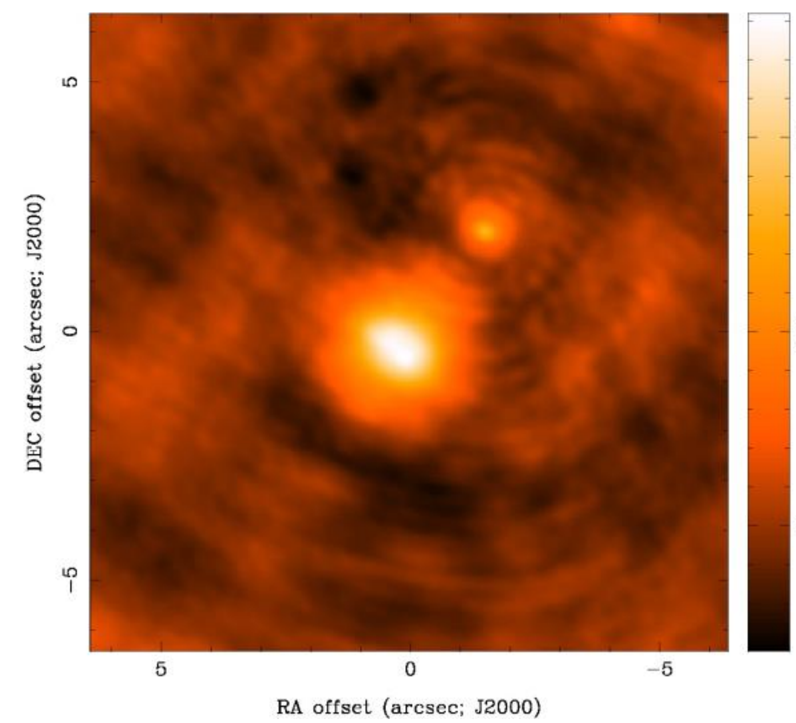

clean example

$T^D(l,m)$

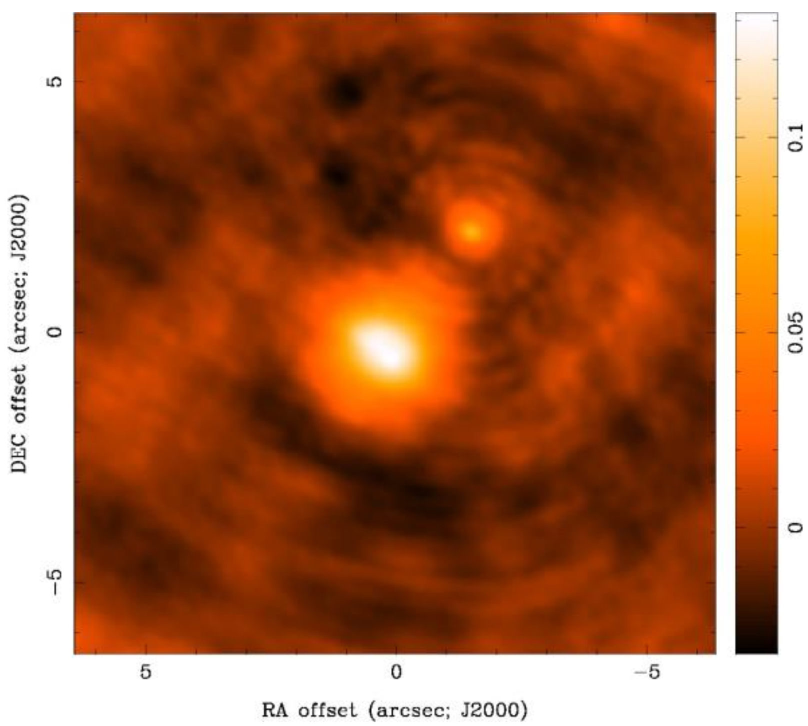

30 clean components

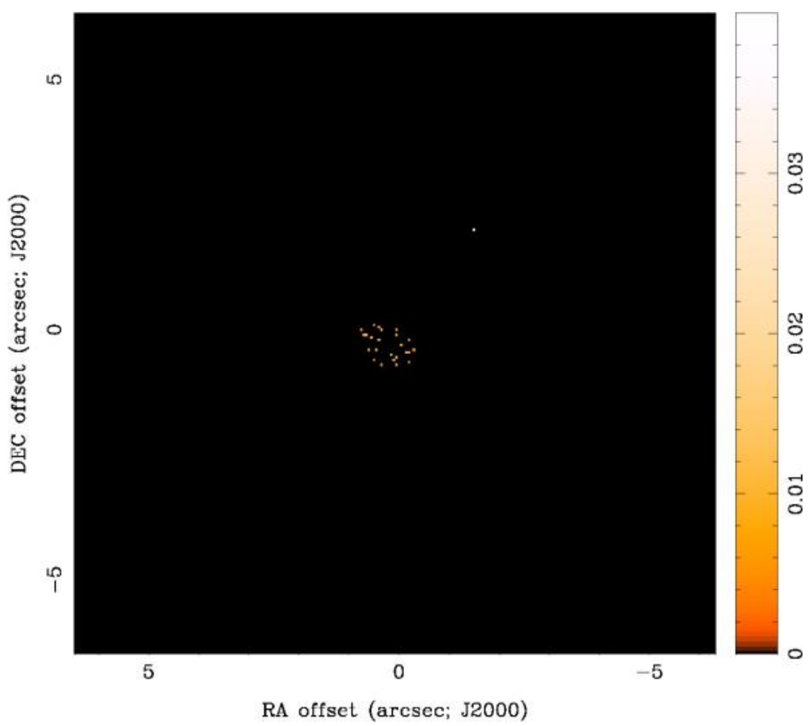

residual map

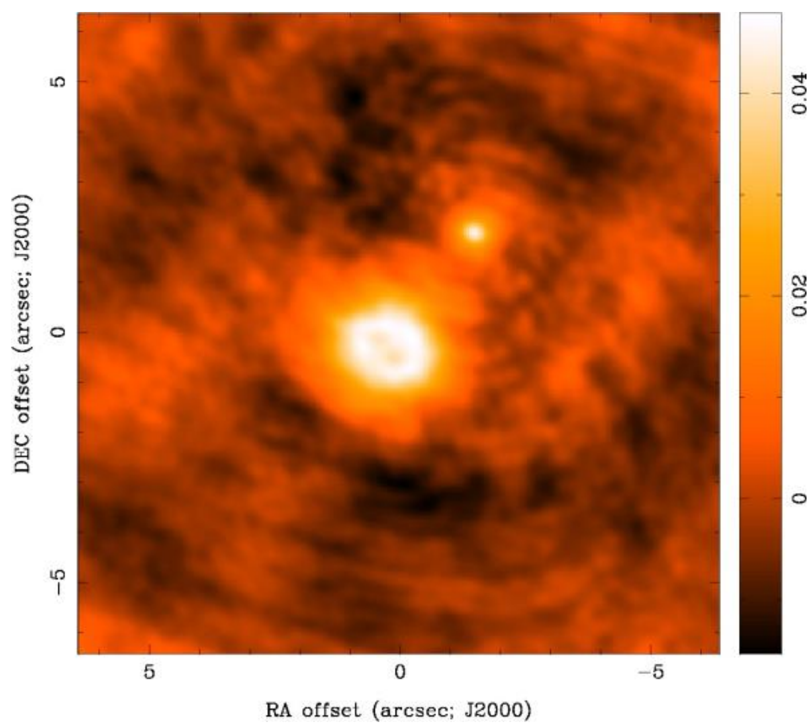

clean example

$T^D(l,m)$

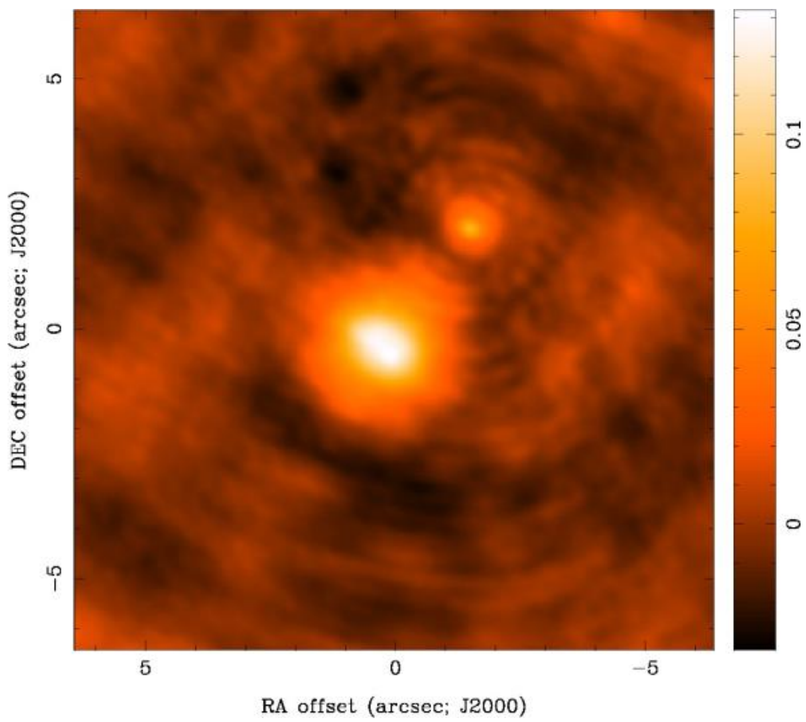

100 clean components

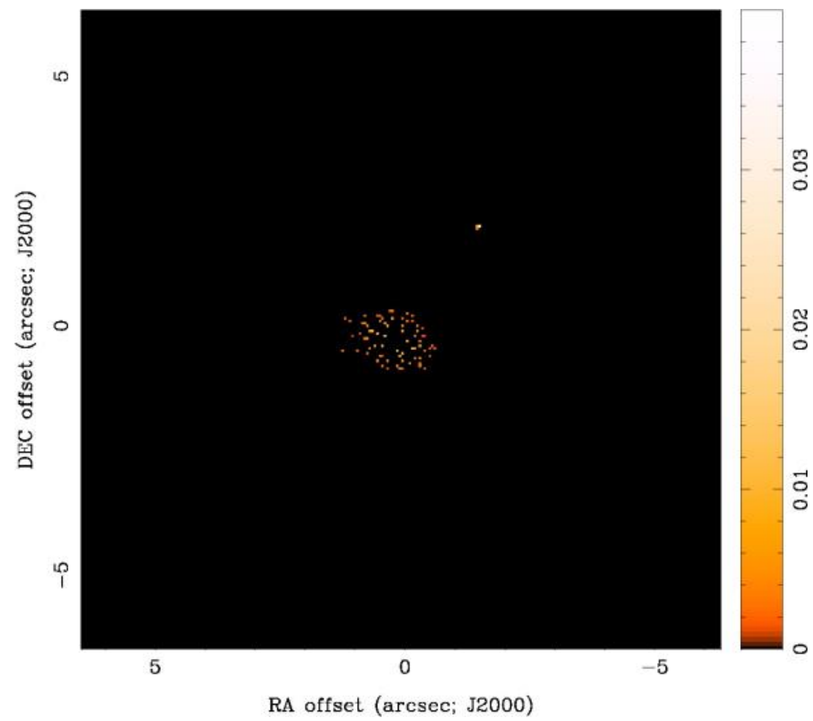

residual map

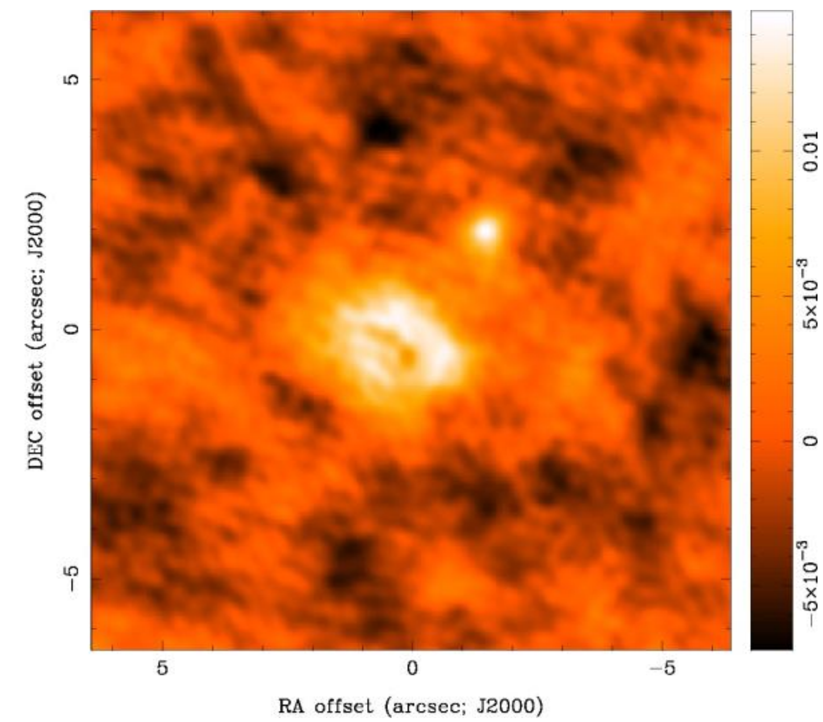

clean example

$T^D(l,m)$

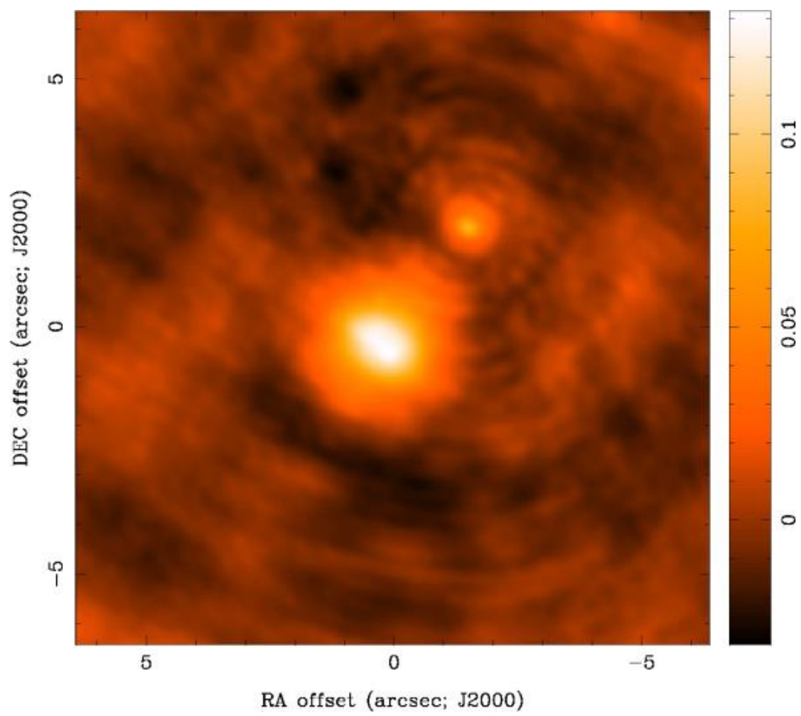

300 clean components

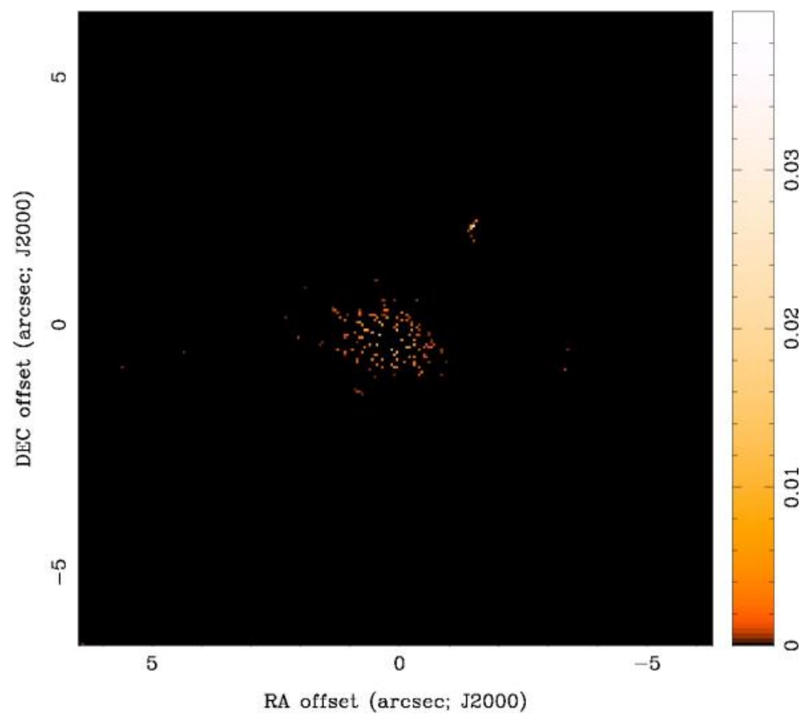

residual map

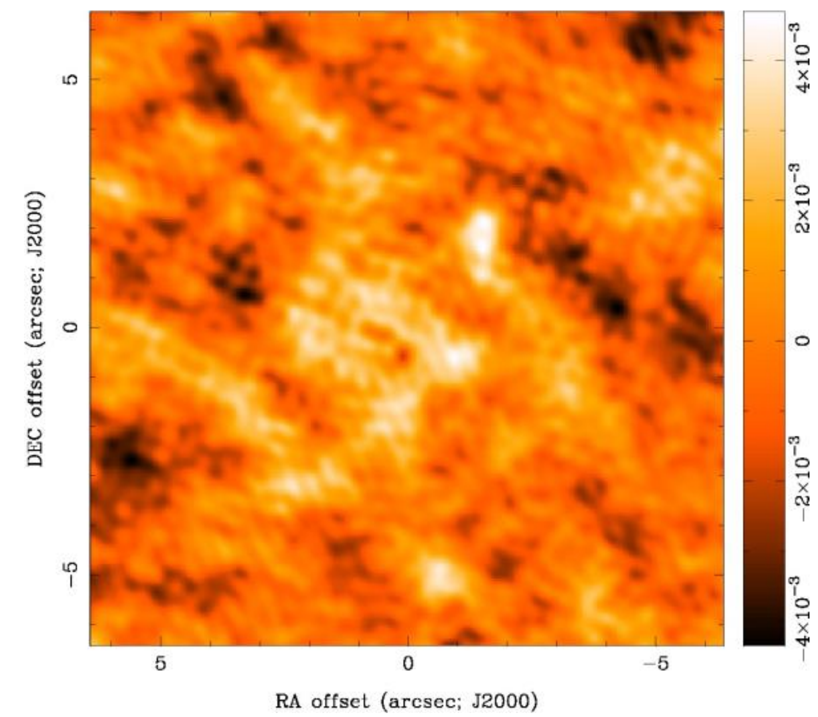

clean example

$T^D(l,m)$

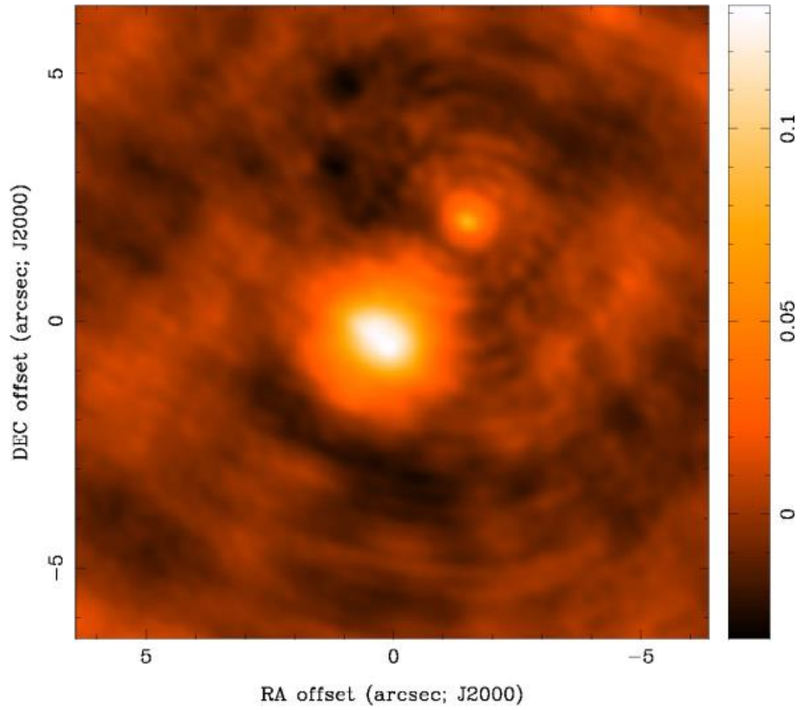

583 clean components

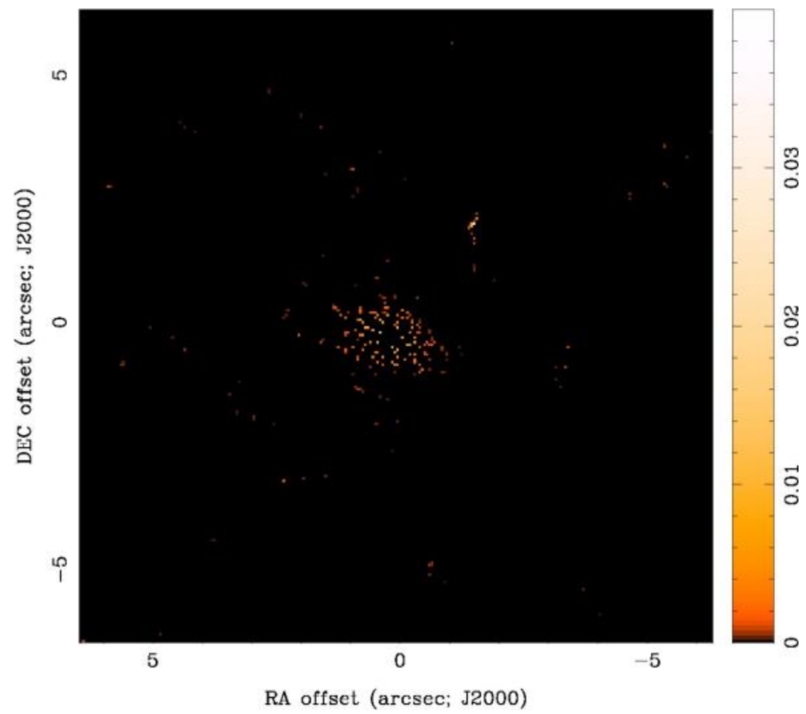

residual map

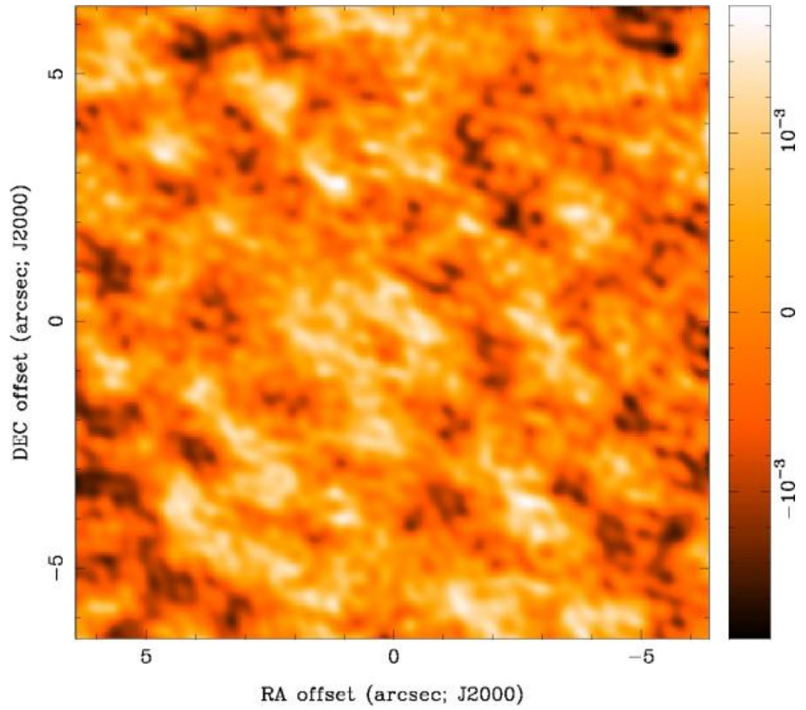

threshold reached

clean example

$T^D(l,m)$

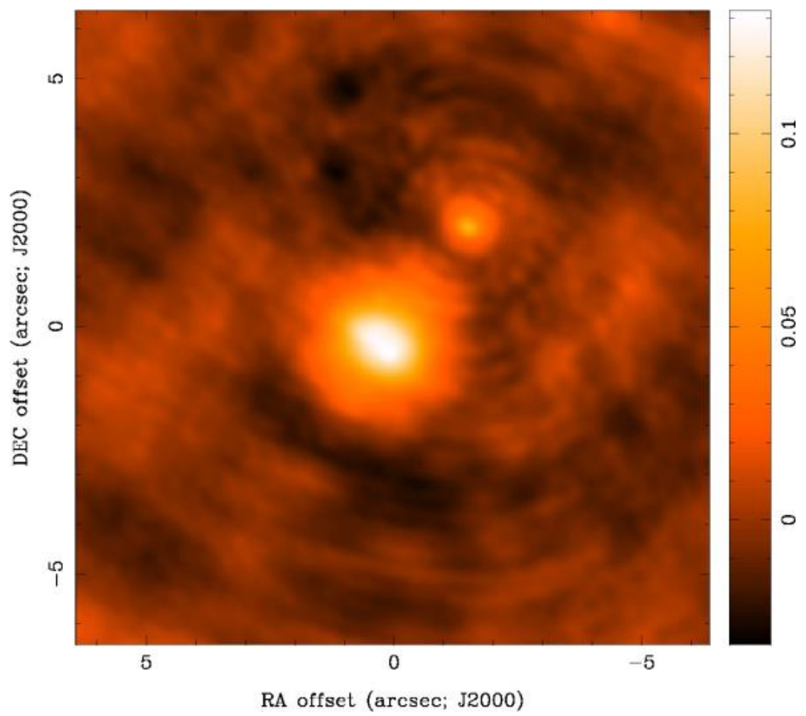

restored image

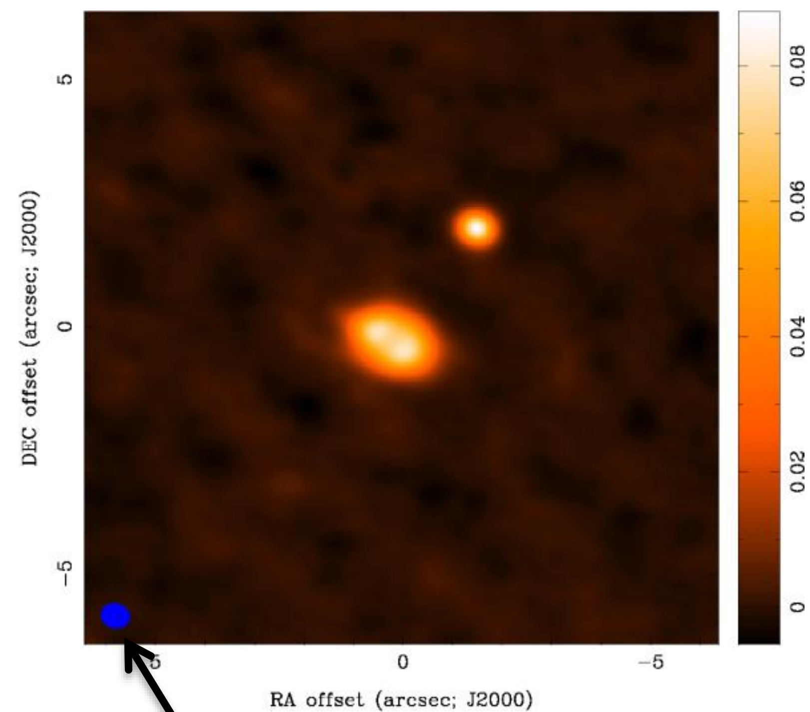

ellipse = clean beam fwhm

final image depends on

imaging parameters (pixel size, visibility weighting scheme, gridding)
and deconvolution (algorithm, iterations, masks, stopping criteria)

Results from Different Weighting Schemes

natural
0.59x0.50

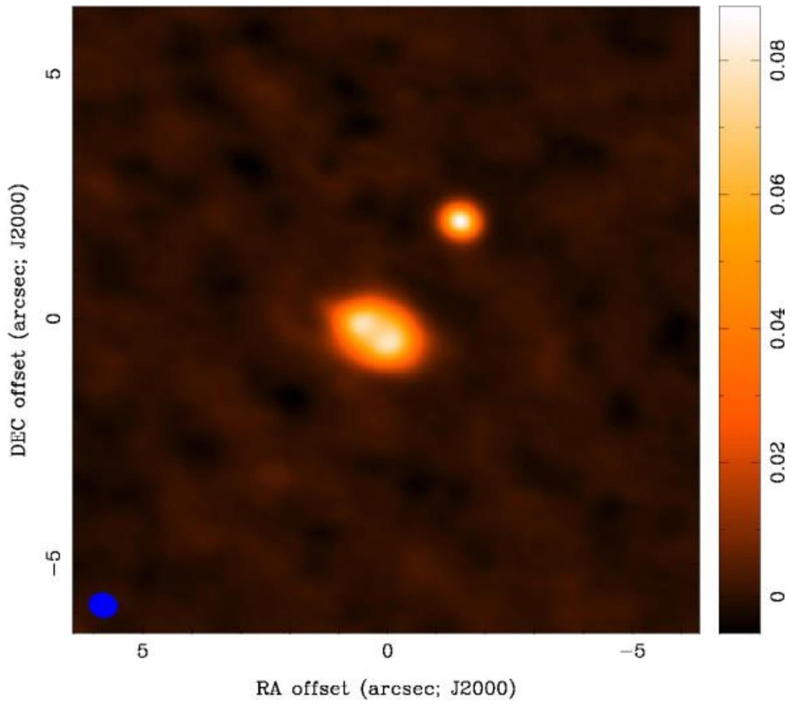

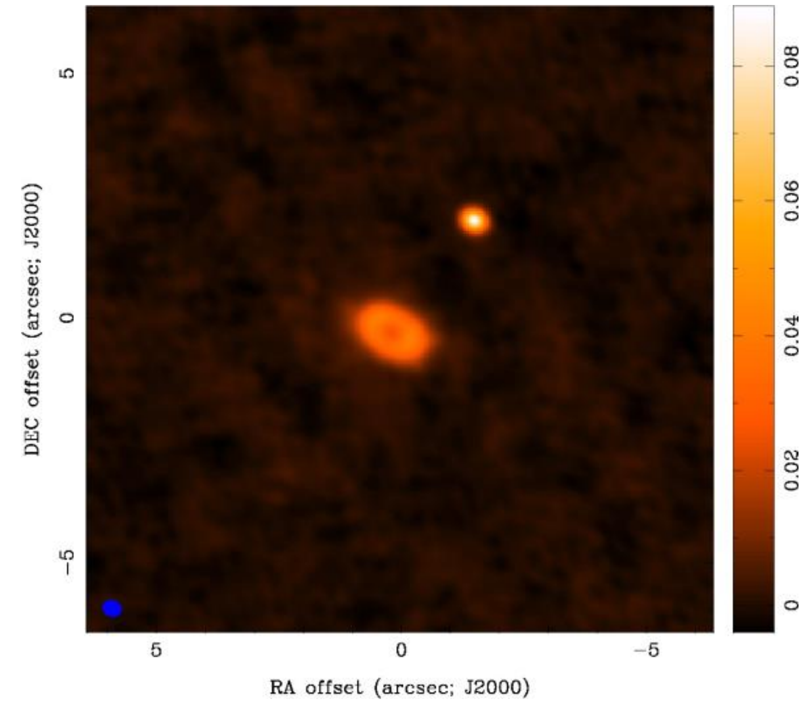

robust=0
0.40x0.34

uniform
0.35x0.30

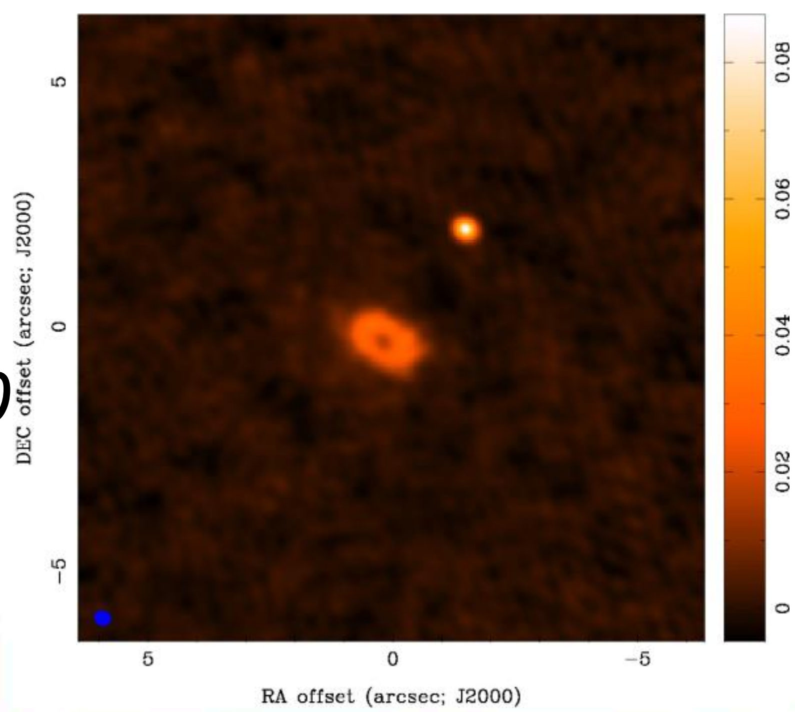

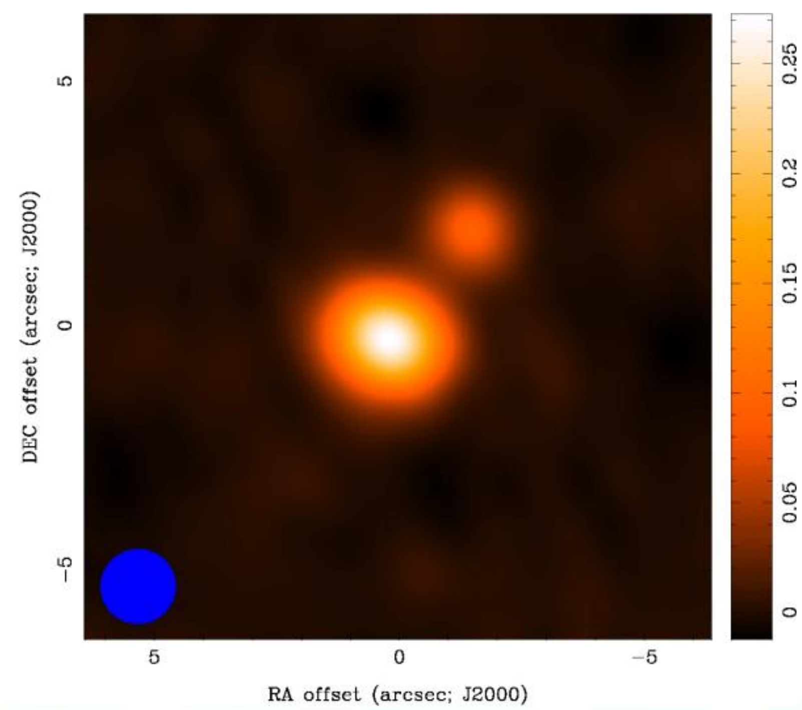

natural
+ taper to
1.5x1.5

Missing Short Baselines: Demonstration

- important structure may be missed in central hole of *(u,v)* plane

- Do the visibilities observed in our example discriminate between these two models of sky brightness *T(l,m)*?

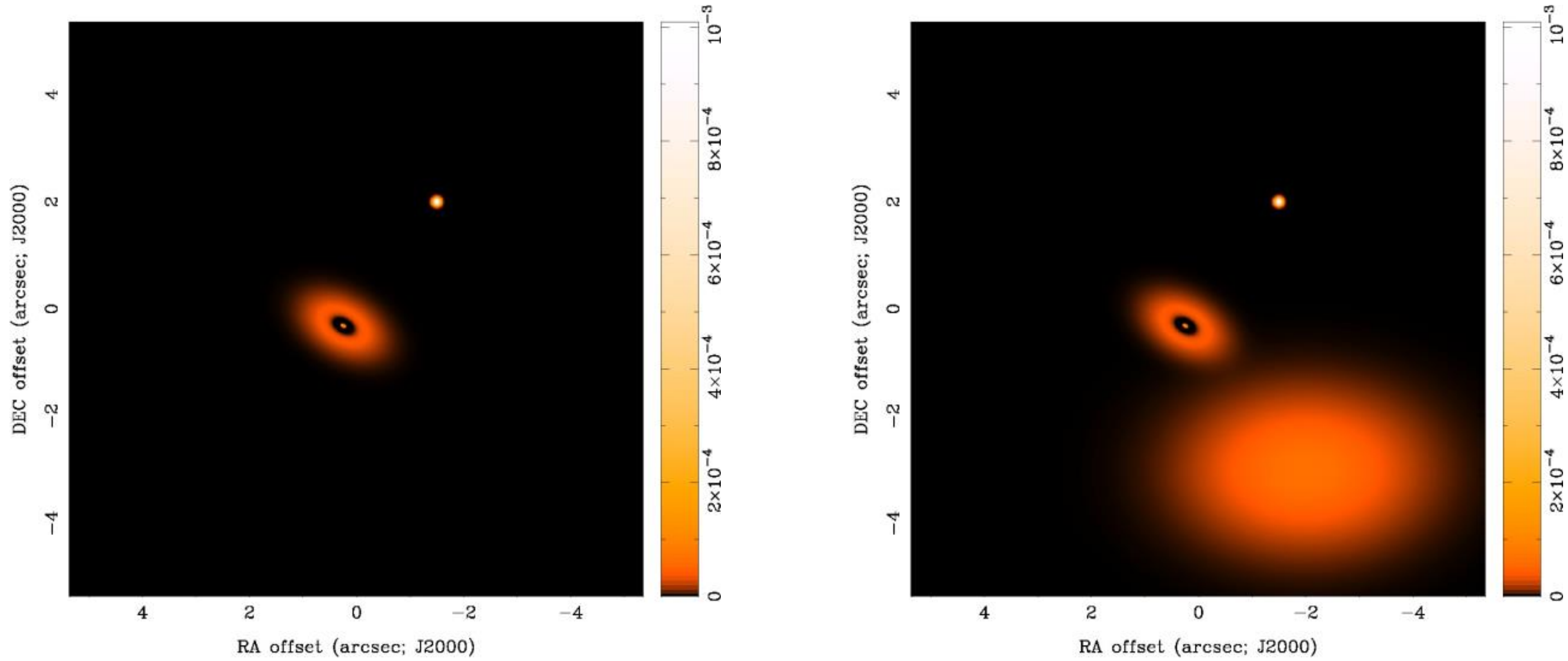

- Yes… but only on baselines shorter than about 75 kλ

Missing Short Baselines: Demonstration

T(l,m) | *natural weight* | $>$ *75 kλ natural weight*

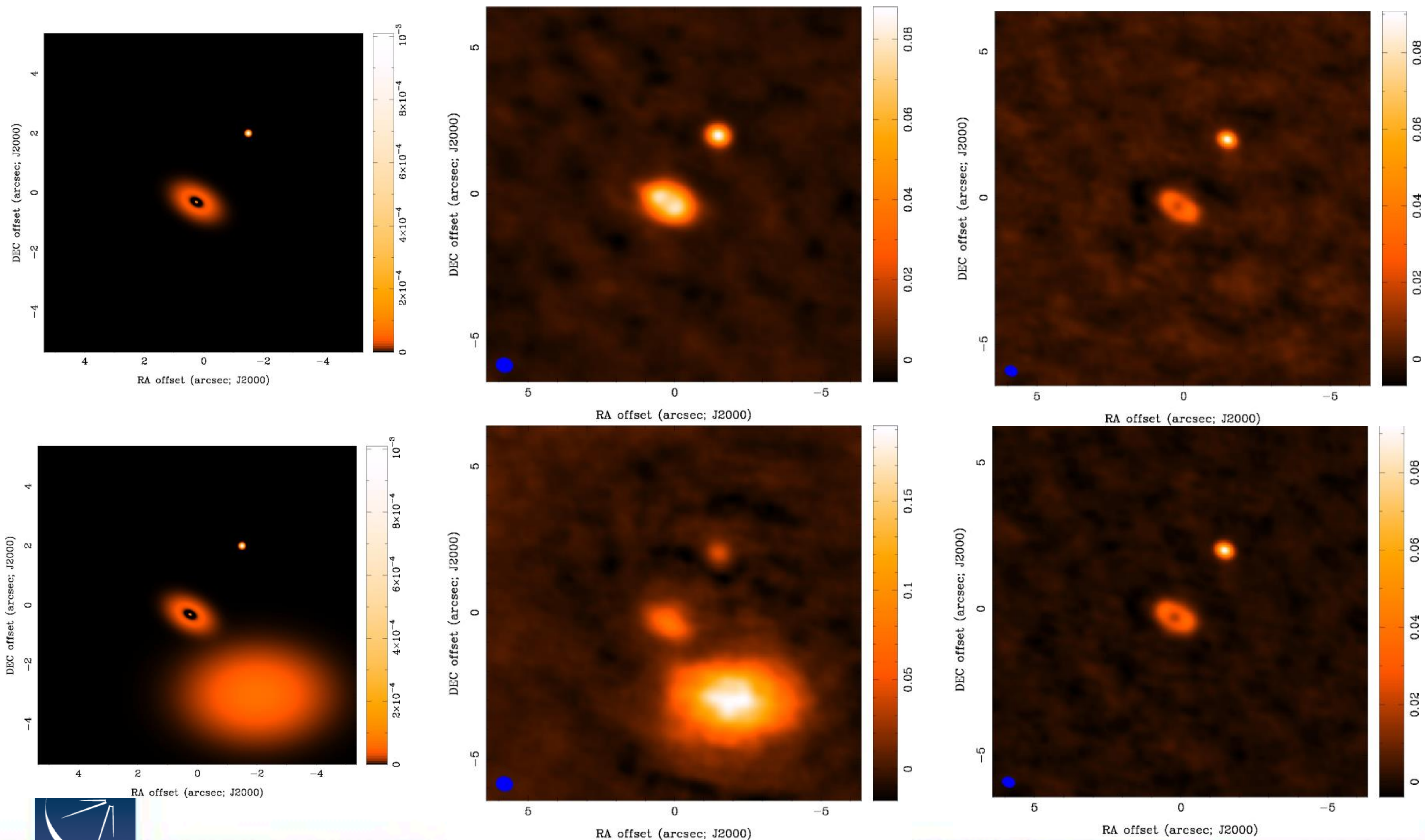

ALMA "Maximum Recoverable Scale"

- adopted to be 10% of the total flux density of a uniform disk (not much!)

	Band	3	4	6	7	8	9	10
	Frequency (GHz)	100	150	230	345	460	650	870
Configuration								
7-m	θ_{res} (arcsec)	12.5	8.4	5.4	3.6	2.7	1.9	1.4
	θ_{MRS} (arcsec)	66.7	44.5	29.0	19.3	14.5	10.3	7.7
C40-1	θ_{res} (arcsec)	3.7	2.5	1.6	1.1	0.80	0.57	0.42
	θ_{MRS} (arcsec)	29.0	19.4	12.6	8.4	6.3	4.5	3.3
C40-2	θ_{res} (arcsec)	2.4	1.6	1.0	0.69	0.52	0.37	0.27
	θ_{MRS} (arcsec)	22.1	14.8	9.6	6.4	4.8	3.4	2.5
C40-3	θ_{res} (arcsec)	1.5	0.97	0.63	0.42	0.32	0.22	0.17
	θ_{MRS} (arcsec)	13.7	9.1	5.9	4.0	3.0	2.1	1.6
C40-4	θ_{res} (arcsec)	0.93	0.62	0.40	0.27	0.20	0.14	0.11
	θ_{MRS} (arcsec)	8.9	5.9	3.9	2.6	1.9	1.4	1.0
C40-5	θ_{res} (arcsec)	0.54	0.36	0.23	0.16	0.12	0.083	0.062
	θ_{MRS} (arcsec)	6.0	4.0	2.6	1.7	1.3	0.93	0.69
C40-6	θ_{res} (arcsec)	0.35	0.23	0.15	0.10	0.076	0.054	0.040
	θ_{MRS} (arcsec)	3.1	2.1	1.3	0.90	0.67	0.48	0.36
C40-7	θ_{res} (arcsec)	0.21	0.14	0.090	0.060	0.045	0.032	0.024
	θ_{MRS} (arcsec)	1.8	1.2	0.77	0.52	0.39	0.27	0.20
C40-8	θ_{res} (arcsec)	0.12	0.079	0.052	0.034	-	-	-
	θ_{MRS} (arcsec)	1.3	0.87	0.57	0.38	-	-	-
C40-9	θ_{res} (arcsec)	0.066	0.044	0.029	-	-	-	-
	θ_{MRS} (arcsec)	0.78	0.52	0.34	-	-	-	-

Table 7.1: Resolution (θ_{res}) and maximum recoverable scale (θ_{MRS}) for the 7-m Array and 12-m Array configurations available during Cycle 4 as a function of a representative frequency in a band. The value of θ_{MRS} is computed using L05 from Table 7.2 and equation 7.7; the value of θ_{res} is the mean size of the interferometric beam obtained through simulation with CASA, using Briggs uv-plane weighting with *robust=0.5*. (This value of *robust* offers a compromise between natural and uniform.) The computations were done for a source at zenith; for sources transiting at lower elevations, the North-South angular measures will increase proportional to 1/sin(ELEVATION).

ALMA Cycle 4 Technical Handbook

Techniques to Obtain Short Baselines (1)

use a large single dish telescope

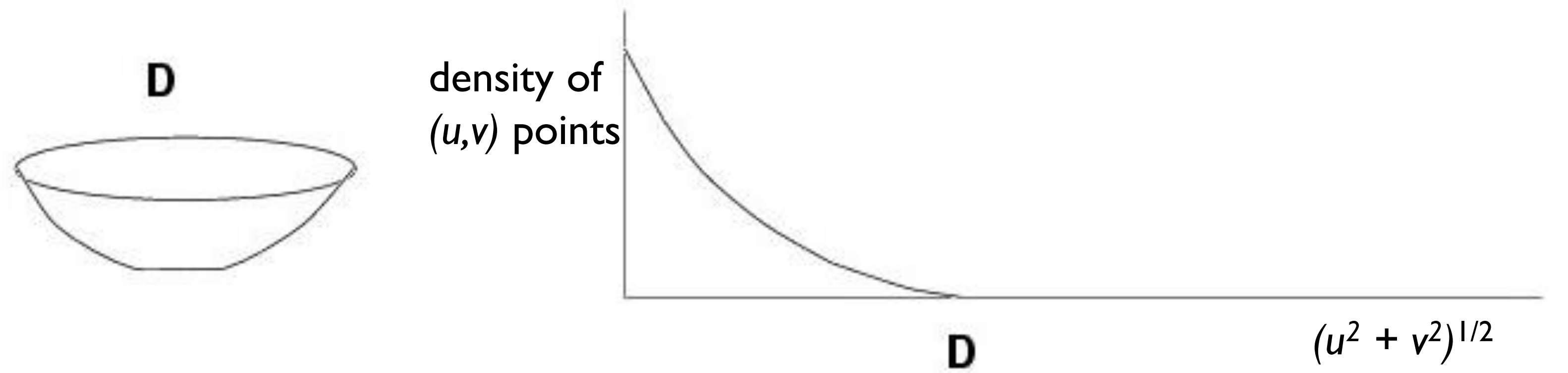

- *all* Fourier components from 0 to D sampled, where D is dish diameter (weighting depends on illumination)
- scan single dish across sky to make an image $T(l,m) * A(l,m)$
  where $A(l,m)$ is the single dish response pattern
- Fourier transform single dish image, $T(l,m) * A(l,m)$, to get $V(u,v)a(u,v)$
  and then divide by $a(u,v)$ to estimate $V(u,v)$ for baselines < D
- choose D large enough to overlap interferometer samples of $V(u,v)$
  and avoid using data where $a(u,v)$ becomes small

Techniques to Obtain Short Spacings (II)

use a separate array of smaller antennas

- small antennas can observe short baselines inaccessible to larger ones
- the larger antennas can be used as single dish telescopes to make images with Fourier components not accessible to the smaller antennas
- example: ALMA main array + ACA

main array
50 x 12m: 12m to 14+ km

ACA
12 x 7m: covers 7-12m
4 x 12m single dishes: 0-7m

Concluding Remarks

- interferometry samples Fourier components of sky brightness
- make an image by Fourier transforming sampled visibilities
- deconvolution attempts to correct for incomplete sampling

- remember
  - there are an infinite number of images compatible with the visibilities
  - missing (or corrrupted) visibilities affect the entire image
  - astronomers must use judgement in imaging and deconvolution
- it's fun and worth the trouble $\rightarrow$ high resolution images!

many, many issues not covered in this talk, see references

Atacama **L**arge **M**illimeter/submillimeter **A**rray

- The largest ground-based astronomical facility
- 50 12-m, 12 7-m, 4 12-m = 66 antennas
- ~5000 m in altitude, Chajnantor plateau, Chile
- East Asia, Europe, North America, & Chile
- https://almascience.org

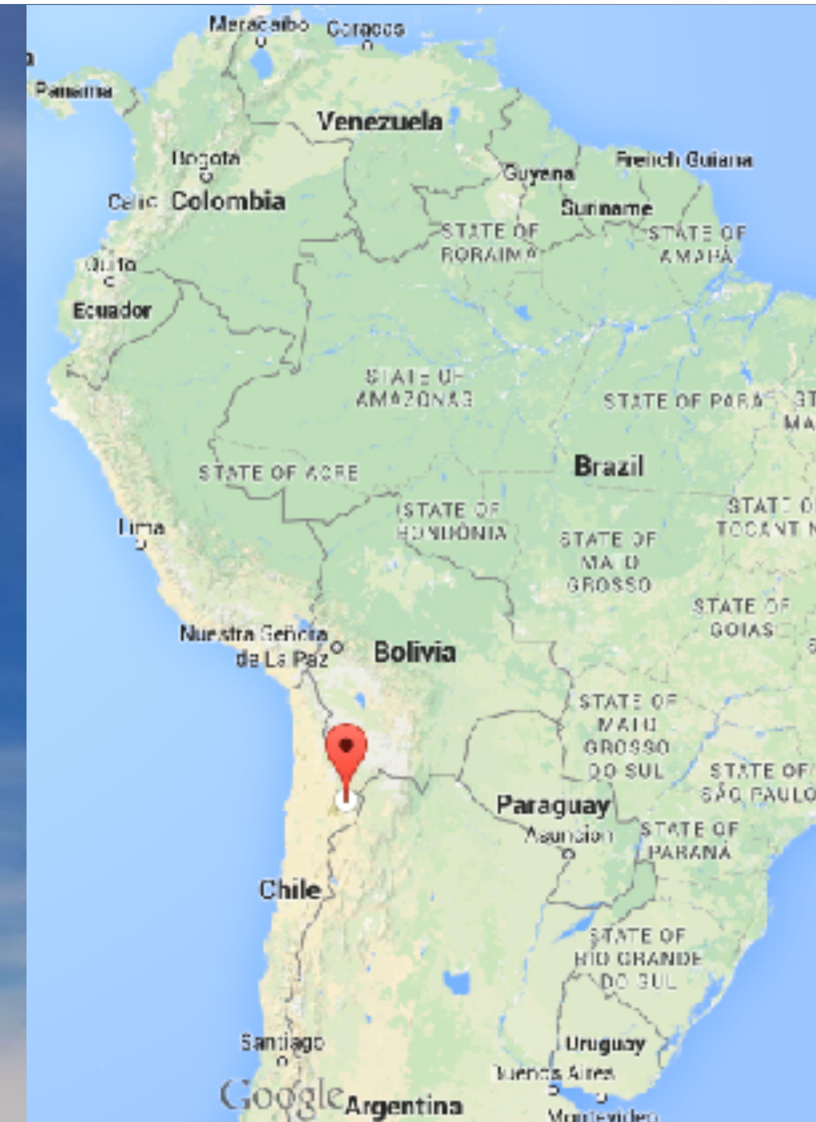

ALMA full Operation's Specifications

	Specification
Number of Antennas	*50×12 m (12-m Array), plus 12×7 m & 4×12 m (ACA)*
Maximum Baseline Lengths	*0.16 - 16.2 km*
Angular Resolution (")	*~0.2" × (300/ν GHz) × (1 km / max. baseline)*
12 m Primary beam (")	*~20.6" × (300/ν GHz)*
7 m Primary beam (")	*~35" × (300/ν GHz)*
Number of Baselines	*Up to 1225 (ALMA correlators can handle up to 64 antennas)*
Frequency Coverage	*All atmospheric windows from 84 GHz - 950 GHz (with extension to ~30 GHz when Bands 1 and 2 are deployed)*
Correlator: Total Bandwidth	*16 GHz (2 polarizations × 4 basebands × 2 GHz/baseband)*
Correlator: Spectral Resolution	*As narrow as 0.008 × (300/ν GHz) km/s*
Polarimetry	*Full Stokes parameters*

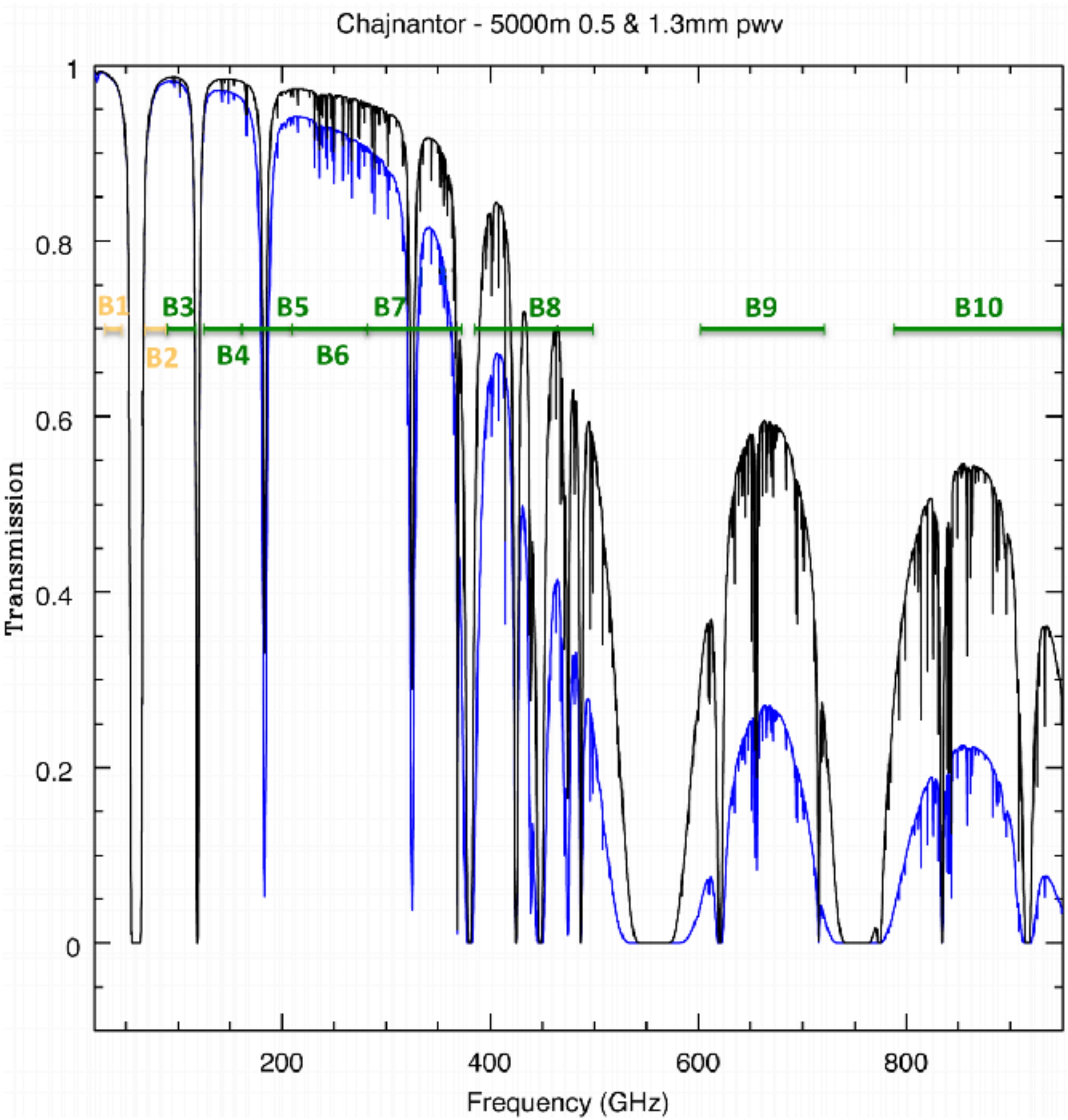

Band	Frequency (GHz)	Wavelength (mm)	Primary Beam (FOV; ″)
3	84-116	3.6-2.6	73-53
4	125-163	2.4-1.8	49-38
5	158-211	1.9-1.4	37-29
6	211-275	1.4-1.1	29-22
7	275-373	1.1-0.8	22-16
8	385-500	0.78-0.6	16-12
9	602-720	0.5-0.42	10-8.5
10	787-950	0.38-0.32	7.8-6.5

2019 Radio meetings

- Townhall meetings
  March & April
- ALMA Summer School
- 2019 Radio Summer School
  August 27—29
- 2019 Radio Telescope User's Meeting
  August 29—30